

**SYNTHESIS OF RETIGABINE ANALOGUES FOR THE TREATMENT OF TINNITUS
AND PROGRESS TOWARDS A CONCISE ROUTE TO XJB-5-131**

By

Nicholas Lawrence Reed

B.Sc. in Chemistry, Purdue University, 2012

Submitted to the Graduate Faculty of
The Kenneth P. Dietrich School of Arts and Sciences in partial fulfillment
of the requirements for the degree of
Master of Science

University of Pittsburgh

2014

UNIVERSITY OF PITTSBURGH
THE KENNETH P. DIETRICH SCHOOL OF ARTS & SCIENCES

This thesis was presented

by

Nicholas Lawrence Reed

It was defended on

November 18th 2014

and approved by

Alexander Deiters, Professor, Department of Chemistry

Dennis P. Curran, Distinguished Service Professor of Chemistry and Bayer Professor,
Department of Chemistry

Thesis Director: Peter Wipf, Distinguished University Professor of Chemistry, Department of
Chemistry

Copyright © by Nicholas Lawrence Reed

2014

SYNTHESIS OF RETIGABINE ANALOGUES FOR THE TREATMENT OF TINNITUS AND PROGRESS TOWARDS A CONCISE ROUTE TO XJB-5-131

Nicholas Reed, M.S.

University of Pittsburgh, 2014

The first part of this thesis describes the synthesis of retigabine analogues for the treatment of tinnitus. Retigabine is a clinically proven anticonvulsant that modulates potassium ion channel activity and has been shown to stop the onset of tinnitus when administered shortly after exposure to extreme levels of sound. Alteration of the fluorophenyl and carbamate functionalities present in the parent compound resulted in the synthesis of a small library of compounds with the goal of improving potency and selectivity for the Kv7.2/3 potassium ion channels. *In vivo* and *in vitro* testing is underway to determine efficacy.

The second part of this thesis describes efforts to develop an improved route to XJB-5-131, a truncated Gramicidin S-derived peptide designed to control reactive oxygen species (ROS) production in mitochondria. A new route to XJB-5-131 was explored utilizing a stereoselective α -alkenylation protocol and starting from vinyl boronic acids.

TABLE OF CONTENTS

LIST OF ABBREVIATIONS	XII
ACKNOWLEDGEMENTS	XVI
1.0 SYNTHESIS OF RETIGABINE ANALOGUES FOR THE TREATMENT OF TINNITUS	1
1.1 INTRODUCTION	1
1.1.1 Tinnitus.....	1
1.1.2 K _v 7 Potassium Ion Channels	3
1.1.3 Retigabine: Development and Drug Profile	7
1.2 RESULTS AND DISCUSSION	11
1.2.1 Analogue Design	11
1.2.2 Analogue Synthesis	18
1.3 CONCLUSIONS	28
2.0 PROGRESS TOWARDS A CONCISE ROUTE TO XJB-5-131	29
2.1 INTRODUCTION	29
2.1.1 Mitochondrial Production of Reactive Oxygen Species and XJB-5-131 ..	29
2.1.2 Stereoselective Alkenylation of Aldehydes: Difficulties and Approaches	35
2.2 RESULTS AND DISCUSSION	45
2.2.1 Synthetic Strategy Towards Amino Acid 2-7	45

2.2.2	Studies Towards Amino Acid 2-7.....	46
2.3	CONCLUSIONS.....	51
3.0	EXPERIMENTAL PART.....	53
3.1	GENERAL EXPERIMENTAL.....	53
3.2	CHAPTER 1 EXPERIMENTAL PART.....	54
3.3	CHAPTER 2 EXPERIMENTAL PART.....	87
4.0	BIBLIOGRAPHY.....	95

LIST OF TABLES

Table 1. <i>N</i> -(6-Substituted-pyridin-3-yl)-3,4-difluorobenzamide Derivatives as $K_v7.2/3$ Activators	13
Table 2. Enantioselective α -Vinylolation of Oxindoles with 1-Bromo-1-propene and β -Bromostyrene.....	38
Table 3. Asymmetric Hiyama Coupling of α -Bromo Esters and Vinyl Silanes	39
Table 4. Attempted Hydroboration to Access a Substituted Boronic Acid 1-34	47
Table 5. Conditions for α -Alkenylation with 2-34	49
Table 6. Attempted α -Alkenylation Using Boronic Acid 2-38	51

LIST OF FIGURES

Figure 1. Structures of Lidocaine and Carbamazepine	3
Figure 2. Structure of K _v AP Voltage-Gated Potassium Ion Channel α -Subunit Showing Pauling-Corey-Branson Helix (left) and Cartoon (right) Representations	5
Figure 3. Structure of the K _v AP Potassium Ion Channel	6
Figure 4. Structures of Flupirtine and Retigabine	7
Figure 5. Proposed Binding Site of Retigabine: A) Three-Dimensional Model of Retigabine Docked to the Active Site of a K _v 7.3 Domain and B) Crucial Amino Acid Residue Interactions	8
Figure 6. Major Metabolites of Retigabine	11
Figure 7. 4-(<i>N</i> -Azacycloalkyl)anilide Derivatives for the Modulation of K _v 7.2/3 Activity	12
Figure 8. Structure-Activity-Relationship of Retigabine	14
Figure 9. 2-Dimensional Representation of the Active Site of Retigabine (red = π - π stacking interaction, blue = hydrophobic interaction, magenta = hydrogen-bonding interaction)	15
Figure 10. Structure of Retigabine and Regions of Modification	15
Figure 11. Examples of Fluorinated and Heterocyclic Retigabine Analogues	17
Figure 12. Covalently Modified MMS-350 and 3-Methyl-3-oxetanemethanol Retigabine Analogues	18
Figure 13. Production of Reactive Oxygen Species in the Electron Transport Chain	30
Figure 14. Mitochondrial Targeting Strategies	31

Figure 15. Structure of Gramicidin S.....	32
Figure 16. Structures of XJB-5-131 and JP4-039.....	33
Figure 17. Difficulties and Desired Transformation Associated with α -Alkylation of Carbonyl Compounds.....	36
Figure 18. New Synthetic Strategy towards XJB-5-131.....	46
Figure 19. Structure of Chiral Imidazolidinones 2-40 and 2-41	48

LIST OF SCHEMES

Scheme 1. Synthesis of Retigabine Dihydrochloride	9
Scheme 2. Synthesis of Retigabine Avoiding Polycarbamylation.....	10
Scheme 3. Reductive Amination of 2-Nitro- <i>p</i> -phenylenediamine and Fluorinated Benzaldehydes	18
Scheme 4. Protection and Carbamylation of Reductive Amination Products	20
Scheme 5. Reduction and Cleavage of Cbz Protecting Group Using Catalytic Hydrogenation	21
Scheme 6. Attempted Nucleophilic Trifluoromethylation of Pentafluorosulfanylimine 1-28	21
Scheme 7. Reductive Amination and Protection Affording Regioisomer 1-30	22
Scheme 8. Carbamylation and Catalytic Hydrogenation of 1-29	22
Scheme 9. Synthesis of Deuterated Reductive Amination Product 1-34	23
Scheme 10. Synthesis of Deuterium-Labeled Retigabine.....	24
Scheme 11. Initial Attempts towards Heterocyclic Analogues of Retigabine.....	25
Scheme 12. Synthesis of Heterocyclic Analogues of Retigabine	26
Scheme 13. Synthesis of Isopropyl Carbamate Analogue 1-44	27
Scheme 14. Synthesis of MMS-350 and 3-Methyl-3-oxetanemethanol Analogues of Retigabine ..	28
Scheme 15. Synthesis of Protected Amino Acid 2-7	34
Scheme 16. Late-Stage Peptide Couplings to Synthesize XJB-5-131	35
Scheme 17. Diastereoselective α -Arylation of Trimethylsilyl Enolates Using Chiral Auxiliaries ..	37
Scheme 18. Enantioselective Palladium-Catalyzed Vinylation of Ketone Enolates	37

Scheme 19. Enantioselective Cross-Coupling of Racemic α -Bromo Ketones with Alkenyl Zirconium Compounds	39
Scheme 20. α -Alkenylation of β -ketoesters using Cinchona Alkaloid-Derived Organocatalysts....	40
Scheme 21. Mechanism of Organo-SOMO Catalysis Using Chiral Imidazolidinones	42
Scheme 22. Anionic Oxy-Cope Strategy to All-Carbon Quaternary Centers	42
Scheme 23. Copper-Catalyzed Coupling of Alkenyl Bromides with Activated Methylene Compounds	43
Scheme 24. α -Alkenylation of Aldehydes with Vinyl Iodonium Triflate Salts Using Copper and Organocatalysis.....	44
Scheme 25. Mechanism of Enantioselective α -Alkenylation of Aldehydes Using Boronic Acids..	45
Scheme 26. Synthesis of Model Boronic Acid 2-34	47
Scheme 27. Synthesis of Amino Boronic Acid 2-38	48
Scheme 28. Preparation of Potassium Trifluoroborate 2-43 and Organo-SOMO Vinylation.....	50
Scheme 29. Synergistic Catalysis Using 2-43	50

LIST OF ABBREVIATIONS

18-C-6	18-crown-6
Å.....	angstroms
Ac	acetyl
aq.....	aqueous
ATP.....	adenosine triphosphate
ATR.....	attenuated total reflectance
Bn.....	benzyl
Boc	<i>tert</i> -butoxycarbonyl
BOP.....	(benzotriazol-1-yloxy)tris(dimethylamino)phosphonium hexafluorophosphate
Brsm.....	based on recovered starting material
Bu.....	butyl
Calcd.....	calculated
CAN.....	ceric ammonium nitrate
cat.....	catalyst
Cbz.....	benzyloxycarbonyl
conc.....	concentrated
Cp.....	cyclopentadienyl

Cy.....cyclohexyl
dba.....dibenzylideneacetone
DCNdorsal cochlear nucleus
DIPEA.....*N,N*-diisopropylethylamine
DMAP4-dimethylaminopyridine
DME.....1,2-dimethoxyethane
DMSOdimethylsulfoxide
drdiastereomeric ratio
e⁻electron
EDC.....1-ethyl-3-(3-dimethylaminopropyl)carbodiimide
eeenantiomeric excess
equiv.....equivalents
Et.....ethyl
Et₃N.....triethylamine
ETCelectron transport chain
FAD.....flavin adenine dinucleotide
FDA.....Food and Drug Administration
GSGramicidin S
HCl.....hydrochloric acid
HESI.....heated electrospray ionization
HOBt.....1-hydroxybenzotriazole
HRMShigh resolution mass spectrometry
Ipcisopinocampheyl

IR.....infrared spectroscopy
K_v7voltage-gated potassium ion channel, family 7
K_vAPvoltage-gated potassium ion channels of *aeropyrum pernix*
LC-MSliquid chromatography-mass spectrometry
Memethyl
mol.molecular
mmolmillimole
NAD.....nicotinamide adenine dinucleotide
NMRnuclear magnetic resonance spectroscopy
PPBplasma protein binding
Pd/C.....palladium on carbon
Pinpinacol
Pivtrimethylacetyl
PTSA.....*p*-toluenesulfonic acid
Q.....coenzyme Q
quant.....quantitative
ROS.....reactive oxygen species
rtroom temperature
TBATtetrabutylammonium difluorotriphenylsilicate
Tf.....trifluoromethanesulfonyl
TFA.....trifluoroacetic acid
TLCthin-layer chromatography
TMEDAtetramethylethylenediamine

UGTuridine 5'-diphospho-glucuronosyltransferase

ACKNOWLEDGEMENTS

First, I would like to thank Professor Peter Wipf for the opportunity to conduct research and my time in his research group. The never-ending emphasis on learning and understanding is a welcome sentiment and was essential to my success. Furthermore, his insistence on excellence has come to shape my understanding of how research should be conducted. I would also like to thank Professors Dennis Curran and Alexander Deiters for serving on my committee throughout my studies. The insight, helpful discussions, and guidance they provided during the composition of this document and the defense process have made this a truly fruitful experience.

I must also express immense gratitude towards the past and present members of the Wipf group, not only for the work that was completed prior to my arrival but also for the helpful discussions, both serious and not, that have made my time in Pittsburgh extremely enjoyable. In particular, I would like to thank Joseph Salamoun, Michael Frasso, John Milligan, Stephanie McCabe, Gilmar Brito, Dr. Joshua Sacher, Dr. Kara George Rosenker, Dr. Christopher Rosenker, and Dr. Raffaele Colombo for their friendship, advice, and positive outlook on life that made working long hours and weeks that much more bearable.

Last, I am extremely grateful for the continual support of my mother, father, sister, brother, and friends during my time in Pittsburgh. They always knew the right thing to say to make a bad day better. A special thank you must be made to Laura Benner who has been my biggest supporter and was with me every step of the way.

1.0 SYNTHESIS OF RETIGABINE ANALOGUES FOR THE TREATMENT OF TINNITUS

1.1 INTRODUCTION

1.1.1 Tinnitus

Tinnitus (Latin for “ringing”) is the perception of sound when no external sound¹ is present. In contrast to auditory hallucinations, which primarily manifest as voices or music, tinnitus involves buzzing, hissing, or ringing. Sound generated from within the ear, termed objective tinnitus, results in noise that is audible to others. Much more common, however, is subjective tinnitus in which sound is perceived only by the affected person and can range from barely audible to high-intensity.¹ Its subjective nature makes tinnitus very difficult to diagnose and rate in terms of severity. Due to its high prevalence around the world,² especially among military veterans,³ efforts to identify and treat the underlying causes of tinnitus have intensified in recent years. Initially thought to be a disorder affecting the cochlea, discouraging preclinical results with a variety of compounds that targeted the cochlea, combined with the development of an effective animal model of the disorder,⁴ have suggested that a central neurological mechanism is responsible for the induction and persistence of tinnitus.

A particularly difficult aspect of treating tinnitus was its ambiguous molecular origin. Tinnitus appears to have a staggering numbers of factors associated with its induction and continuation. Objective tinnitus tends to result from vascular abnormalities⁵ or spontaneous otoacoustic emissions⁶ while cochlear lesions (damage or reduced function of the cochlea) are the most obvious physical cause of subjective tinnitus. Those with tinnitus typically have cochlear dead regions⁷ or outer hair cell damage.⁸ These observations only explain the induction of tinnitus, however, and not its persistence after the initial injury.

Recently, it has been found that a homeostatic response affecting the neuronal activity of the auditory system could be responsible for compensatory auditory stimulation that leads to tinnitus.⁹ Building on previous work that identified the dorsal cochlear nucleus (DCN) as the critical component in the induction of tinnitus,¹⁰ Tzounopoulos and coworkers have described the pathogenic plasticity of $K_v7.2/3$ heteromeric potassium ion channels in the DCN as the primary mechanism of tinnitus induction. Reduction of $K_v7.2/3$ potassium channel activity was shown to increase neuronal excitability through modulation of the resting membrane potential, the action potential threshold, the membrane potential spike that occurs after depolarization, and subthreshold excitability.¹¹ In particular, reduced K_v7 ion channel activity prevents the termination of action potentials, leading to simulated auditory input (i.e. tinnitus).

In spite of intense research to identify and understand the underlying causes of tinnitus, there is currently no standard therapy or treatment. Most treatments aim to alleviate symptoms or related abnormalities. In addition to behavioral¹² and sound therapy,¹³ hearing aids have been used to compensate for decreased input in the impaired frequency range.¹⁴ These therapies are limited to those with hearing loss and cannot be used in the high frequency range. The use of

cochlear implants to restore input to the auditory system¹⁵ has also been shown to be effective in patients that exhibit bilateral sensorineural hearing loss.

Pharmaceutical research has thus far resulted in no approved drugs in either the United States or Europe for the treatment of tinnitus. The analgesic lidocaine has been shown to have transiently effective properties in the treatment of tinnitus when administered intravenously¹⁶ and for those patients with psychiatric disorders and tinnitus, carbamazepine has regularly been prescribed as a dual treatment in spite of studies showing a negligible benefit when compared with placebo (figure 1).¹⁷ With a stunning lack of options for those affected by tinnitus, examination of compounds that modulate K_v7 ion channel activity could lead to the development of an effective treatment.



Figure 1. Structures of Lidocaine and Carbamazepine

1.1.2 K_v7 Potassium Ion Channels

Early work in the area of ion channels by Hodgkin and Huxley, who were able to derive a rigorous mathematical treatment of action potential initiation and propagation by likening the event to an electrical circuit, led to the 1963 Nobel Prize in Physiology and Medicine.¹⁸ Since that seminal work, significant efforts have been made to elucidate the mechanistic and structural features of specific types of ion channels¹⁹ (which resulted in the 2003 Nobel Prize in Chemistry) including voltage-gated potassium ion channels. Unlike sodium and calcium ion channels, which have pore-forming proteins primarily derived from one gene, the subunits of potassium ion

channels are encoded by separate genes and then assemble on various membranes to form ion channels.²⁰ Subunits from different families of voltage-gated potassium ion channels can also combine to create biologically relevant ion channels,^{21,22} and, because of this heterogeneity, potassium ion channels serve a multitude of functions. Voltage-gated potassium ion channels (K_v ion channels) have 12 subfamilies distinguished by their amino acid sequence (abbreviated with $K_vX.Y$ nomenclature, where X is the family and Y, the specific family member) and almost exclusively terminate action potentials in neurons.

Structurally, K_v ion channels in vertebrates are comprised of four α -subunits that each contain six transmembrane helices (figure 2, S1-S6).²³ Helices 1 to 3 arrange around the periphery of the ion channel and are joined by a conformationally flexible voltage sensing domain (S4) that responds to changes in the membrane potential.²⁴ In particular, the S3 and S4 domains form a hydrophobic helix-turn-helix structure that excludes several arginine residues (figure 2, indicated in green) and constitutes the voltage sensor paddle. This structure, in light of contradictory electrochemical data,²⁵ is thought to be conformationally flexible, allowing the voltage paddle to move freely around the outer edge of the ion channel. The S5 and S6 domains form the lining of the pore domain through which potassium ions flow with the S6 domain forming the inner lining. Opening and closing of the pore domain is controlled by a glycine-gating hinge that was identified through analysis of crystal structures of open and closed bacterial potassium ion channels.²⁶ The two domains maintain a roughly antiparallel alignment, indicating that the opening of the pore may occur by pulling the S5 helix away causing the S6 helix to follow.

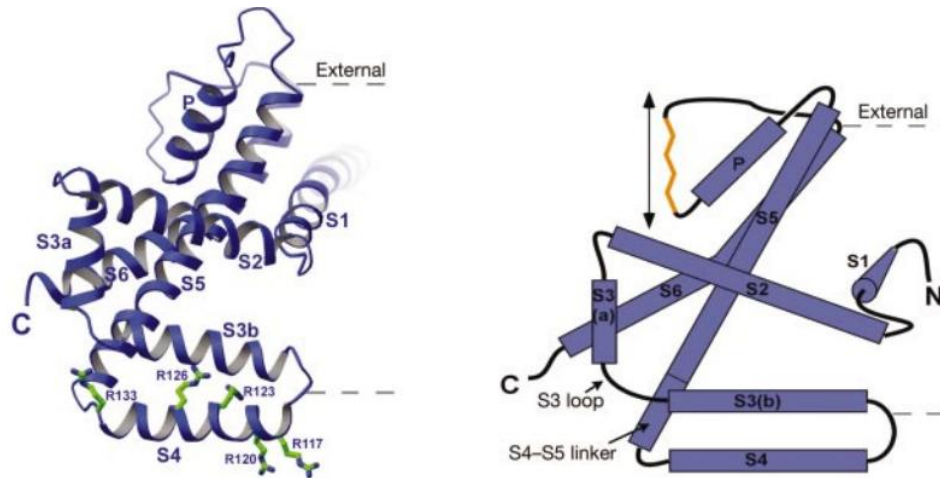


Figure 2. Structure of K_v AP Voltage-Gated Potassium Ion Channel α -Subunit showing Pauling-Corey-Branson Helix (left) and Cartoon (right) Representations.²³ Reproduced with permission from Ref. 23.

The macrostructure of the K_v ion channel is comprised of four subunits arranged around a water-filled pore helix in a “teepee” structure that is in accordance with previously characterized bacterial ion channels and was confirmed by X-ray diffraction of crystallized K_v AP ion channels from the extremophile *aeropyrum pernix* (figure 3).²³ The high potassium ion selectivity is due to a signature sequence in the S6 domain that lines most of the pore helix, allowing for solvation of dehydrated potassium ions by the backbone carbonyl groups while excluding sodium or calcium ion on the basis of their size.²⁷ The path through the pore itself is not a uniform structure, ranging from 3 Å at its narrowest to 15 Å at its widest and becomes a water-filled cavity half-way through. Travel through the channels is controlled primarily through concentration gradients along the cell membrane and the channel itself which closes due to fluctuations in the membrane potential.

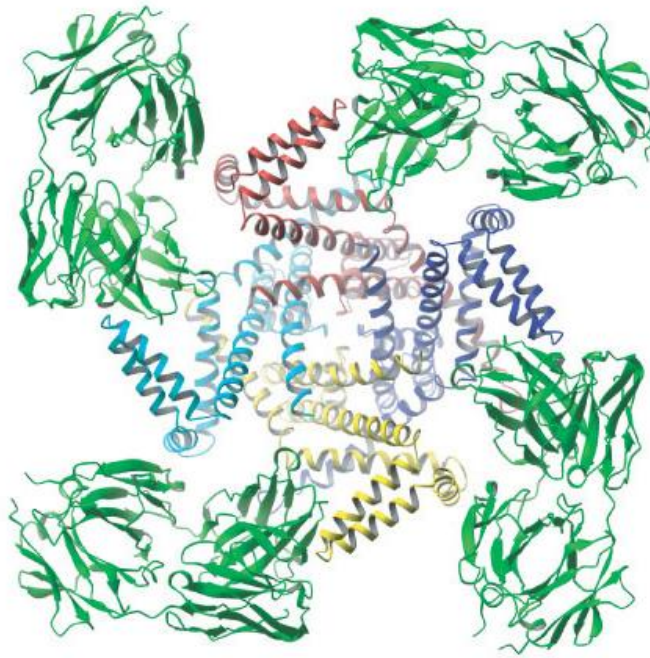


Figure 3. Structure of the K_v AP Potassium Ion Channel. ²³ Reproduced with permission from Ref. 23.

KCNQ genes encode for the five members of the K_v7 family of potassium channel subunits. In the nervous system, $K_v7.2$ to $K_v7.5$ form the α -subunits of the low-threshold voltage-gated potassium channel²⁸ and most channels are comprised of $K_v7.2$ and $K_v7.3$ heteromeric²⁹ or $K_v7.2$ homomeric subunits.³⁰ These types of channels activate at subthreshold potentials and do not inactivate, providing a steady current that serves to stabilize the membrane potential and prevents burst-firing of neurons. Because of their central role in modulating neuronal excitability, mutation of K_v7 ion channels has been associated with several disorders. Mutation of $K_v7.1$, for example, can lead to several different inherited arrhythmias including long QT syndrome.³¹ Thus, it should not be surprising that recent studies by Tzounopoulos and coworkers have implicated reduced $K_v7.2/3$ potassium ion channel activity in fusiform cells of the dorsal cochlear nucleus as a potential cause of tinnitus.¹¹ Moreover, a recently approved drug for the treatment of partial-onset seizures, retigabine, is known to activate K_v7 ion channels.

1.1.3 Retigabine: Development and Drug Profile

Retigabine traces its origins to flupirtine, a structurally-related analgesic that derives its effectiveness through activation of K_v7 potassium ion channels. This mechanism of action is now thought to be responsible for the variety of beneficial effects that have been observed for flupirtine including anticonvulsant,³² neuroprotective,³³ and antiparkinsonian³⁴ activity. A large number of compounds were developed by Asta Medica (now Viatris) that resulted in the deazaflupirtine derivative D-20443 (retigabine, **1-1**) which was extensively studied.³⁵

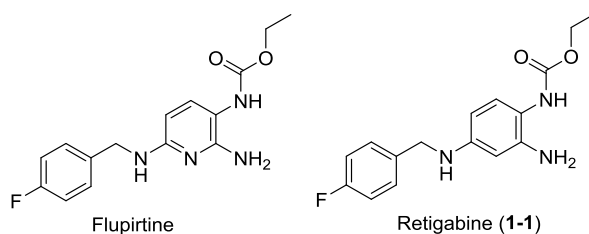


Figure 4. Structures of Flupirtine and Retigabine (**1-1**)

Early studies showed retigabine to have a broad spectrum of activity in animals models of epilepsy.³⁶ The mechanism of action was later shown to involve the opening of neuronal potassium ion channels, specifically $K_v7.2-5$ ion channels.³⁷ A combination of electrochemical and site-directed mutagenesis experiments have determined that retigabine acts as a positive allosteric modulator of $K_v7.2-5$ with some selectivity for opening $K_v7.2/3$ heteromeric dimers over other subunit combinations. This action controls neuronal excitability through hyperpolarization of the membrane, leading to reduced epileptic susceptibility.³⁸ In addition, other ion channel and receptor families show no significant activity until high concentrations of the compound are reached,³⁷ highlighting retigabine's high selectivity. The active site of the K_v7

ion channel has been deduced primarily on the basis of site-directed mutagenesis and electrochemical experiments³⁹ which have identified crucial tryptophan, threonine, and leucine residues (figure 5). The active site of K_v7.3 was then modeled with bound retigabine using a homology model derived from a K_v7.1 ion channel X-ray structure. Given the location of the active site, retigabine likely does not alter the voltage sensing properties of the channel, instead stabilizing the open conformation of the ion channel through the S5 and S6 domains.

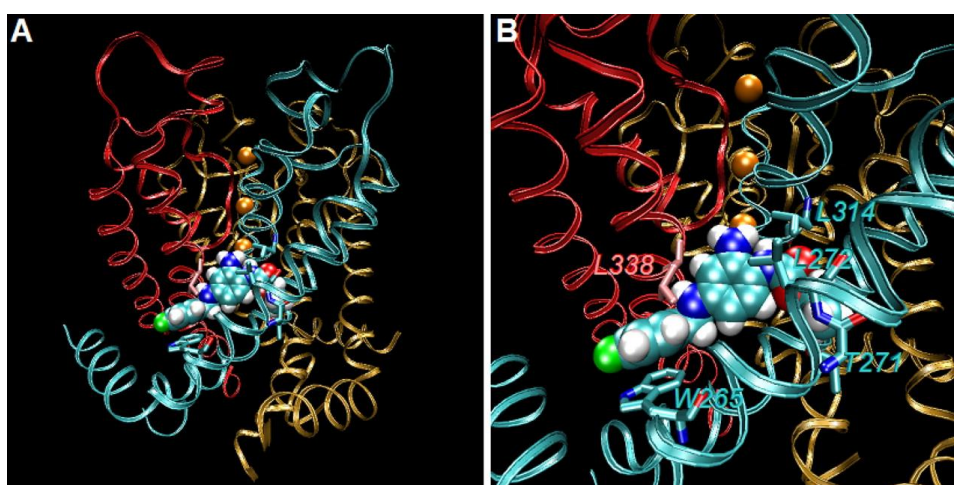
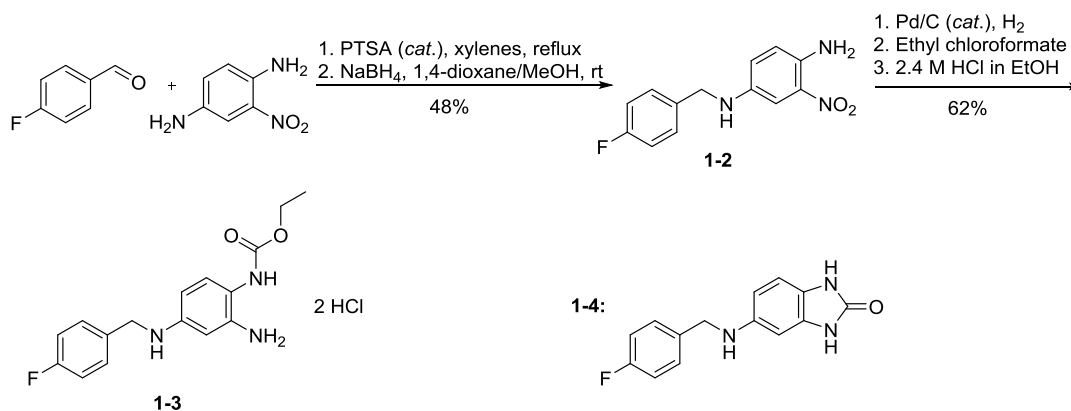


Figure 5. Proposed Binding Site of Retigabine: A) Three-Dimensional Model of Retigabine Docked to the Active Site of a K_v7.3 Domain and B) Crucial Amino Acid Residue Interactions.³⁹ Adapted with permission from Ref. 39.

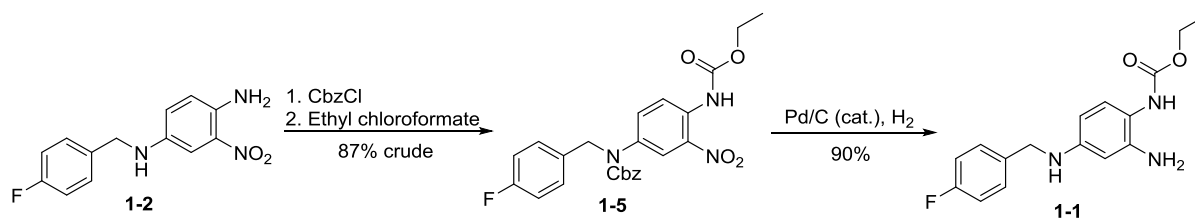
Based on favorable animal studies and preclinical studies, retigabine entered clinic trials in the early 2000s (after being licensed to several different pharmaceutical companies throughout the 1990s) and was found to reduce the frequency of seizures by 23 to 35% versus placebo with the most common side effects being dizziness, confusion, and slurred speech.⁴⁰ Retigabine was approved by the FDA in 2010 under the name Potiga™, and has been consistently prescribed for partial-onset seizures.

Retigabine and related analogues are available via several short synthetic routes. Reductive amination of 2-nitro-*p*-phenylenediamine and 4-fluorobenzaldehyde gives diamine **1-2** in modest yield (scheme 1). A three-step sequence beginning with catalytic hydrogenation, treatment with ethyl chloroformate to give **1-1**, and addition of ethanolic HCl gives retigabine as dihydrochloride salt **1-3** in 62% yield.⁴¹ Simple purification of the final compound makes this method advantageous for gram-scale synthesis, but **1-3** is unstable and converts to cyclic urea **1-4** when stored for long periods of time, even at -20 °C.⁴²



Scheme 1. Synthesis of Retigabine Dihydrochloride

Selective carbamoylation of the diamine derived from **1-2** with ethyl chloroformate required slow addition of the chloroformate to minimize formation of bis-ethyl carbamate byproducts. A second route utilizing the carbobenzyloxy (Cbz) protecting group was devised to avoid this problem (scheme 2).⁴³ Intermediate **1-2** was protected with CbzCl and DIPEA and then carbamoylation using ethyl chloroformate gave **1-3** in good yield without the need for purification. Subsequent cleavage of the Cbz protecting group and reduction of the nitro group using Pd/C and H₂ gave retigabine (**1-1**) on gram-scale and in excellent overall yield.



Scheme 2. Synthesis of Retigabine Avoiding Polycarbamylation

Several studies to determine the pharmacokinetic parameters of retigabine have been performed.⁴⁴ Retigabine is rapidly absorbed and distributed with an oral bioavailability of 60% and a volume of distribution around 6.2 L/kg, reflecting its relatively high plasma protein binding (80%).⁴⁵ Retigabine achieves a maximum concentration between 600-800 ng/mL in 1.5-2 hours and has a half-life of approximately 8 to 10 hours.⁴⁶ Patients typically receive doses of the compound two to three times daily which, when adjusted for plasma protein binding, results in a free concentration in plasma and the brain (due to its ability to easily cross the blood-brain barrier) near 1 μM .⁴⁷

Retigabine is resistant to first-pass metabolism, being metabolized primarily via hepatic glucuronidation and acetylation at the N-2 and N-4 positions (figure 6), with the N2 position being preferred.⁴⁸ UGT1A1 and UGT1A4 appear to be the primary glucuronosyltransferases that affect retigabine and a constant ratio between the decay of retigabine and its main metabolite has been found, suggesting the two compounds may be linked through enterohepatic circulation and a glucuronidation cycle.⁴⁸ This is beneficial because glucuronidation via multiple UGT enzymes is a well-protected process, even in patients with a wide variety of hepatic diseases. Due to slow UGT formation in the liver, however, this treatment is unlikely to be useful in very young children. Retigabine also exhibits a moderate dependence on gender⁴⁵ and race⁴⁹ in terms of efficacy and metabolism, respectively. Excretion of retigabine occurs renally, with roughly 84%

of the compound being recoverable as either the parent or a major metabolite when using ^{14}C -labelled compound.⁵⁰

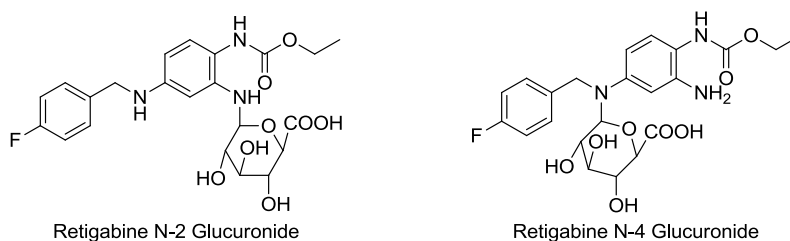


Figure 6. Major Metabolites of Retigabine

1.2 RESULTS AND DISCUSSION

1.2.1 Analogue Design

Structure-activity-relationship information for retigabine has been slow to appear⁵¹ and so far limited data has been reported for $\text{K}_{\text{v}7.2/3}$ ion channels. Several patents have been published that report a variety of structures but are target multiple disease states and with limited evaluation of biological properties.⁵² Valeant pharmaceuticals reported several 4-(*N*-azacycloalkyl)anilide derivatives that were found to be potent $\text{K}_{\text{v}7.2/3}$ activators with EC_{50} values ranging from 1-500 nM (figure 7).⁵³ The most important features were substitutions at both *ortho* positions around the carbamate, steric restriction of the benzyl amine as part of a tetrahydroisoquinoline ring, and replacement of the ethyl carbamate with a *neo*-pentyl amide. Several small groups were tolerated *ortho* to the carbamate (figure 7, R_1) with methyl, methoxy, trifluoromethyl, and trifluoromethoxy substitution at both R_1 and R_2 leading to increased activity.

In addition, substitution of the tetrahydroisoquinoline ring was tolerated as well with fluorinated functional groups (F, CF₃) in the 6 or 7 position being most potent (figure 7, R).

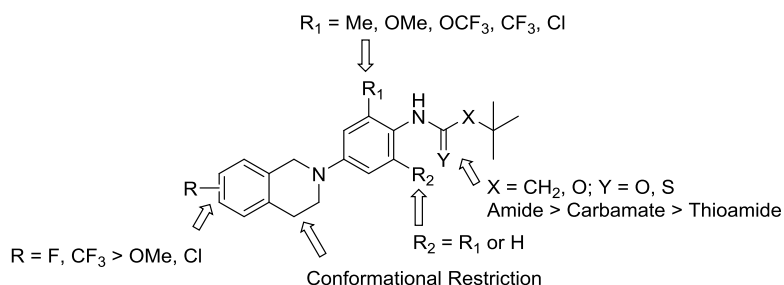
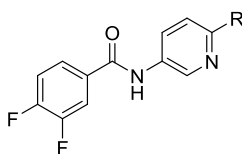


Figure 7. 4-(N-Azacycloalkyl)anilide Derivatives for the Modulation of K_v7.2/3 Activity

Icagen has also disclosed inhibitors that are structurally related to retigabine through elimination of two aniline nitrogen atoms from the core phenyl ring.⁵⁴ Further replacement of the benzyl amine with an amide linkage resulted in compounds that had similar activity to retigabine (table 1). Substituting the 2-position of the pyridine ring led to enhanced selectivity for K_v7.2/3 channels compared to other heteromeric and dimeric channels although these compounds were also active towards K_v7.1 indicating an altered mechanism of action. Indeed, it was determined that these compounds do not bind to the S5 and S6 domain as retigabine does, indicating that the aryl diamine core is a necessary component of the structure.

Table 1. *N*-(6-Substituted-pyridin-3-yl)-3,4-difluorobenzamide Derivatives as $K_v7.2/3$ Activators

Entry	R	$K_v7.2/3$ EC ₅₀ (μ M)
1	F	4.8
2	Me	6.8
3	OMe	>10
4	CF ₃	>10
5	Cl	0.38
6	OH	>10
7	NH-cyclopropyl	2.7
8	pyrrolidin-1-yl	0.48

The groups of Nan and Gao have described the synthesis of bis-*N*-acylated retigabine derivatives that selectively inhibit $K_v7.2$ ion channels.⁵⁵ Inhibition of $K_v7.2$ ion channels could be achieved at 100 nM by substituting various alkyl and allyl chains of medium length (*n*-propyl, 1,1-disubstituted allyl) at *N*-4 and an ethyl carbamate at *N*-2. Substitution at *N*-2 or *N*-4 alone leads to a loss of inhibitory activity for $K_v7.2$ but it is unknown whether the compounds activate the channels once more. $K_v7.2/3$ potassium ion channels were not evaluated but it would be reasonable to suspect that heteromeric channels comprised of $K_v7.2$ subunits would also be inhibited.

With regards to retigabine, several trends can be identified (figure 8) based on this literature precedent. First, simultaneous substitution of both aniline nitrogen atoms is not tolerated. Substitution *ortho* to the ethyl carbamate is tolerated well as long as both positions are substituted as is replacement of the ethyl carbamate with sterically-hindered amides. The 4-fluorophenyl ring can be substituted with a variety of functional groups but fluorinated functional groups tend to give greater potency compared to other heteroatoms. The benzyl

amine can be conformationally constrained within a ring and might lead to greater potency by itself but substitution of the benzyl amine for an amide may result in an altered mechanism of action. Replacement of the aryl diamine core with pyridine was also not tolerated.

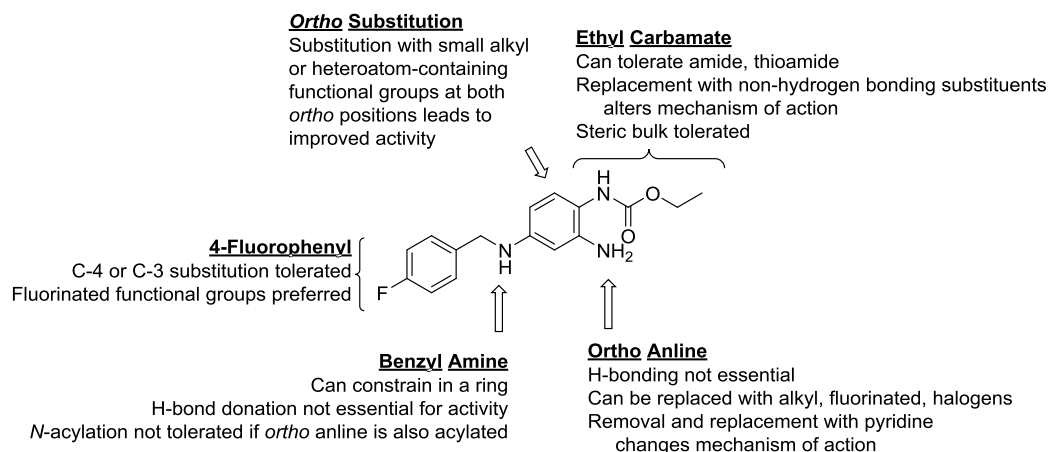


Figure 8. Structure-Activity-Relationship of Retigabine

The binding pocket of retigabine has been shown to contain a crucial tryptophan residue (figure 5, figure 9).³⁹ Several leucine residues and a threonine residue also comprise the currently known binding site, although the exact shape and structure are unknown in the absence of crystallographic data. The initial analogue design focused on altering two different sites on retigabine: first, the fluorophenyl functionality in zone 1 which targets the crucial tryptophan residue and second, the carbamate functionality in zone 2 (figure 10) which likely sits in a hydrophobic pocket in the active site but may also have a hydrogen-bonding interaction with T271. The fluorophenyl functionality allows for the incorporation of several different aromatic and heteroaromatic structures with varying degrees of fluorination, in accord with the Wipf group's keen interest in the selective incorporation of fluorine and fluorine-containing functional groups to natural products, peptides, and bioactive molecules.⁵⁶ The second site of alteration

allows for the use of methodology previously utilized in the Wipf group⁵⁷ to introduce several highly functionalized carbamates including those derived from the bis-oxetane sulfoxide, MMS-350 (figure 12, **1-13**),⁵⁸ and 3-methyl-3-oxetanemethanol.⁵⁹

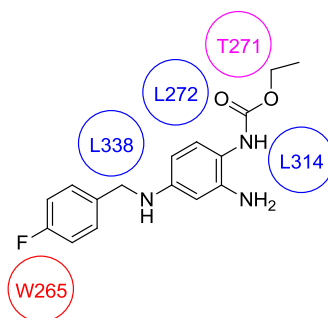


Figure 9. 2-Dimensional Representation of the Active Site of Retigabine (red = π - π stacking interaction, blue = hydrophobic interaction, magenta = hydrogen-bonding interaction)

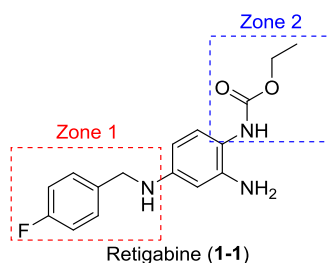


Figure 10. Structure of Retigabine and Regions of Modification

Fluorine has been commonly employed as a bioisosteric replacement for the hydrogen atom due to its chemical inertness, ability to modulate pharmacokinetic parameters like pK_a and lipophilicity, and increased metabolic stability relative to hydrogen.⁶⁰ Higher order fluorinated functional groups like the trifluoromethyl- and pentafluorothio- (SF_5) groups have also been used when a bulkier, more strongly electron-withdrawing functional group is wanted. In particular, the SF_5 group is rarely used in the synthesis of bioactive compounds despite its ability to greatly

increase lipophilicity and decrease metabolism across several atoms due to its difficulty of synthesis.⁶¹ Previous studies in the Wipf group have shown that selective incorporation of higher order fluorinated functional groups (CF₃ and SF₅) in bioactive molecules like Gramicidin S and Mefloquine can lead to improved peptide mimicry, potency, and selectivity.^{56a, 56b}

It was envisioned that trifluoromethyl- (**1-5** and **1-6**) and pentafluorothiophenyl analogues (**1-7** and **1-8**), as well as thiophene (**1-11**) and thiazole analogues (**1-12**) would allow us to probe the structure-activity relationship of retigabine. A thorough analysis of the fluorinated benzene derivatives might reveal an electronic or steric requirement in the active site binding region of retigabine. In addition, reports of SF₅-containing compounds (**1-5** and **1-6**) are relatively scarce, especially in the context of bioactive analogues. Thiophene is a typical benzene isostere and maintains roughly the same steric bulk and planar structure while being more electron-rich and polar, resulting in a lower logP value. This could result in enhanced aqueous solubility. The thiazole substitution has all of the above benefits as well as an additional nitrogen atom that could participate in hydrogen-bonding interactions with nearby donors, complementing the crucial π - π interaction of tryptophan-265 (figure 9) and leading to enhanced selectivity. Additionally, alteration of the benzylic position (**1-9** and **1-10**) would allow for manipulation of the adjacent nitrogen atom by decreasing its basicity via inductive withdrawal or steric blocking. The first pK_a of retigabine as the free base has been calculated to be 13.1 at the *N*-2 position,⁶² a primary site of glucuronidation. Decreasing the basicity of the secondary aniline could decrease clearance of the compound.

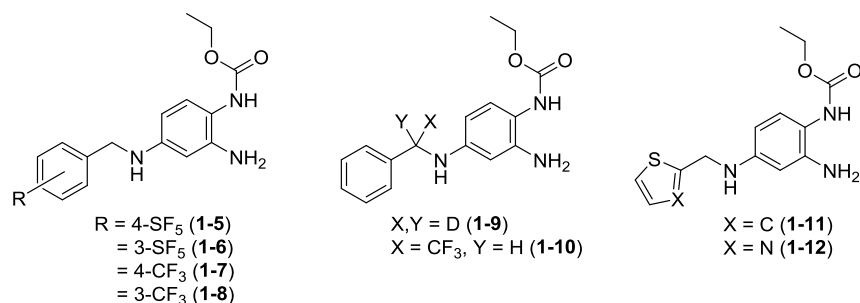


Figure 11. Examples of Fluorinated and Heterocyclic Retigabine Analogues

Alteration of zone 2 (figure 10) had a more focused set of objectives. Of particular interest to us were the isopropyl, MMS-350, and 3-methyloxetanemethanol derived carbamates. The isopropyl carbamate would function to probe the steric requirements around the core diamine. MMS-350 (**1-13**) has gained attention as a method of combating radiation exposure⁶³ and as an additive to increase the aqueous solubility of small organic molecules (figure 12).⁵⁸ More recently, the Wipf group demonstrated its ability to enhance the solubility of bioactive molecules through covalent attachment.⁵⁷ The covalently modified compounds showed increased solubility and membrane permeability. Retigabine itself is very insoluble in aqueous solution (calculated to be 45 mg/L)⁶² with the hydrochloride salt being only sparingly soluble as well.⁶⁴ Given the hydrochloride salt's instability towards long-term storage,⁴² it was envisioned that a covalently modified MMS-350 derivative of retigabine (**1-14**) could impart aqueous solubility without negatively impacting stability (figure 12). In the same vein, covalently linking 3-oxetanemethanol (**1-15**) could improve aqueous solubility and has the potential for additional hydrogen bond interactions.

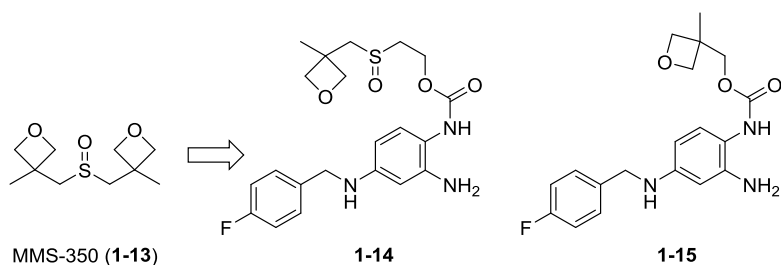
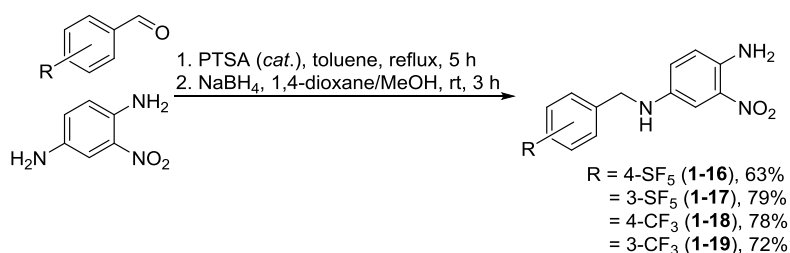


Figure 12. Covalently modified MMS-350 and 3-Methyl-3-oxetanemethanol Retigabine Analogues

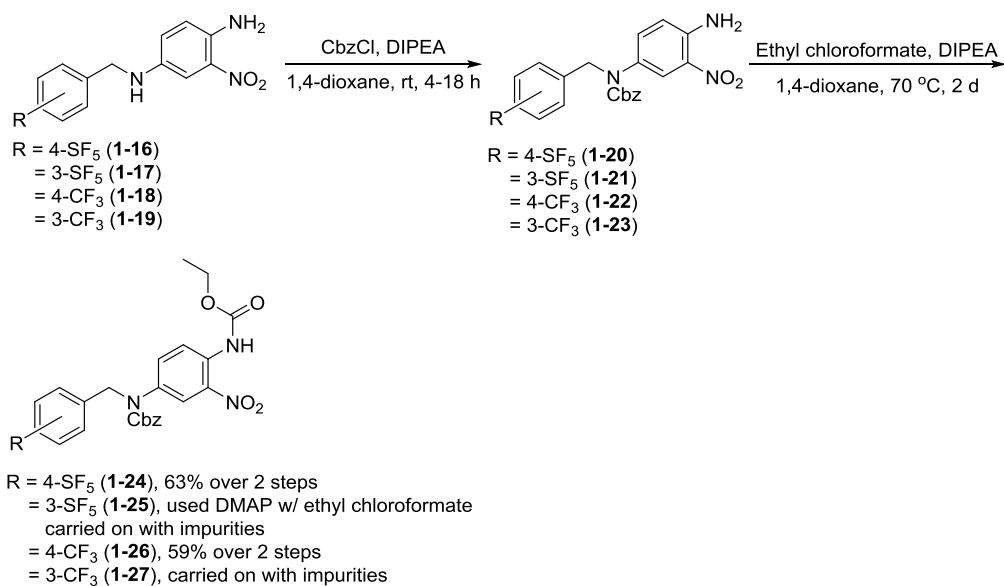
1.2.2 Analogue Synthesis

With the first set of analogues determined, initial synthetic efforts focused on synthesizing the fluorinated benzene derivatives of Retigabine. Polycarbamylation was anticipated to be a problem, therefore, protection of the secondary amine with CbzCl was seen as a preferable approach to access the desired compounds. Condensation under Dean-Stark conditions in toluene and subsequent reduction of the intermediate imines with sodium borohydride furnished diamines **1-16** to **1-19** in good yield (scheme 3). Severe streaking during chromatography even on Et₃N deactivated SiO₂ resulted in decreased isolated yields of **1-16** and necessitated purification of the intermediate imine before reduction with NaBH₄. This was accomplished by filtration through a small pad of SiO₂ and removal of the residual solvent.



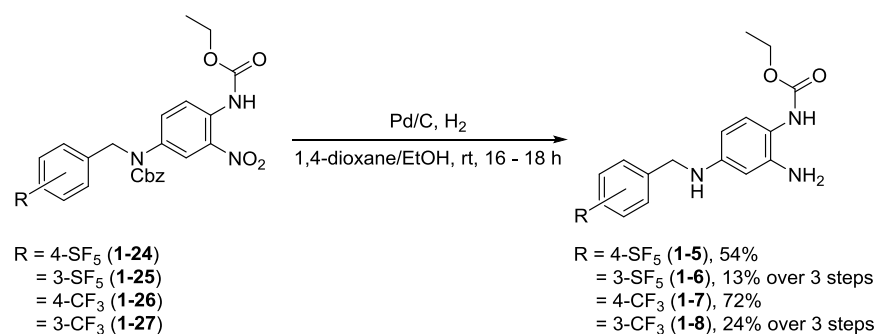
Scheme 3. Reductive Amination of 2-Nitro-*p*-phenylenediamine with Fluorinated Benzaldehydes

Protection of the secondary amine of **1-16** with CbzCl and DIPEA proceeds readily at room temperature (scheme 4). Isolation of Cbz-protected amine **1-20** proved difficult due to streaking during chromatography on SiO₂, thus crude **1-20** was treated with ethyl chloroformate and DIPEA in 1,4-dioxane to give **1-24**. Initial attempts to form the desired ethyl carbamate using a single equivalent of ethyl chloroformate did not proceed to completion even after heating and gave low yields of **1-24**. The reaction also appeared to stall after 48 hours with significant amounts of **1-20** remaining. Several equivalents of ethyl chloroformate (2-5 equiv.) and DIPEA (2-5 equiv.), elevated temperatures, and extended reaction times were needed to achieve synthetically useful yields of **1-24**. Compounds **1-25**, **1-26**, and **1-27** were synthesized in a similar sequence. The low reactivity of the aniline was attributed to the presence of an *ortho*-nitro group as well as the electron deficient nature of the core aromatic ring overall. In addition, the 3-substituted phenyl derivatives (**1-25** and **1-27**) gave products that could not be purified by chromatography on SiO₂ due to inseparable byproducts resulting from polycarbamylation.



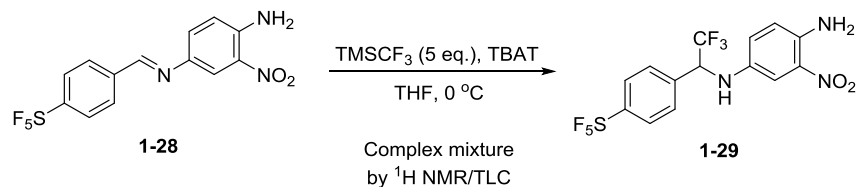
Scheme 4. Protection and Carbamylation of Reductive Amination Products

All attempts to increase the effectiveness of the reaction using N-methyl amines (DMAP) or NaH as the base failed to give increased yields. By ¹H NMR analysis, the primary byproduct appeared to be polycarbamoylated compounds resulting from unreacted starting material in the protection step (several quartet-triplet pairs indicating ethyl groups were present). Hydrogenolysis of the Cbz group and reduction of the nitro group were accomplished using Pd/C and H₂ to give **1-5** to **1-8** in good yields (scheme 5). The 3-substituted phenyl derivatives gave decreased yields over the 3 step sequence due to low conversion in the protection step. This resulted in more residual starting material (**1-17** or **1-19**) that could give polycarbamoylated side products when treated with ethyl chloroformate.



Scheme 5. Reduction and Cleavage of Cbz Protecting Group Using Catalytic Hydrogenation

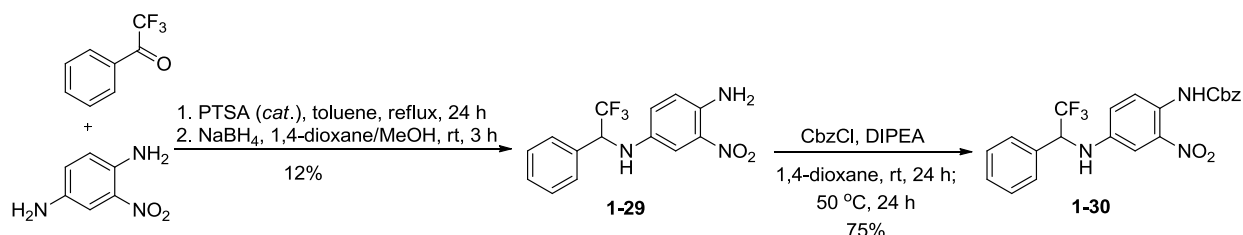
Compound **1-10** could be envisioned to arise from addition of trifluoromethyl anion (derived from the Ruppert-Prakash reagent and a fluoride source) into an electron deficient imine like **1-28** (itself obtained by condensation of 4-pentafluorothiobenzaldehyde and 2-nitro-*p*-phenylenediamine in 64% yield). These attempts were met with failure. Conditions known to add trifluoromethyl anion into electrophilic imines under acidic conditions⁶⁵ gave only recovered starting material or complex mixtures by LC-MS and ¹H NMR (scheme 6). In light of these difficulties, the previously described reductive amination strategy was used to access compound **1-29**.



Scheme 6. Attempted Nucleophilic Trifluoromethylation of Pentafluorosulfanylimine **1-28**

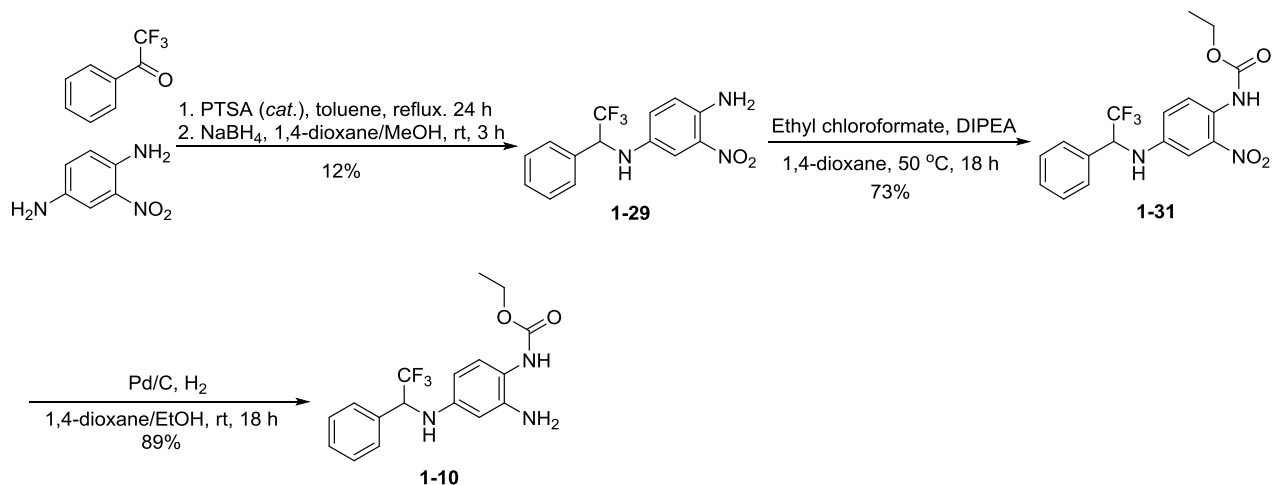
Reductive amination of 2,2,2-trifluoroacetophenone and 2-nitro-*p*-phenylenediamine under Dean-Stark conditions in toluene lead to poor conversion and isolated yields (*ca.* 12%) of **1-29** (Scheme 7) with significant quantities of residual starting material even after extended

reaction times. Comparable yields were obtained utilizing a procedure promoted by $\text{AlMe}_3/\text{BH}_3\cdot\text{SMe}_2$ ⁶⁶ and no product was observed using molecular sieves at room temperature. Attempted protection of the secondary aromatic amine of **1-29** resulted in the incorrect regioisomer **1-30** in 75% yield. This serendipitous result indicated that the trifluoromethyl group inductively deactivated the adjacent amine enough to do away with the use of a protecting group.



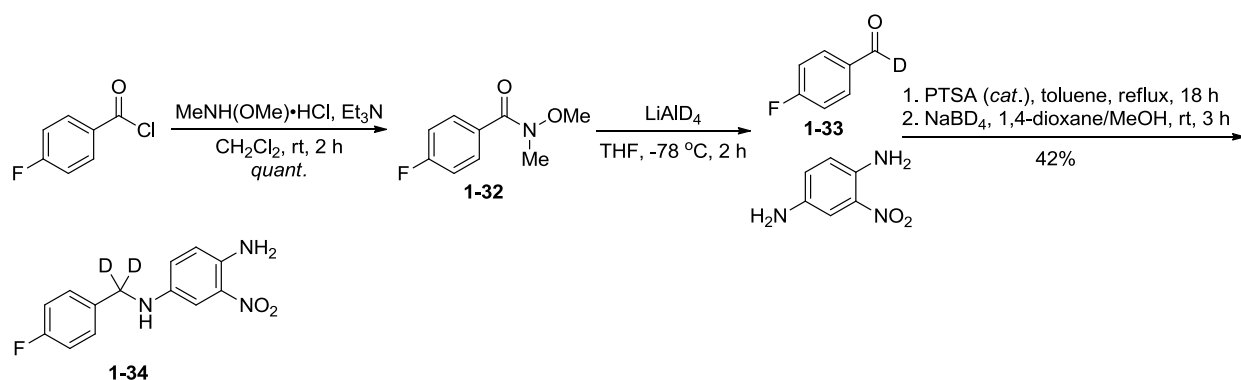
Scheme 7. Reductive Amination and Protection Affording Regioisomer **1-30**

Thus, treatment of **1-29** with ethyl chloroformate at room temperature for 24 h and then at 50 °C for a further 24 h gave ethyl carbamate **1-31** in 73% yield (scheme 8). Subsequent reduction with Pd/C and H_2 proceeded in excellent yield to give **1-10**.



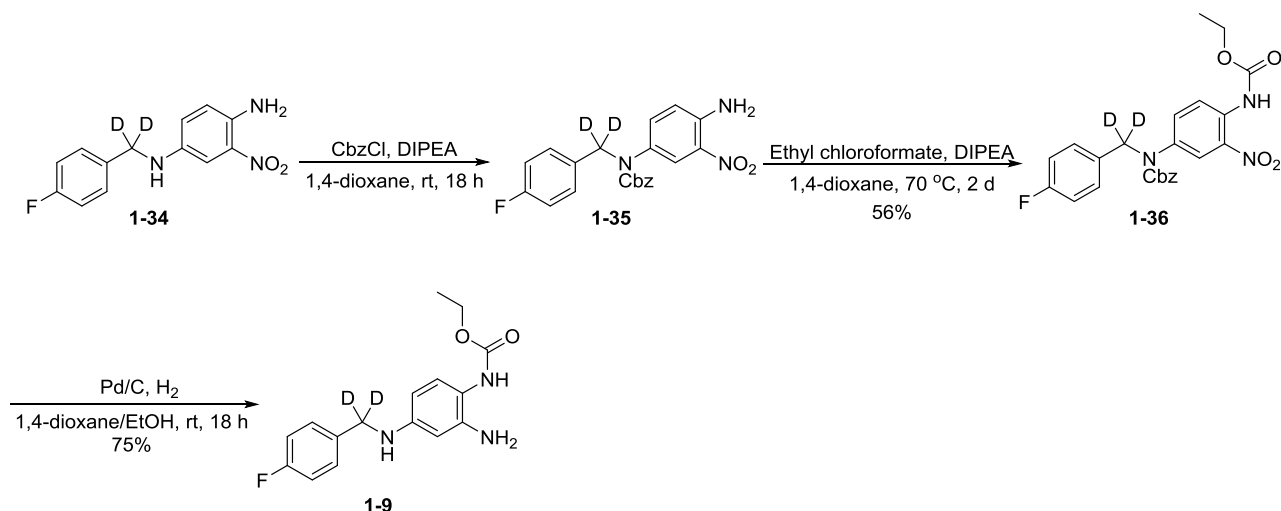
Scheme 8. Carbamylation and Catalytic Hydrogenation of **1-29**

Deuterated analogue **1-9** required the synthesis of deuterated benzaldehyde **1-33**, which commenced with formation of Weinreb amide **1-32**⁶⁷ in quantitative yield (Scheme 9). Reduction using LiAlD₄ gave **1-33** which was subjected as a crude mixture to the previously described reductive amination conditions using NaBD₄ to give **1-34** in a moderate 42% yield over 2 steps. Attempts to isolate **1-33** proved difficult due to volatility.



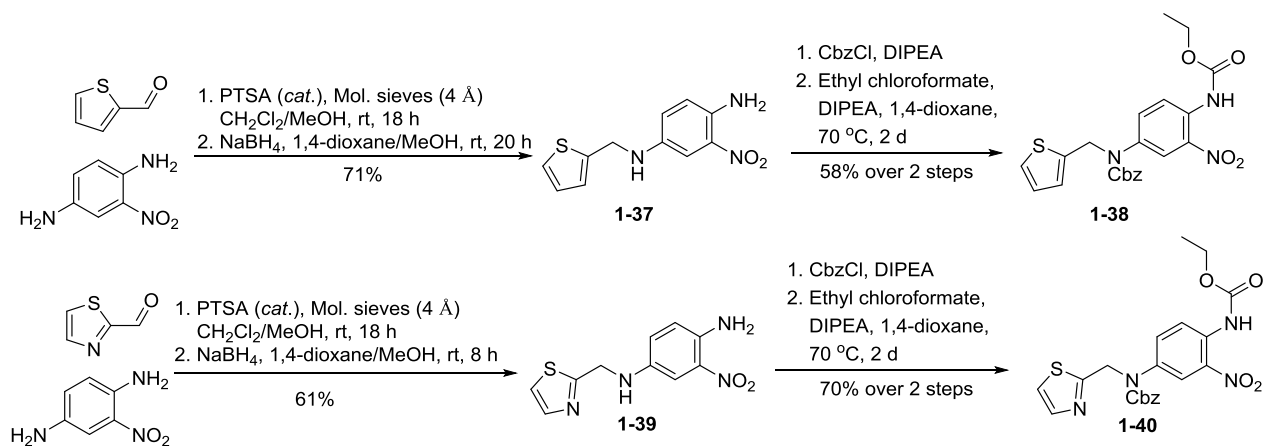
Scheme 9. Synthesis of Deuterated Reductive Amination Product **1-34**

Protection and carbamoylation proceeded in comparable yield (56%) to previously prepared analogues to give **1-36**. Reduction of the nitro group and cleavage of the Cbz protecting group using Pd/C and H₂ gave the desired deuterated analogue **1-9** in 75% yield (scheme 10).



Scheme 10. Synthesis of Deuterium-Labelled Retigabine

The final compounds to be made with alterations in zone 1 incorporated heteroaromatic structures. Reductive amination using the previously described conditions (PTSA, toluene, reflux) gave impure material in diminished yield due to unknown side reactions. Purification was also complicated by the increased polarity of the heteroaromatic rings. A new reductive amination procedure employing molecular sieves was adapted from a previously reported procedure.⁶⁸ Use of molecular sieves and PTSA as a catalyst at room temperature allowed for the isolation of diamines **1-37** and **1-39** in 71% and 61% yield, respectively (scheme 11) without the need for column chromatography. Interestingly, **1-37** seemed to form a 1:1 mixture with the intermediate imine during reduction with NaBH_4 and required prolonged reaction times to proceed to completion. Protection and treatment with ethyl chloroformate gave ethyl carbamates **1-38** and **1-40** in good yield over 2 steps.

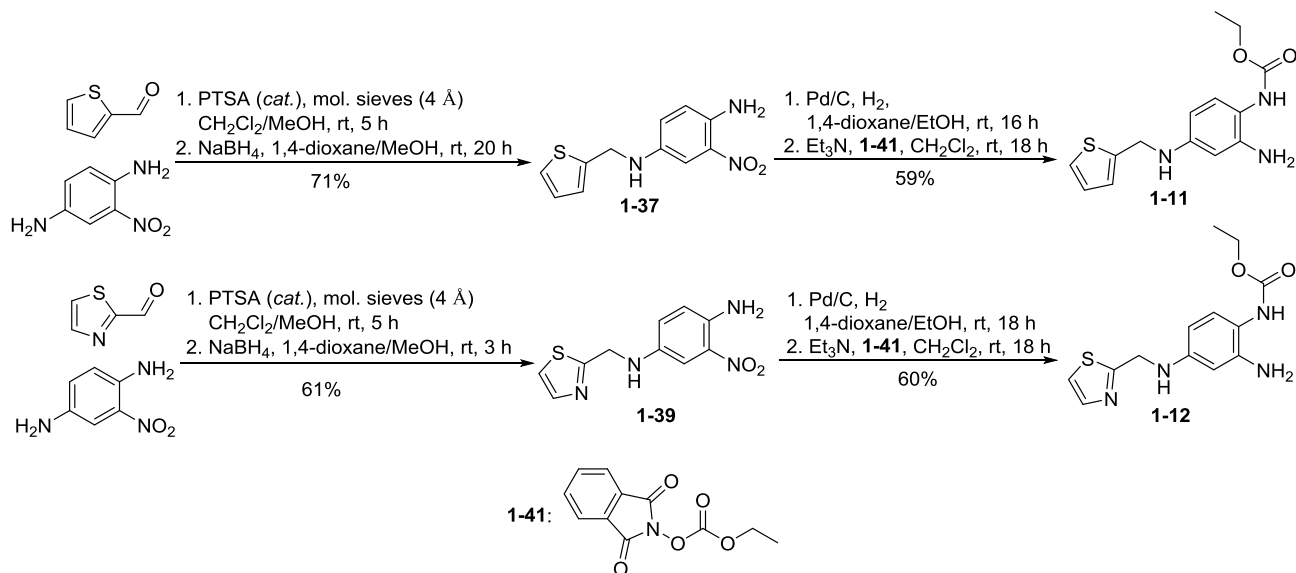


Scheme 11. Initial Attempts towards Heterocyclic Analogues of Retigabine

Reduction of the nitro group of **1-40** or its thiophene counterpart was easily accomplished using Pd/C and H₂, but removal of the Cbz group and isolation of the desired compounds could not be realized under a variety of conditions including high pressure and temperature catalytic hydrogenation, transfer hydrogenation, and strongly acidic conditions. Strongly acidic conditions using HBr in AcOH resulted in intramolecular condensation leading to a cyclic urea that coeluted by TLC with the desired product. Reversing the reaction order (cleavage of the Cbz group followed by reduction of the nitro group with Pd/C) did not afford desired product **1-12** in pure form or acceptable yields either.

A revised route was obviously needed. Eschewing the use of a protecting group, reduction of the nitro group of **1-37** or **1-39** leading to an aryl triamine followed by treatment with an attenuated ethyl chloroformate equivalent could lead to the desired compounds without polycarbamylation. Previous studies in the Wipf group involving MMS-350 had utilized mixed phthalimidyl carbonates and observed that they react readily with aromatic amines to give covalently linked MMS-350 derived carbamates.⁵⁷ Similar reagents have also been shown to be effective carbamoylating agents.⁶⁹ Reduction of the nitro group of **1-37** and **1-39** using Pd/C and

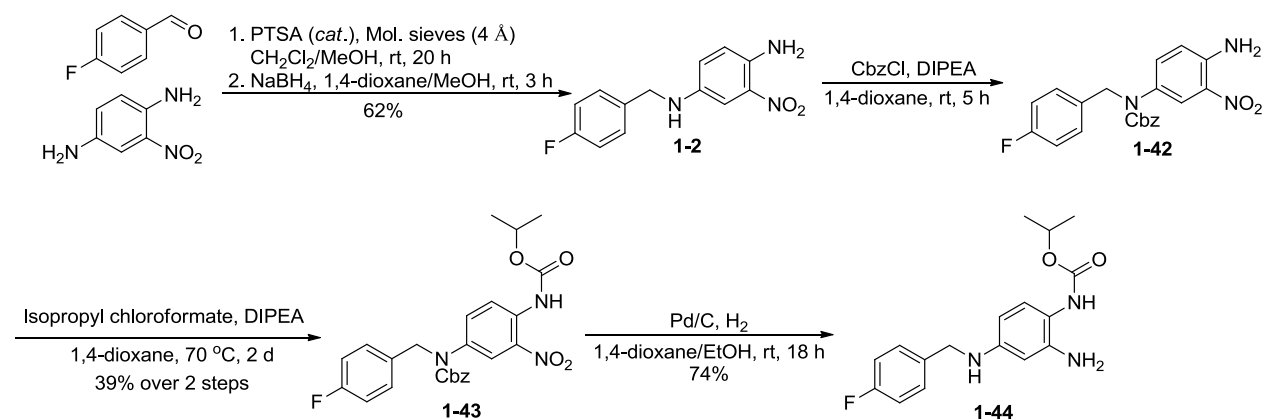
H₂ and subsequent reaction with mixed phthalidimidyl carbonate **1-41** and Et₃N in CH₂Cl₂ gave the desired heterocyclic analogues (**1-11** and **1-12**) in good yield over 2 steps (scheme 12). This sequence has several advantages including the use of air and moisture stable carbamoylating reagents, shorter overall step count, and comparable overall yields.



Scheme 12. Synthesis of Heterocyclic Analogues of Retigabine

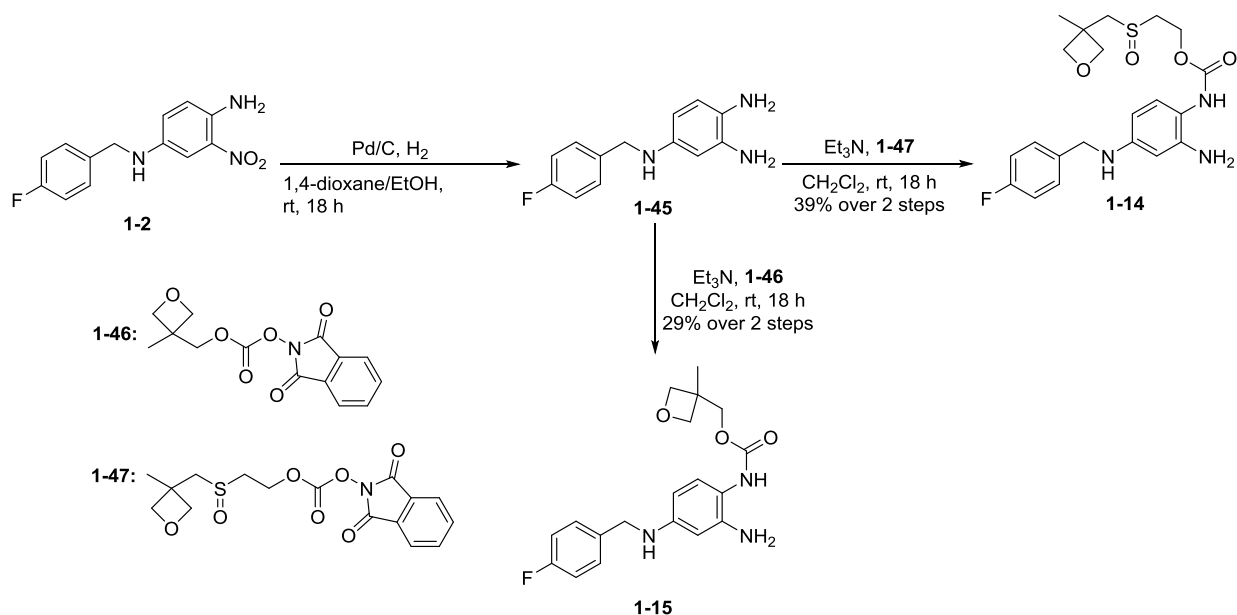
The analogues with alterations in zone 2 of retigabine were surprisingly difficult to access. Initial attempts to prepare the desired compounds involved the previously described reductive amination-protection-carbamoylation sequence to yield **1-43**. Attempts to prepare functionalized carbamate equivalents using carbonyl diimidazole-derived reagents⁷⁰ led only to recovered starting material and formation of the corresponding isocyanate of **1-42** with phosgene⁷¹ and addition of the corresponding alcohols led to mixtures of products by LC-MS that were inseparable by TLC. The only compound successfully prepared via this route was isopropyl carbamate analogue **1-44** due to the ready availability of isopropyl chloroformate.

Reductive amination gave diamine **1-2** in 62% yield which was then protected and treated with isopropyl chloroformate, affording only 39% of the desired product over 2 steps (scheme 13). Catalytic hydrogenation of **1-43** using Pd/C and H₂ gave **1-44** in good yield (74%).



Scheme 13. Synthesis of Isopropyl Carbamate Analogue **1-44**

The synthesis of **1-44** drew our attention to a key limitation of our strategy; acid-sensitive functionalities would likely not survive the formation of the chloroformate using traditional methods⁷² and yields would likely be low. In particular, MMS-350 had previously shown acid instability. Thus, taking lessons learned from the heterocyclic analogues of retigabine and the work done in the Wipf group,⁵⁷ mixed phthalidimidyl carbonates appeared to be a superior method to access these compounds. **1-46** and **1-47** could be prepared from diphthalidimidyl carbonate and enabled controlled carbamoylation without any evidence of polycarbamoylation (scheme 14). Thus, catalytic hydrogenation of **1-2** yielded triamine **1-45** which was then treated with a mixed carbonate (**1-46** or **1-47**) and Et₃N. Purification of compound **1-15** was complicated by closely eluting impurities but could be obtained in 29% yield over 2 steps. The MMS-350 derived compound **1-14** was obtained in better, albeit still modest, 39% yield.



Scheme 14. Synthesis of MMS-350 and 3-Methyl-3-Oxetanemethanol Modified Analogues

1.3 CONCLUSIONS

A small collection of retigabine analogues was synthesized exploring various alterations which included fluorinated phenyl, heteroaromatic, benzylic, and carbamate alterations to the parent compound. Initially, several analogues were prepared utilizing a protecting group sequence that exhibited severe limitations. A new, shorter route was developed involving reductive amination, reduction of the nitro group, and treatment with mixed phthalidimidyl carbonates to deliver the final compounds in good overall yields. Overall, 11 compounds were synthesized and are awaiting *in vitro* and *in vivo* biological evaluation.

2.0 PROGRESS TOWARDS A CONCISE ROUTE TO XJB-5-131

2.1 INTRODUCTION

2.1.1 Mitochondrial Production of Reactive Oxygen Species and XJB-5-131

The “free radical theory of aging” proposed by Harman in 1956 hypothesized that free radicals, most likely produced within an organism, lead to the detrimental effects of aging.⁷³ Since Harman’s seminal publication, reactive oxygen species (ROS) have been associated with the a variety of detrimental cellular effects and disease states⁷⁴ including Alzheimer’s disease, Parkinson’s disease, stroke, and cancer.⁷⁵ The theory has also been expanded to include oxidizing oxygen species like peroxides, singlet oxygen, and ozone. With the vast majority of ROS being produced in the mitochondria during the oxidative phosphorylation (OxPhos) process (Figure 13),⁷⁴ it comes as no surprise that most efforts to control ROS production target the mitochondria.⁷⁶

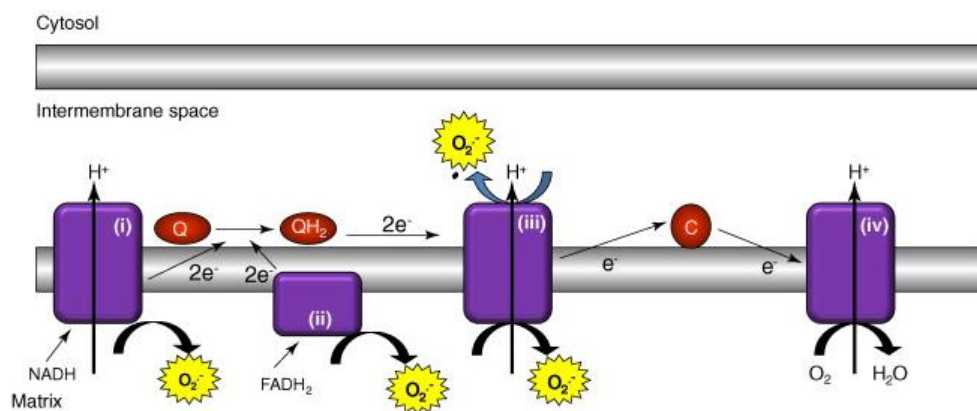


Figure 13. Production of Reactive Oxygen Species in the Electron Transport Chain.⁷⁷ Adapted by permission from Ref 77.

Because antioxidants have proven ineffective at combating oxidative damage in animal models due to localization problems,⁷⁸ targeting of the inner mitochondrial membrane by external ROS scavengers has been achieved in a variety of ways. Taking advantage of several distinct features of the inner mitochondrial membrane,⁷⁹ most targeting methods can be described as either non-peptidic or peptidic in nature (Figure 14). Non-peptidic methods (lipophilic cations, sulfonyl urea compounds, anthracyclines, etc.) typically involve modulation of the mitochondrial membrane potential (either inadvertently or by design) or damage of mitochondrial membrane proteins.⁷⁶ Each of these processes can be useful in targeting mitochondria but they have significant side effects that limit their effectiveness, such as destabilization of the mitochondrial membrane which can lead to eventual cell death.

Peptide mimics have also been shown to localize effectively in mitochondria. The Szeto-Schiller (SS) peptides utilize a 2',6'-dimethyltyrosine unit that acts as the ROS scavenging payload with the rest of the peptide consisting of alternating basic and aromatic residues serving to localize the compound in the inner mitochondrial membrane,⁸⁰ with enhancements of up to 600-fold being achieved. Wipf and Xiao synthesized a variety of truncated Gramicidin S-

derived ROS scavengers that localize in the inner mitochondrial membrane⁸¹ and utilize a stable nitroxide radical, 4-amino-TEMPO, as the ROS scavenging moiety.

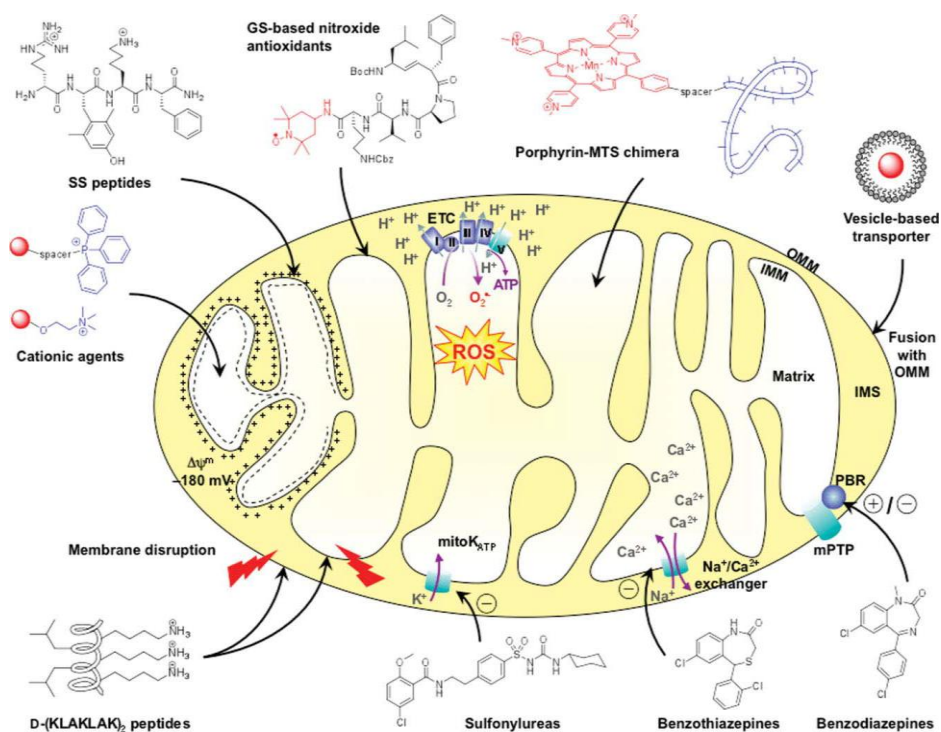


Figure 14. Mitochondrial Targeting Strategies.⁷⁶ Adapted by permission from Ref. 76.

XJB-5-131 (figure 16) was the result of extensive experimentation with Gramicidin S (figure 15), a mitochondrial membrane-active decapeptide that contains 2 type II' β -turns, an unnatural *D*-phenylalanine residue, and an ornithine residue. Gramicidin S was initially used as a topical antibiotic in World War II due to its wide spectrum antibiotic and antifungal properties. Crystallographic structural confirmation was not obtained until 1978 when Dodson and coworkers solved the crystal structure of a Gramicidin S-urea complex to 1 Å resolution,⁸² indicating a slightly distorted conformation from that proposed by Hodgkin and Schmidt.⁸³ The

crystal structure confirmed the presence of two type II' β -turns as well four internal hydrogen bonds that serve to stabilize the dimeric structure.

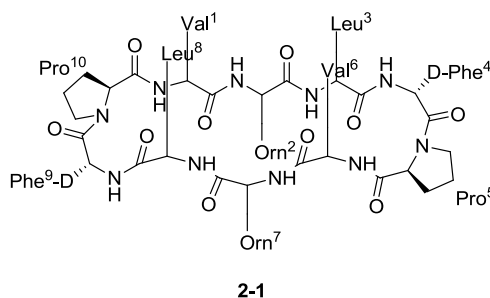


Figure 15. Structure of Gramicidin S

Utilizing a truncated version of **2-1** that incorporates an ROS scavenging moiety, directed delivery could be achieved with a compound that would be more amenable to synthesis and diversification. Thus, Xiao and Wipf synthesized a variety of truncated Gramicidin S derivatives. XJB-5-131 (Figure 16, **2-2**) was found to localize in mitochondria based on analysis of electron-spin resonance spectra.⁸¹ As a consequence of its localization properties, **2-2** has shown promise in animal models of radiation sickness,⁶³ neurodegeneration,⁸⁴ and lethal hemorrhagic shock.⁸⁵ Attempts to further simplify the structure of XJB-5-131 led to the development of JP4-039⁸⁶ (Figure 16) which has shown to be particularly effective in combating radiation exposure.⁸⁷

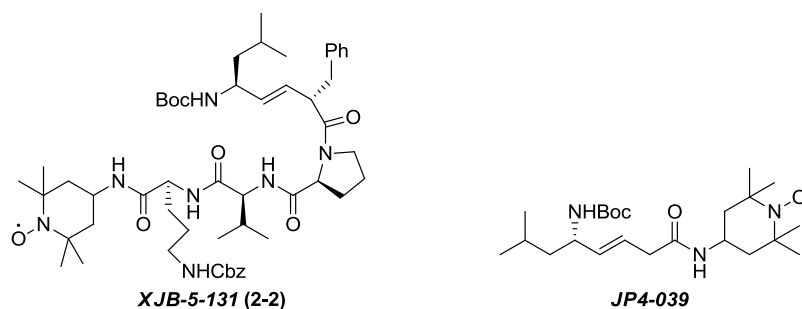
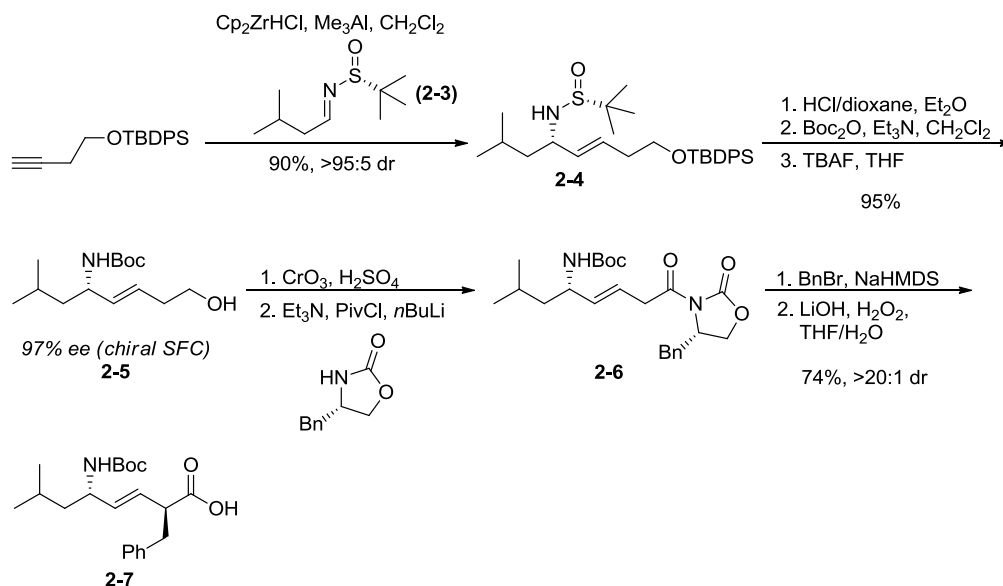


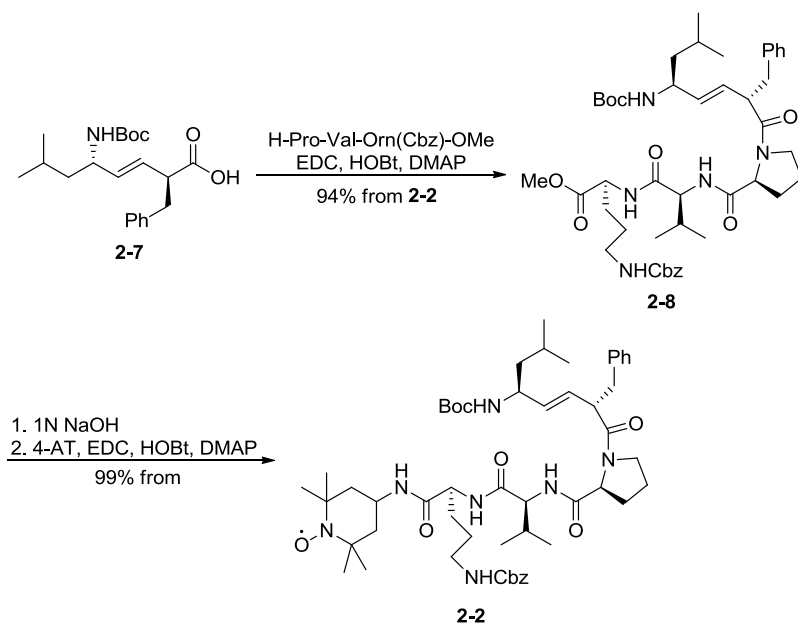
Figure 16. Structures of XJB-5-131 and JP4-039

The initial synthesis of XJB-5-131 required nearly 20 steps and the separation of a 1:1 mixture of diastereomers. While delivering the final compound in good overall yield and allowing for the preparation of enough material for initial biological assays, the length of this synthetic sequence would make gram-scale quantities of the target compound difficult to access. A shortened route was developed⁸⁸ starting from commercially available homopropargyl alcohol that utilized zirconium transmetalation methodology previously developed in the Wipf group (scheme 15).⁸⁹ Hydrozirconation of homopropargyl alcohol with Schwartz's reagent, transmetalation from Zr to Al, and then addition into sulfinimine **2-3** gave **2-4** with high diastereoselectivity. Interestingly, this process was hypothesized to proceed through a 4-membered chelate transition state. Several protecting group manipulations gave alcohol **2-5** which was subsequently oxidized and the Evan's auxiliary appended to give **2-6**. Alkylation with benzyl bromide and cleavage of the chiral auxiliary with LiOH and H₂O₂ gave **2-7** in excellent overall yield.



Scheme 15. Synthesis of Protected Amino Acid **2-7**

With the most difficult part of the molecule synthesized, peptide coupling of **2-7** with H-Pro-Val-Orn(Cbz)-OMe using EDC and HOBT gave **2-8** in excellent yield and hydrolysis of the pendant methyl ester and subsequent peptide coupling with 4-amino-TEMPO (4-AT) affords **2-2** (scheme 16). Overall, 12 steps (LLS) deliver the desired compound in 34% yield, and this route has been used to synthesize gram-scale quantities of the target compound. In spite of its high efficiency, six steps in this route serve to manipulate either protecting groups or chiral auxiliaries and represent nearly half of the actual synthetic sequence. In addition, stoichiometric quantities of each chiral auxiliary are needed, representing a significant dollar cost if large quantities of material are needed. Thus, we began looking at new disconnections towards amino acid **2-7** in an attempt to streamline the synthesis. In particular, recent advances in the stereoselective synthesis of α -alkenylated carbonyl compounds seemed like a good starting point in our endeavors.



Scheme 16. Late-Stage Peptide Couplings to Synthesize XJB-5-131

2.1.2 Stereoselective Alkenylation of Aldehydes: Difficulties and Approaches

The stereoselective α -alkenylation of carbonyl compounds has been a long sought-after transformation. It is often not possible to employ traditional procedures involving enolate chemistry for a variety of reasons (figure 17). First, even if satisfactory enantioenrichment occurs, the resulting products would be more acidic than the starting materials. Quantitative enolate formation is an option but requires carefully controlled reaction conditions and the use of dangerously reactive chemicals. Second, olefin isomerization to give α,β -unsaturated carbonyl compounds is a potential problem, especially when transition metal complexes are used. The olefin reaction partners are usually not electrophilic enough to directly participate in these types of transformations either and require an electron-withdrawing functionality (α,β -unsaturated ketone, ester, nitrile, nitro, etc.) and a terminal leaving group (vinyl halide, tosylate, etc.) to achieve the same reactivity patterns as alkyl halides or sulfonates.

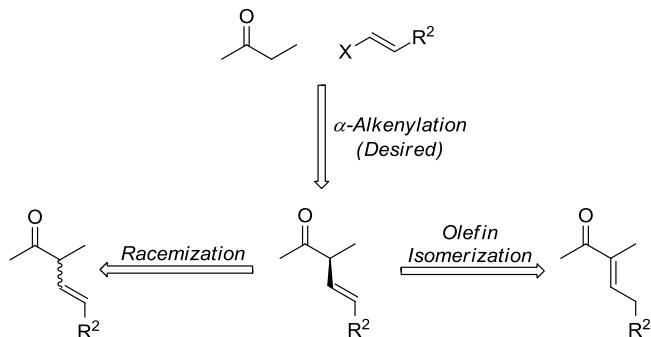
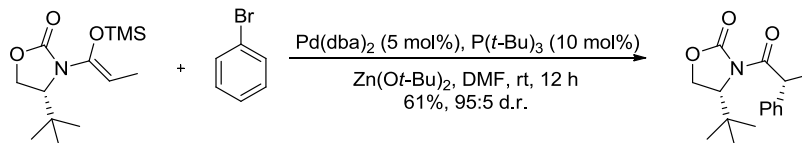


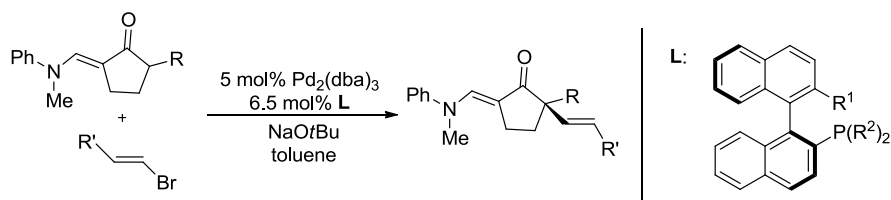
Figure 17. Difficulties and Desired Transformation Associated with α -Alkylation of Carbonyl Compounds

The α -alkenylation of carbonyl compounds is a direct extension of earlier work to develop α -arylation procedures. Several groups, particularly those of Buchwald and Hartwig, have developed suitable procedures⁹⁰ that utilize basic conditions to enolize various types of carbonyl compounds. The resulting products were racemic and non-enolizable, so racemization was not a concern. In order to allow for a wider variety of substrates, Hartwig and coworkers have also developed milder procedures utilizing preformed silyl enol ethers and Lewis acid catalysts which have been found to avoid epimerization of the resulting stereocenters, react more quickly, and give higher selectivity.⁹¹ The scope with regards to the silyl enol ether was broad allowing even sterically hindered enolates to be successfully arylated with high selectivity in synthetically useful yields. Particularly useful was the use of chiral oxazolidinones allowing highly diastereoselective couplings of aryl bromides (scheme 17).



Scheme 17. Diastereoselective α -Arylation of Trimethylsilyl Enolates Using the Evans' Auxiliary

In recent years, catalytic and stereoselective methods for generating α -alkenyl carbonyl compounds have emerged. Beginning with stereoselective α -arylation procedures,⁹² α -vinylation has gained popularity as more powerful methods of catalysis are developed. Buchwald and coworkers have demonstrated that palladium can competently couple vinyl bromides and ketone enolates (Scheme 18).⁹³ Enantiomeric excesses of up to 94% were realized by using axially chiral phosphine ligands and catalytic $\text{Pd}_2(\text{dba})_3$, but this achievement was tempered by the fact that the reaction is highly substrate dependent. Enantiomeric excesses were greatly diminished when *cis* olefins or cyclohexanones were used. This methodology also requires the use of a blocking group in the α' -position due to the strongly basic reaction conditions.

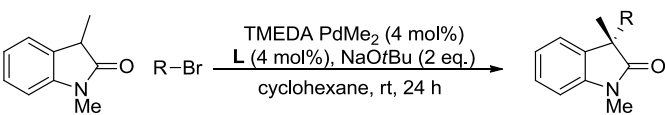


Scheme 18. Enantioselective Palladium-Catalyzed Vinylation of Ketone Enolates

In 2009, the same group was able to show that oxindoles were suitable substrates for α -arylation and α -vinylation when axially-chiral P-stereogenic ligands were used in combination with a palladium precatalyst.^{92b} All examples of arylation proceed in good to excellent yield with excellent enantioselectivity but interestingly, alkenylation using *trans*- and *cis*-1-bromo-1-

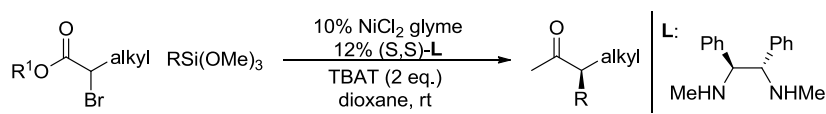
propene gave highly divergent selectivity (Table 2, entries 1 and 2) though no explanation was put forth to explain the discrepancy. 2-Bromopropene was a competent substrate (Table 2, entry 3) giving good yields and excellent selectivity. Likewise, a mixture of *cis/trans* isomers of β -bromostyrene was subjected to vinylation conditions and a mixture of products was obtained with the *cis*-isomer showing significantly higher enantioinduction than the *trans*-isomer (Table 2, entry 4).

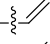
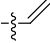
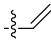
Table 2. Enantioselective α -Vinylation of Oxindoles with 1-Bromo-1-propene and β -Bromostyrene



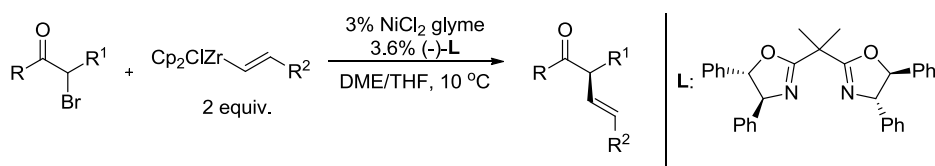
entry	vinyl bromide	isolated yield (%)	ee (%)
1	<i>cis</i> -1-bromo-1-propene	79	94
2	<i>trans</i> -1-bromo-1-propene	87	54
3	2-bromopropene	63	96
4	<i>cis/trans</i> - β -bromostyrene	73 (<i>trans</i>) / 10 (<i>cis</i>)	78 (<i>trans</i>) / 98 (<i>cis</i>)

The Fu group has investigated the Hiyama coupling of racemic α -bromoesters with aryl and vinyl silanes using a chiral nickel-diamine catalyst system (Table 3).⁹⁴ The reaction proceeded in moderate yield with high enantioselectivity. This process likely proceeds through the standard oxidative insertion-transmetallation-reductive elimination sequence common to palladium and nickel catalytic cycles with isomerization possible through a η^3 π -complex. Alkenyl (Table 3, entries 1 and 3) and styrenyl (Table 3, entry 2) silanes were able to deliver the corresponding alkenylation products in good yield and high enantioselectivity.

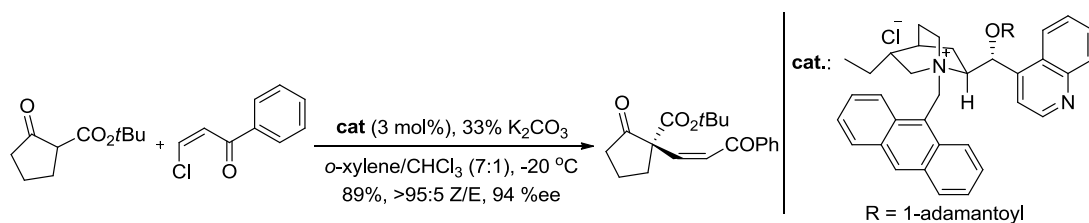
Table 3. Asymmetric Hiyama Coupling of α -Bromo Esters and Vinyl Silanes

Entry	Alkyl	R	Isolated yield (%)	Ee (%)
1	<i>n</i> -Bu		66	93
2	<i>n</i> -Bu		72	92
3	Et		70	91

The same group was later able to show that alkenylzirconium compounds were competent substrates in this transformation.⁹⁵ Reaction with α -bromo ketones using a chiral nickel-bisoxazoline system gave the desired α -alkenylation products with good to excellent enantioinduction (80-95 %ee) and good yields (Scheme 19). The most commonly used substrates were aryl ketones, though some alkyl and benzyl ketones were also used and gave comparable yields and selectivity. This type of transformation complements a broader class of similar transition-metal catalyzed reactions that have been developed with a variety of organometallic reaction partners (boron, zinc, magnesium, silicon, tin, and indium compounds).⁹⁶ This process has limited functional group compatibility, however, due to the hydrozirconation reaction used to generate the requisite substrates.

**Scheme 19.** Enantioselective Cross-Coupling of Racemic α -Bromo Ketones with Alkenyl Zirconium Compounds

Organocatalytic methods for α -alkenylation have recently begun to surface as alternatives to traditional transition-metal mediated processes that typically suffer from limited substrate scope and modest functional group compatibility. These types of processes have several advantages when compared to transition metal mediated processes, including mild reaction conditions and reduced likelihood of product racemization. The most direct method of enantioselective α -alkenylation was developed by Jørgensen and coworkers who utilized cyclic β -ketoesters in a conjugate addition-elimination procedure under phase-transfer conditions mediated by cinchona alkaloid-derived catalysts (Scheme 20).⁹⁷ The reaction gave good to excellent yields with excellent enantioselectivity. The mechanism of this transformation is thought to involve enolization of the β -ketoester forming a chiral ion-pair, which can then undergo conjugate addition with the β -chloroenone to generate a set of diastereomeric enolates. Expulsion of the halide results in a stereospecific regeneration of the alkene to generate the desired α -alkenylation product. In order to expand the types of substrates that can be used, however, a more general approach had to be developed that does not rely on premade olefins and the creation of non-enolizable stereocenters.

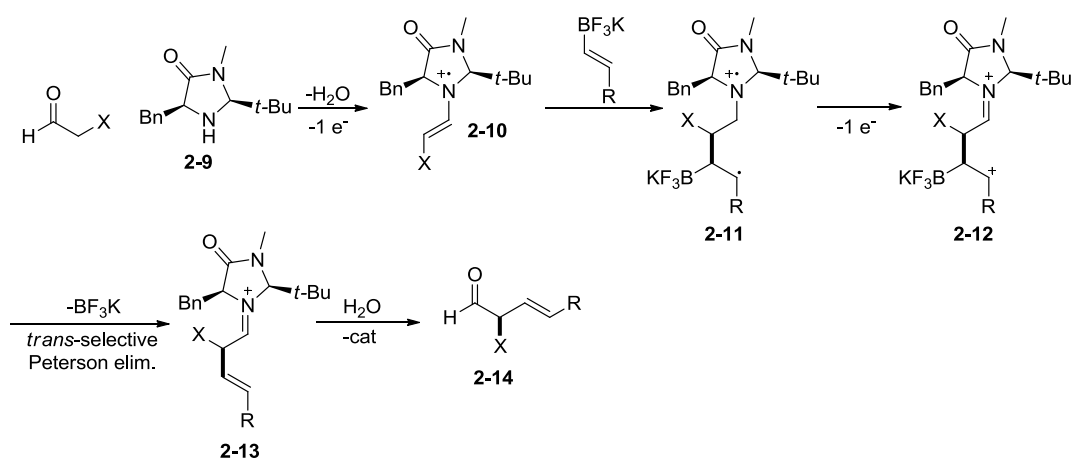


Scheme 20. α -Alkenylation of β -Ketoesters using Cinchona Alkaloid-Derived Organocatalysts

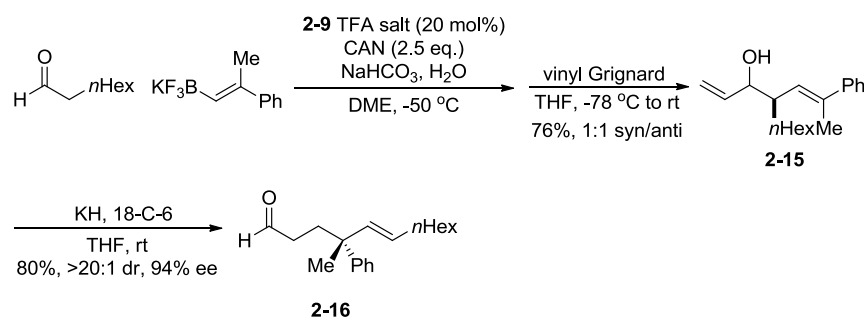
More recently, the MacMillan group has reported several different methods of preparing α -alkenylation products using aldehydes as the carbonyl component. Due to the mild reaction

conditions and the nature of the organocatalyst, racemization of the resulting α -alkenyl aldehydes is disfavored. Furthermore, the versatility of the resulting aldehydes (reduction to alcohols, oxidation to carboxylic acids, reduction to alkyl chains, Wittig reaction, addition of nucleophiles, reductive amination, homologation to the terminal alkyne, etc.) makes this strategy attractive for complex molecule synthesis.⁹⁸

Early work in this area utilized alkenyl trifluoroborate salts and aldehydes under organo-SOMO catalysis conditions (Scheme 21).⁹⁹ Initial condensation of imidazolidinone catalyst **2-9** with an aldehyde gives an enamine which can be oxidized by CAN to give radical cation **2-10**. Subsequent radical addition to the alkenyl trifluoroborate reaction partner gives radical cation **2-11** which can then be oxidized further to dication **2-12**. A *trans*-selective Peterson-type elimination leads to enantioenriched α -alkenylation product **2-13** which can be hydrolyzed to give **2-14** and regenerate catalyst **2-9**. This procedure was used with a variety of aldehydes (alkyl, alkene-containing, cycloalkanes, benzyl, protected alcohols, and protected amines) and alkenyl trifluoroborate salts (substituted styrenes and alkyl) giving good yields and excellent enantioselectivity in all cases. This methodology was applied to the synthesis of a challenging all-carbon quaternary center (Scheme 22). The initial α -alkenylation product was treated with vinyl Grignard reagent to give a 1:1 diastereomeric mixture of **2-15** which could be subjected to anionic Oxy-Cope conditions to give aldehyde **2-16** with excellent enantio- and diastereoselectivity.



Scheme 21. Mechanism of Organo-SOMO Catalysis Using Chiral Imidazolidinones

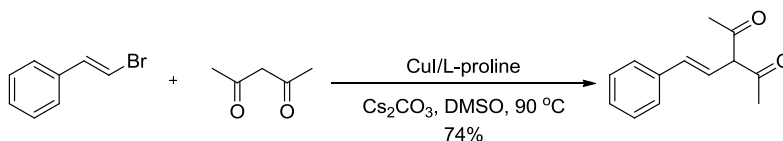


Scheme 22. Anionic Oxy-Cope Strategy to All-Carbon Quaternary Centers

Synergistic catalysis takes advantage of two separate catalytic cycles that can intersect each other with intermediates that react to give the desired product and regenerate one or both of the catalysts in the process. This type of transformation has become prominent in recent years.⁹⁸

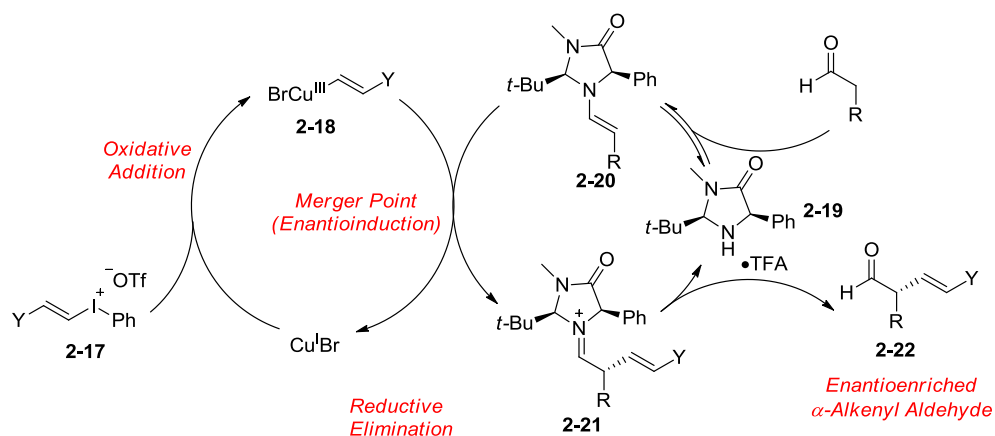
¹⁰⁰ Copper catalysis has been used in previous procedures that couple aryl groups with various nucleophiles. Electrophilic organocopper species (specifically organo-Cu^I, Cu^{II}, and Cu^{III} intermediates) have been implicated in many reactions such as the Chan-Evans-Lam coupling,¹⁰¹ Ullmann-Goldberg coupling,¹⁰² and an aromatic Glaser-Hay-type coupling.¹⁰³ Oxidative insertion of Cu^I or transmetalation and subsequent oxidation with an external oxidant (often molecular O₂) to generate an organo-Cu^{III} intermediate can be attacked by a nucleophile and

reductively eliminate the desired coupling product. This type of process has been used to access α -alkenylation products via reaction of an alkenyl-Cu^{III} intermediate with a wide variety of activated methylene compounds (Scheme 23).¹⁰⁴



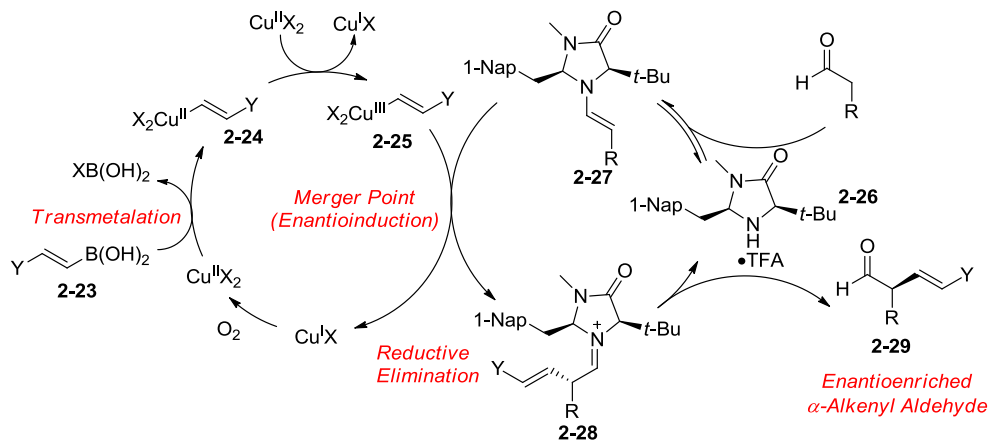
Scheme 23. Copper-Catalyzed Coupling of Alkenyl Bromides with Activated Methylene Compounds

MacMillan and coworkers have used a combination of transition metal and organocatalysis to effect several challenging transformations.^{98, 100a} Initial forays in the area of α -alkenylation were extensions of previous work to develop synergistic catalysis protocols that afforded α -arylation¹⁰⁵ and α -trifluoromethylation¹⁰⁶ products with high enantioinduction. Much of the early work used hypervalent iodine reagents (in particular, iodonium salts) which could be manipulated easily via transition metal or photoredox catalysis. Thus, the first α -alkenylation procedure using synergistic catalysis utilized iodonium triflate salts and aldehydes under organo- and copper catalysis conditions to generate α -alkenyl aldehydes in high enantiomeric excess and good yield (scheme 24). The transformation was postulated to proceed via oxidative insertion of Cu^I into the carbon-iodine bond of **2-17** to give alkenyl Cu^{III} species **2-18** which could then be attacked by nucleophilic enamine **2-20** derived from condensation of imidazolidinone salt **2-19** with an aldehyde. The resulting organometallic species can reductively eliminate to give a regenerated Cu^I catalyst and iminium ion **2-21** which can be hydrolyzed to give the desired α -alkenylation product **2-22**.



Scheme 24. α -Alkenylation of Aldehydes with Vinyl Iodonium Triflates Using Copper and Organocatalysis

A later report by MacMillan and Stevens utilized readily prepared alkenyl boronic acids^{100a} with organo- and copper catalysis that could deliver the same class of compounds in comparable yields and selectivity. In this case, boronic acid **2-23** can transmetallate with Cu^{II} and be oxidized by O_2 to arrive at the same putative alkenyl Cu^{III} species **2-25** as before (Scheme 25). Nucleophilic attack by transiently generated enamine **2-27** and subsequent reductive elimination gives iminium ion **2-28**. Hydrolysis gives **2-29** and regenerates organocatalyst **2-26**. A broad range of substrates including electron-deficient and electron-rich substrates could be used and the reaction conditions were functionally simple. This reactivity coupled with the ready accessibility of alkenyl boronic acids¹⁰⁷ prompted us to examine this procedure as a better method of accessing amino acid **2-7** *en route* to XJB-5-131.



Scheme 25. Mechanism of Enantioselective α -Alkenylation of Aldehydes Using Boronic Acids

2.2 RESULTS AND DISCUSSION

2.2.1 Synthetic Strategy towards Amino Acid 2-7

We sought to take advantage of the high yielding peptide coupling steps that complete the synthesis of **2-2** and instead focus on constructing carboxylic acid **2-7** in a more efficient manner. To that end, we envisioned that the previously discussed α -alkenylation using synergistic organocatalysis and copper catalysis^{100a} could be used to arrive at carboxylic acid **2-7** (Figure 18). Boronic acid **2-30** could be synthesized from commercially available *N*-Boc-leucine via hydrozirconation chemistry. We also envisioned that using a model system **2-31** would allow us to probe the complexities of the key coupling step and answer several important questions. First, while free N-H bonds have been used with MacMillan's organocatalysis procedures,¹⁰⁸ they have not been used in combination with metal catalysis in a vinylation procedure. Second, while protected amines have been used in previous MacMillan alkenylation

procedures,⁹⁸⁻⁹⁹ protected allylic amines have not and can drastically change a substrate's steric and electronic properties.

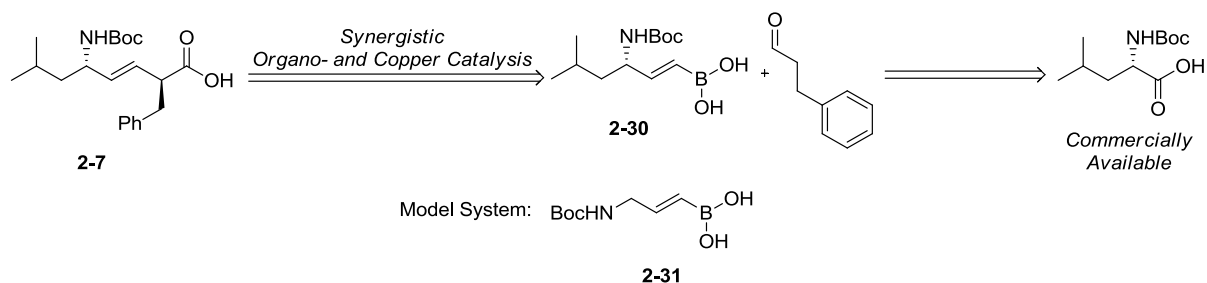


Figure 18. New Synthetic Strategy Towards XJB-5-131

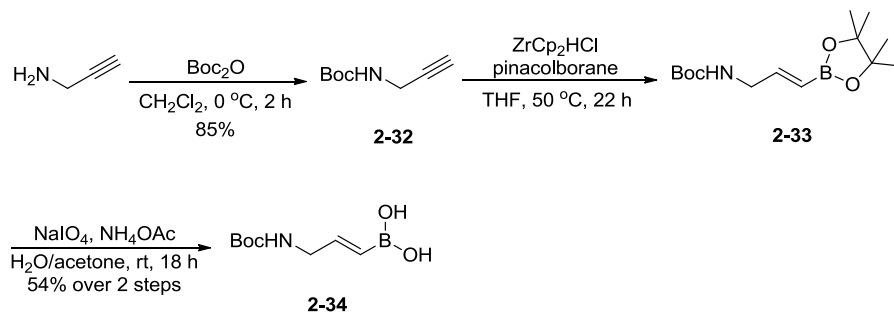
2.2.2 Studies towards Amino Acid 2-7

Initial studies were directed towards the synthesis of model system **2-31**. Boc protection of propargyl amine¹⁰⁹ gave **2-32** in 85% yield which was subjected to a variety of hydroboration conditions that could be used to gain access to the desired boronic acid or the pinacolboronate ester. Loss of the Boc protecting group was likely due to the formation of strong acids during the course of the reaction (Table 4, entries 1, 2, and 5). All other hydroborating agents failed to give the desired product, presumably due to insufficient reactivity of the alkyne towards hydroboration, even when dialkylboranes were used (Table 4, entries 3-6).

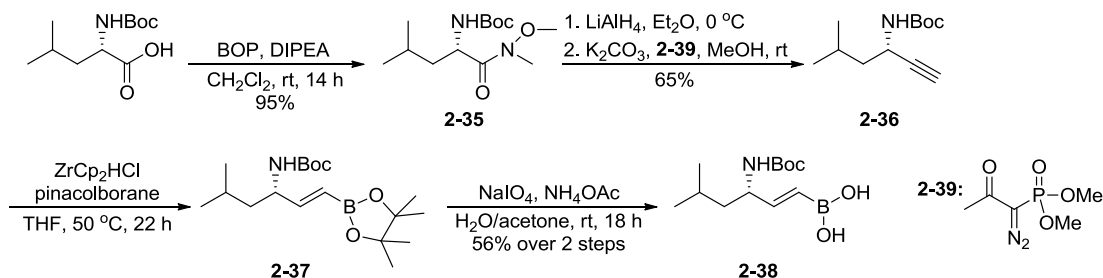
Table 4. Attempted Hydroboration to Access a Substituted Boronic Acid

Entry	Conditions	Result
1	HBBBr ₂ SMe ₂ , CH ₂ Cl ₂ , -78 °C; NaOH, H ₂ O	No product
2	HBBBr ₂ SMe ₂ , pinacol, CH ₂ Cl ₂ , -78 °C	No Product
3	(lpc) ₂ BH, 0 °C	No product
4	Catecholborane, THF, 70 °C, 1 h; H ₂ O, rt	Incomplete conversion
5	Catecholborane, THF, 70 °C, 20 h; H ₂ O, rt	Loss of Boc group
6	Cy ₂ BH (cat.), pinacolborane, rt	Recovered starting material
7	ZrCp ₂ HCl, HBPIn, THF, 50 °C, 22 h	100% conversion by ¹ H NMR

Ultimately, a zirconium-catalyzed hydroboration procedure modified from the original work of Pereira and Srebnik¹¹⁰ gave access to pinacolboronate ester **2-33** which decomposed when subjected to chromatography on SiO₂ (Scheme 26). The crude pinacolboronate ester was oxidatively cleaved using NaIO₄ and NH₄OAc in aqueous acetone¹¹¹ to give **2-34** which was also not isolable by chromatography on SiO₂ due to decomposition. Crystallization of the crude material from CH₂Cl₂ at -20 °C gave gram-scale quantities of **2-34** in 54% yield over 2 steps.

**Scheme 26.** Synthesis of Model Boronic Acid **2-34**

Boronic acid **2-38** could also be prepared via a similar route. Alkyne **2-36** was prepared according to a two-step protocol involving formation of Weinreb amide **2-35** and a reduction/Ohira-Bestmann homologation sequence¹¹² to give **2-36** (Scheme 27). Preparing the Ohira-Bestmann reagent (**2-39**) *in situ* and subsequent reaction with the crude amino aldehyde (from LiAlH₄ reduction)^{112a} gave lower yields (*ca* 30%) compared to preparing and isolating the reagent beforehand.¹¹³ Zirconium-catalyzed hydroboration of **2-36** followed by oxidative cleavage¹¹¹ gave amino boronic acid **2-38** in 56% yield over 2 steps following crystallization from CH₂Cl₂. Chiral imidazolidinones **2-40** and **2-41** (Figure 19) could be prepared according to literature protocols¹¹⁴ from the corresponding amino acids or purchased from commercial vendors. The corresponding trifluoroacetate salts were prepared by treatment with TFA in Et₂O.



Scheme 27. Synthesis of Amino Boronic Acid **2-38**

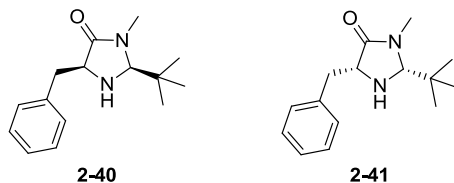
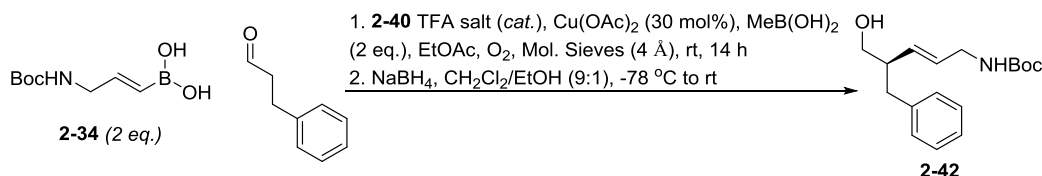


Figure 19. Structure of Chiral Imidazolidinones **2-40** and **2-41**

Initial attempts to alkenylate boronic acid **2-34** gave complex mixtures that were found to contain hydrocinnamyl alcohol, protodeboronation products, a mixed boronic anhydride

resulting from cyclodehydration with methylboronic acid and **2-34**, and a small amount of **2-42** (Table 5, entry 1). Screening reaction conditions indicated the necessity of excess water in the reaction (even in the presence of molecular sieves) to achieve synthetically useful yields. Eventually a maximum yield of 33% (Table 5, entry 7) was achieved using 500 wt% of 4 Å molecular sieves and 30 mol% of **2-40** TFA salt, and allowing the reaction to proceed for two days at room temperature. Attempts to use **2-34** as the limiting reagent gave significant amounts of protodeboronation product and no detectable amount of **2-42**. Heating the reaction mixture gave no product by ^1H NMR and 3 Å molecular sieves in pellet form led to decreased yields.

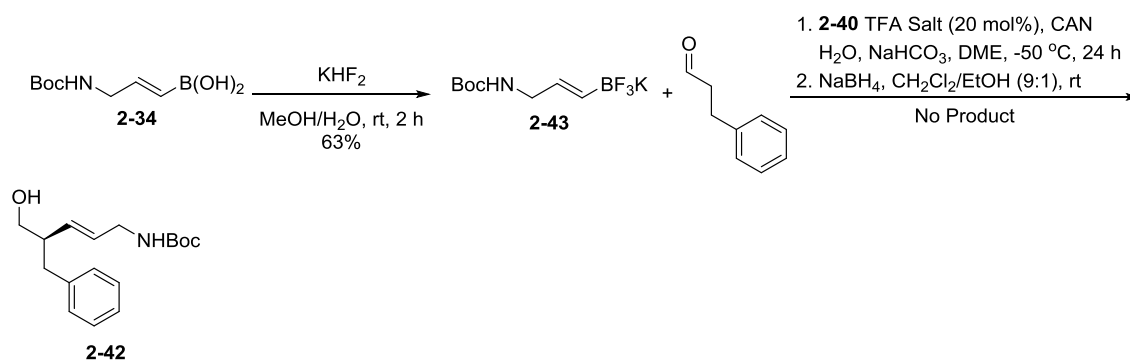
Table 5. Conditions for α -Alkenylation with Boronic Acid **2-34**



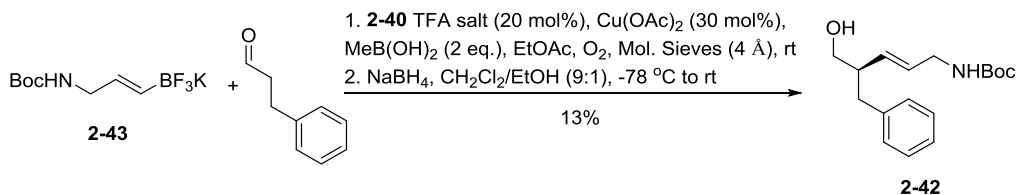
Entry	2-40 TFA Salt (mol%)	Mol. Sieves (wt%)	Misc.	Yield
1	20	1000	n/a	11%
2	20	1000	1 drop of H_2O added	26%
3	20	1000	Boronic acid as L.R.	trace by ^1H NMR
4	20	500	n/a	18%
5	20	0	$50\text{ }^\circ\text{C}$ during part 1	No Pdt
6	20	500	3 Å mol. sieves, pellet	10%
7	30	500	48 h	33%

In addition, potassium trifluoroborate salt **2-43** was prepared to test its utility in both the synergistic catalysis protocol^{100a} and the previously described organo-SOMO procedure.⁹⁹ Zirconium-catalyzed hydroboration of **2-32** followed by treatment with aq. KHF_2 gave **2-43** in 63% yield (Scheme 28). Organo-SOMO catalysis conditions using CAN as the oxidant gave no desired product while reaction under synergistic catalysis conditions gave the desired product in

comparable yield to **2-34** (13%, compare to Table 5, entry 1). Exclusion of molecular sieves and methyl boronic acid gave no desired product, presumably due to insolubility of the trifluoroborate salt. These results indicated that the electron-deficient nature of the olefinic reaction partner may disfavor formation of key electron-deficient intermediates (Scheme 25, **2-25**) and lead to low yields of desired product.



Scheme 28. Preparation of Potassium Trifluoroborate **2-43** and Organo-SOMO Vinylation

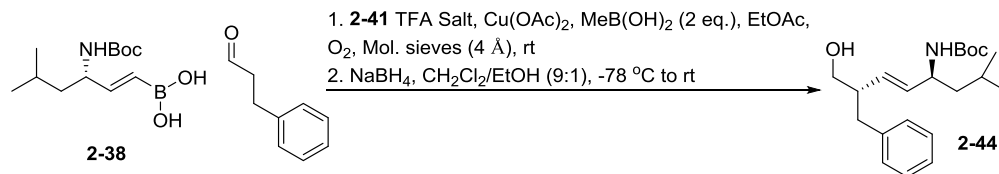


Scheme 29. Synergistic Catalysis Using Potassium Trifluoroborate **2-43**

It was thought that the isobutyl chain of **2-38** would help to stabilize electron-deficient intermediates that are formed during the copper catalytic cycle. Thus, boronic acid **2-38** was subjected to α -alkenylation conditions. No desired product was obtained using our optimized reaction conditions. Stoichiometric organocatalyst (Table 6, entry 2) and stoichiometric Cu(OAc)₂ (Table 6, entry 3) were used but failed to deliver any detectable amount of alcohol **2-**

44. Extended reaction times (Table 6, entry 4) did not give any trace of the desired product either even with stoichiometric organocatalyst. Possibly there may be an unidentified effect of the protecting group effect that subtly modulates the reactivity of the boronic acid.

Table 6. Attempted α -Alkenylation Using **2-38**



Entry	2-41 TFA Salt (mol%)	$\text{Cu}(\text{OAc})_2$ (mol%)	Time	Result
1	30	30	2 d	No pdt by TLC/ ^1H NMR
2	100	30	14 h	No pdt by TLC/ ^1H NMR
3	20	200	14 h	No pdt by TLC/ ^1H NMR
4	100	30	2 d	No pdt by TLC/ ^1H NMR

2.3 CONCLUSIONS

A concise route to XJB-5-131 was explored that relied on the diastereoselective α -alkenylation of hydrocinnamaldehyde with boronic acid **2-38**.^{100a} Model system boronic acid **2-34** was synthesized and used to explore various reaction parameters that could affect the transformation, including water content, limiting reagent, and the loading of molecular sieves. A 33% yield of alkenylation product **2-42** was obtained, indicating that the desired transformation is feasible but difficult to achieve. Boronic acid **2-38** was synthesized starting from enantiomerically enriched *N*-Boc-leucine in 5 steps and 36% overall yield. Attempts to use this

compound in the α -alkenylation procedure did not lead to desired product under a variety of conditions.

3.0 EXPERIMENTAL PART

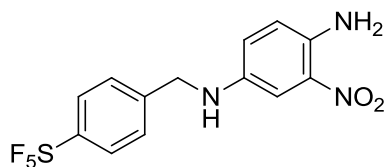
3.1 GENERAL EXPERIMENTAL

All reactions were performed under an N₂ atmosphere and all glassware was dried in an oven at 130 °C for at least 2 h prior to use and allowed to cool under an atmosphere of dry N₂ or Ar unless otherwise stated. Reactions carried out below 0 °C employed an acetone/dry ice bath or a cryocool and an acetone bath. THF and Et₂O were distilled over sodium/benzophenone ketyl, CH₂Cl₂ and toluene were distilled over CaH₂, and 1,4-dioxane, MeOH, and MeCN were dried batchwise over 3 Å molecular sieves unless otherwise noted. Et₃N and DIPEA were distilled from CaH₂ and stored over KOH. Concentration under reduced pressure refers to the use of a rotary evaporator connected to a PIAB Lab Vac H40 to remove solvent and drying under high vacuum refers to the use of a Fischer Scientific Maxima C *Plus* vacuum pump (0.5-4 mmHg) to remove traces of solvent.

All flash column chromatography was performed with normal phase SiO₂ (Silicycle, 40-63 µm particle size). Reactions were monitored by thin-layer chromatography (Merck pre-coated silica gel 60 F₂₅₄ plates, 250 µm layer thickness) and visualization was accomplished with a 254 nm UV light, by staining with KMnO₄ solution (1.5 g of KMnO₄ and 1.5 g of K₂CO₃ in 100 mL of a 0.1% NaOH solution), or by staining with *p*-anisaldehyde solution (2.5 mL of *p*-anisaldehyde, 2 mL of AcOH, and 3.5 mL of conc. H₂SO₄ in 100 mL of 95% EtOH).

Melting points were obtained using a Laboratory Devices Mel-Temp II using open capillaries and are uncorrected. ^1H and ^{13}C NMR spectra were obtained on Bruker Avance 300, 400, or 500 instruments as indicated. ^1H spectra were obtained at 300, 400, or 500 MHz in CDCl_3 and $(\text{CD}_3)_2\text{SO}$ unless otherwise noted. Chemical shifts were reported in parts per million with the residual solvent peak used as an internal standard. ^1H NMR spectra were obtained and are tabulated as follows: chemical shift, multiplicity (s = singlet, d = doublet, t = triplet, q = quartet, quint = quintet, dd = double of doublets, dt = doublet of triplets, m = multiplet, br = broad, app = apparent), number of protons, and coupling constant(s). ^{13}C NMR were run at 75, 100, 125, or 175 MHz as specified using a proton-decoupled pulse sequence and are tabulated by observed peak. Infrared spectra were measured on a PerkinElmer Spectrum100 FT-IR Spectrometer (ATR). High resolution mass spectra were obtained on a Thermo Fisher Exactive Orbitrap LC-MS using heated electrospray ionization (HESI). Compounds **2-39**¹¹³, **2-40**, and **2-41**¹¹⁴ were prepared according to literature protocols.

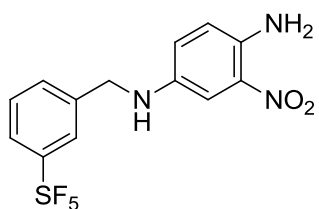
3.2 CHAPTER 1 EXPERIMENTAL PART



1-16

(4-Amino-3-nitrophenyl)[(4-pentafluorothiophenyl)methyl]amine (1-16). To a solution of 2-nitro-*p*-phenylenediamine (0.751 g, 4.66 mmol) and PTSA (0.045 g, 0.24 mmol) in toluene (25 mL) was added 4-(pentafluorothio)-benzaldehyde (1.115 g, 4.707 mmol). The

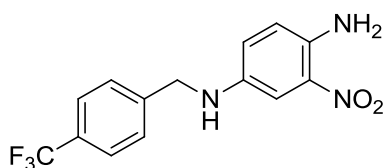
resulting solution was heated to reflux with a Dean-Stark trap for 21 h, the mixture was filtered through a Buchner funnel packed with a thin pad of SiO₂, and the filtrate was stirred and allowed to cool to rt. The solvent was removed under reduced pressure to give the crude imine (1.10 g) as a bright orange-red solid, that was suspended in a mixture of 1,4-dioxane (5.2 mL) and MeOH (1.3 mL) and NaBH₄ (0.120 g, 3.14 mmol) was added in 3 portions at 15 min intervals. The resulting solution was allowed to stir at rt for 3 h, quenched with H₂O (25 mL) and the resulting solid collected by filtration. The crude compound was washed with H₂O (500 mL) and dried under high vacuum to give **1** (1.09 g, 2.95 mmol, 63%) as a dark purple powder: Mp 129-130 °C (H₂O); IR (ATR) 3522.90, 3397.94, 1576.91, 1531.83, 1327.68, 1216.31 cm⁻¹; ¹H NMR (CDCl₃, 400 MHz) δ 7.73 (d, 2 H, *J* = 8.4 Hz), 7.61 (d, 2 H, *J* = 8.4 Hz), 7.27 (d, 1 H, 2.8 Hz), 6.84 (dd, 1 H, *J* = 9.2, 2.8 Hz), 6.71 (d, 1 H, *J* = 8.8 Hz), 5.74 (br s, 2 H), 4.37 (s, 2 H), 3.92 (br s, 1 H); ¹³C NMR (CDCl₃, 100 MHz) δ 153.2 (app. t, *J* = 17.5 Hz), 143.0, 138.9, 138.5, 132.6, 127.7, 126.5 (quint., *J* = 4.6 Hz), 125.3, 120.4, 106.2, 48.1; HRMS (HESI) *m/z* calcd for C₁₃H₁₃N₃O₂F₅S (M+H) 370.0643, found 370.0645.



1-17

(4-Amino-3-nitrophenyl)[(3-pentafluorothiophenyl)methyl]amine (1-17). A solution of 2-nitro-*p*-phenylenediamine (0.756 g, 4.69 mmol) and PTSA (0.054 g, 0.28 mmol) in toluene (25 mL) was treated with 3-(pentafluorothio)benzaldehyde (1.10 g, 4.56 mmol) via syringe and the resulting solution was heated to reflux with a Dean-Stark trap for 5 h. The mixture was

filtered through a Buchner funnel packed with a thin pad of SiO₂ and the filtrate was stirred and allowed to cool to rt. The solvent was removed under reduced pressure to give the crude imine (1.571 g) as a bright orange-red solid, that was suspended in a mixture of 1,4-dioxane (5.2 mL) and MeOH (1.3 mL) and NaBH₄ (0.126 g, 3.30 mmol) was added in 3 portions at 15 min intervals. The resulting solution was allowed to stir at rt for 3 h, quenched with H₂O (25 mL), and extracted from brine with CH₂Cl₂ (3 x 200 mL). The solvent was removed under reduced pressure and the resulting residue dried under high vacuum at 60 °C for 12 h to give **1-17** (1.36 g, 3.69 mmol, 79%) as a dark red-purple powder: Mp 128-129 °C (CH₂Cl₂); IR (ATR) 3477.56, 3422.45, 3360.67, 3109.99, 1574.79, 1515.17, 1206.56; ¹H NMR (CDCl₃, 400 MHz) δ 7.77 (s, 1 H), 7.68 (d, 1 H, *J* = 8.4 Hz), 7.53 (d, 1 H, 7.6 Hz), 7.47-7.43 (m, 1 H), 7.30 (d, 1 H, *J* = 2.8 Hz), 6.86 (dd, 1 H, *J* = 8.8, 2.8 Hz), 6.72 (d, 1 H, *J* = 8.8 Hz), 5.75 (br s, 2 H), 4.37 (s, 2 H), 3.89 (br s, 1 H); ¹³C NMR (CDCl₃, 100 MHz) 154.4 (quint., *J* = 18.0 Hz), 140.3, 139.0, 138.5, 132.6, 130.7, 129.3, 125.4, 125.3-125.1 (overlapping quint.), 120.4, 106.4, 48.6; HRMS (HESI) *m/z* calcd for C₁₃H₁₃N₃O₂F₅S (M+H) 370.0643, found 370.0641.

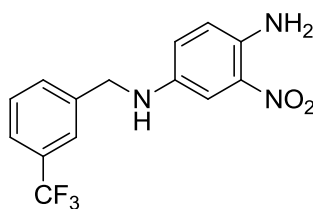


1-18

(4-Amino-3-nitrophenyl){[4-(trifluoromethyl)phenyl]methyl}amine (1-18).

A solution of 2-nitro-*p*-phenylenediamine (0.754 g, 4.68 mmol) and PTSA (0.054 g, 0.28 mmol) in toluene (25 mL) was treated via syringe with 4-(trifluoromethyl)benzaldehyde (0.640 mL, 4.69 mmol) and the resulting solution was heated at reflux with a Dean-Stark trap for 5 h. The mixture

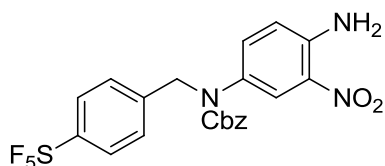
was filtered through a Buchner funnel packed with a thin pad of SiO₂ and the filtrate was stirred and allowed to cool to rt. The solvent was removed under reduced pressure to give the crude imine (1.23 g) as a bright orange-red solid, that was suspended in a mixture of 1,4-dioxane (5.2 mL) and MeOH (1.3 mL) and NaBH₄ (0.120 g, 3.14 mmol) was added in 3 portions at 15 min intervals. The resulting solution was allowed to stir at rt for 3 h, quenched with H₂O (25 mL) and extracted from brine with CH₂Cl₂ (3 x 200 mL). The solvent was removed under reduced pressure and the residue dried under high vacuum at 60 °C to give **1-18** (1.141 g, 3.666 mmol, 78%) as a dark purple oil: IR (CH₂Cl₂) 3483.58, 3370.03, 1573.93, 1521.07, 1324.97 cm⁻¹; ¹H NMR (CDCl₃, 400 MHz) δ 7.60 (d, 2 H, *J* = 8.0 Hz), 7.48 (d, 2 H, *J* = 8.0 Hz), 7.28 (d, 1 H, *J* = 2.8 Hz), 6.85 (dd, 1 H, *J* = 8.8, 2.8 Hz), 6.71 (d, 1 H, *J* = 8.8 Hz), 5.47 (br s, 2 H), 4.37 (s, 2 H), 3.92 (br s, 1 H); ¹³C NMR (CDCl₃ 100 MHz) δ 143.1, 139.1, 138.4, 132.6, 129.9 (q, *J* = 32.1 Hz), 127.8, 125.8 (q, *J* = 3.6 Hz), 125.3, 124.2 (q, *J* = 270.0 Hz), 120.3, 106.1, 48.5; HRMS (HESI) *m/z* calcd for C₁₄H₁₃N₃O₂F₃ (M+H) 312.0954, found 312.0955.



1-19

(4-Amino-3-nitrophenyl){[3-(trifluoromethyl)phenyl]methyl}amine (1-19). A solution of 2-nitro-*p*-phenylenediamine (0.753 g, 4.67 mmol) and PTSA (0.050 g, 0.26 mmol) in toluene (25 mL) was treated via syringe with 3-(trifluoromethyl)benzaldehyde (0.620 mL, 4.64 mmol). The resulting solution was heated to reflux with a Dean-Stark trap for 5 h, filtered through a Buchner funnel packed with a thin pad of SiO₂, and allowed to cool to rt. The solvent

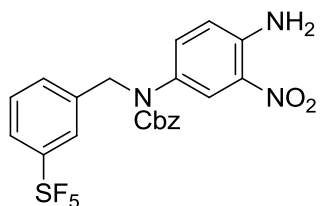
was removed under reduced pressure to give the crude imine (1.203 g) as bright orange solid, that was suspended in a mixture of 1,4-dioxane (3.7 mL) and MeOH (0.90 mL) and NaBH₄ (0.117 g, 0.655 mmol) was added in 3 portions at 15 minute intervals. The resulting solution was allowed to stir at rt for 3 h, quenched with H₂O (25 mL), and extracted with CH₂Cl₂ (3 x 100 mL). The combined organic extracts were washed with brine, dried (Na₂SO₄), filtered, and the solvent evaporated under reduced pressure to give crude **1-19** (1.141 g). Purification by chromatography on SiO₂ (70% CH₂Cl₂ in hexanes) gave **1-19** (1.10 g, 3.35 mmol, 72%) as a dark purple powder: Mp 95-96 °C (CH₂Cl₂); IR (ATR) 3456.00, 3396.67, 3330.69, 1515.08, 1323.54 cm⁻¹; ¹H NMR (CDCl₃, 400 MHz) δ 7.64 (s, 1 H), 7.55 (m, 2 H), 7.47 (m, 1 H), 7.29 (d, 1 H, *J* = 2.8 Hz), 6.86 (dd, 1 H, *J* = 8.8, 2.8 Hz), 6.71 (d, 1 H, *J* = 8.8 Hz), 5.74 (br s, 2 H), 4.36 (s, 2 H), 3.89 (br s, 1 H); ¹³C NMR (CDCl₃, 100 MHz) δ 140.0, 139.16, 138.5, 132.6, 131.2 (q, *J* = 32 Hz), 131.0, 129.3, 125.4, 124.5 (q, *J* = 3.7 Hz), 124.4 (q, *J* = 3.8 Hz), 124.2 (q, *J* = 271 Hz), 120.3, 106.2, 48.6; HRMS (ESI) *m/z* calcd for C₁₄H₁₃N₂O₃F₃ (M+H) 312.0954, found 312.0947.



1-20

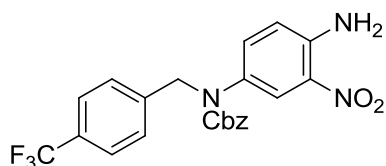
***N*-(4-Amino-3-nitrophenyl)(phenylmethoxy)-*N*-[[4-(pentafluorothio)phenyl]methyl]carboxamide (1-20).** A solution of **1-16** (0.207 g, 0.544 mmol) and DIPEA (0.110 mL, 0.665 mmol) in 1,4-dioxane (2.8 mL) at rt was treated dropwise via syringe with benzyl chloroformate (0.100 mL, 0.682 mmol). The resulting solution was allowed to stir for 18 h and was then quenched with 1:1 H₂O:CH₂Cl₂ (6.5 mL). The phases were separated and the aqueous phase extracted with CH₂Cl₂ (3 x 5 mL). The combined organic phases were washed with brine, dried

(Na₂SO₄), filtered, and the solvent evaporated to give crude **1-20** (0.280 g) as an orange foam that was used without further purification.



1-21

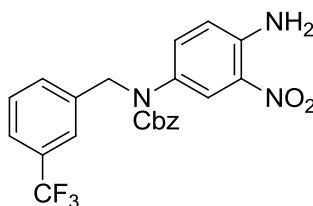
***N*-(4-Amino-3-nitrophenyl)(phenylmethoxy)-*N*-{[3-(pentafluorothio)phenyl]methyl} carboxamide (1-21).** A solution of **1-17** (0.202 g, 0.531 mmol) and DIPEA (0.090 mL, 0.54 mmol) in 1,4-dioxane (2.8 mL) at rt was treated dropwise via syringe with benzyl chloroformate (0.080 mL, 0.55 mmol). The resulting solution was allowed to stir for 3 h and was then quenched with 6.50 mL of 1:1 H₂O:CH₂Cl₂. The phases were separated and the aqueous phase extracted with CH₂Cl₂ (3 x 5 mL). The combined organic phases were washed with brine, dried (Na₂SO₄), filtered, and the solvent evaporated to give crude **1-21** (0.309 g) as an orange oil which was used without further purification.



1-22

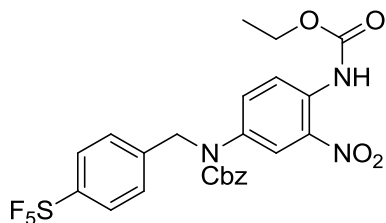
***N*-(4-Amino-3-nitrophenyl)(phenylmethoxy)-*N*-{[4-(trifluoromethyl)phenyl]methyl} carboxamide (1-22).** A solution of **1-18** (0.199 g, 0.639 mmol) and DIPEA (0.110 mL, 0.666 mmol) in 1,4-dioxane (3.2 mL) at rt was treated dropwise via syringe with benzyl chloroformate

(0.100 mL, 0.682 mmol). The resulting solution was allowed to stir for 4 h and was then quenched with 1:1 H₂O:CH₂Cl₂ (6.5 mL). The phases were separated and the aqueous phase extracted with CH₂Cl₂ (3 x 5 mL). The combined organic phases were washed with brine, dried (Na₂SO₄), filtered, and the solvent evaporated to give crude **1-22** (0.328 g) as a dark orange oil which was used without further purification.



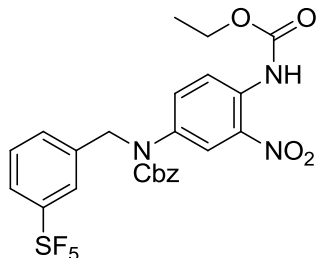
1-23

***N*-(4-Amino-3-nitrophenyl)(phenylmethoxy)-*N*-{[3-(trifluoromethyl)phenyl]methyl} carboxamide (1-23).** A solution of **1-19** (0.205 g, 0.659 mmol) and DIPEA (0.115 mL, 0.696 mmol) in 1,4-dioxane (3.5 mL) at rt was treated dropwise via syringe with benzyl chloroformate (0.100 mL, 0.682 mmol). The resulting solution was allowed to stir for 4 h at rt and was then quenched with 1:1 H₂O:CH₂Cl₂ (10 mL), the layers were separated, and the aqueous phase was extracted with CH₂Cl₂ (2 x 15 mL). The combined organic phases were washed with H₂O and brine, dried (Na₂SO₄), filtered, and the solvent evaporated to give crude **1-23** (0.331 g) as an orange oil which was used without further purification.



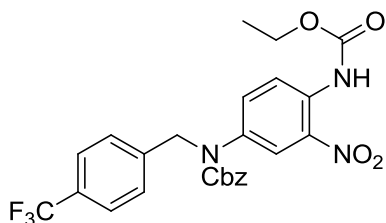
1-24

Ethoxy-*N*-(4-*N*-[(4-pentafluorothiophenyl)methyl](phenylmethoxy)carbonylamino}-2-nitrophenyl)carboxamide (1-24). A solution of crude **1-20** (0.050 g, 0.099 mmol) and DIPEA (0.050 mL, 0.30 mmol) in 1,4-dioxane (1.0 mL) at rt was treated dropwise via syringe with ethyl chloroformate (0.030 mL, 0.31 mmol). The resulting solution was allowed to stir at 70 °C for 24 h and was then quenched with 1:1 H₂O:CH₂Cl₂ (5 mL). The phases were separated and the aqueous phase extracted with CH₂Cl₂ (3 x 20 mL). The combined organic phases were washed with H₂O and brine, dried (MgSO₄), filtered, and the solvent evaporated under reduced pressure to give crude **1-24** (0.050 g) as an orange oil. The crude residue was purified by chromatography on SiO₂ (30% EtOAc in hexanes) to give **1-24** (0.036 g, 0.063 mmol, 63%, 82% brsm) as an orange oil: IR (CH₂Cl₂) 3365.79, 2094.66, 1738.05, 1706.74, 1515.21 cm⁻¹; ¹H NMR (CDCl₃, 400 MHz) δ 9.77 (s, 1 H), 8.54 (d, 1 H, *J* = 9.2 Hz), 8.04 (br s, 1 H), 7.68 (d, 2 H, *J* = 8.8 Hz), 7.33-7.27 (m, 5 H), 7.24-7.22 (m, 2 H), 5.19 (s, 2 H), 4.92 (s, 2 H), 4.26 (q, 2 H, *J* = 7.2 Hz), 1.34 (t, 3 H, *J* = 7.2 Hz); ¹³C NMR (CDCl₃, 100 MHz) δ 155.2, 153.4 (quint., *J* = 18.0 Hz), 153.2, 153.2, 141.0, 135.8, 135.7, 134.2, 128.8, 128.8, 128.2, 127.9, 126.6 (app. t, *J* = 4.6 Hz), 123.6, 121.4, 68.5, 62.3, 53.4, 14.5; HRMS (HESI) *m/z* calcd for C₂₄H₂₃N₃O₆F₅S (M+H) 576.1222, found 576.1221.



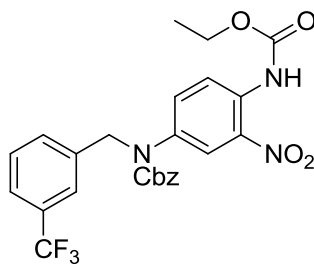
1-25

Ethoxy-*N*-(4-{*N*-[(4-pentafluorothiophenyl)methyl](phenylmethoxy)carbonylamino}-2-nitrophenyl)carboxamide (1-25). A solution of crude **1-21** (0.326 g), DIPEA (0.280 mL, 1.69 mmol), and DMAP (0.003 g, 0.02 mmol) in 1,4-dioxane (4 mL) at rt was treated dropwise via syringe with ethyl chloroformate (0.155 mL, 1.58 mmol). The resulting solution was allowed to stir at 70 °C for 2 d and was then quenched by the addition of 1:1 H₂O:CH₂Cl₂ (10 mL). The phases were separated and the aqueous phase extracted with CH₂Cl₂ (3 x 20 mL). The combined organic phases were washed with H₂O, 1 M aq. HCl, and brine, dried (MgSO₄), filtered, and the solvent evaporated under reduced pressure to give crude **1-25** (0.340 g) as an orange oil. The crude residue was purified by chromatography on SiO₂ (20% EtOAc in hexanes) to give **1-25** (0.052 g) as a yellow oil which was used without further purification.



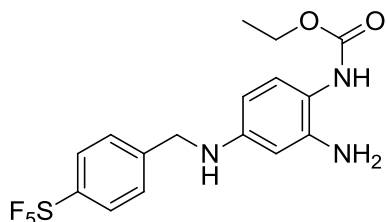
1-26

Ethoxy-*N*-[2-nitro-4-((phenylmethoxy)-*N*-{[4-(trifluoromethyl)phenyl]methyl} carbonylamino)phenyl]carboxamide (1-26). A solution of crude **1-22** (0.310 g) and DIPEA (0.670 mL, 4.05 mmol) in 1,4-dioxane (5.2 mL) at rt was treated dropwise via syringe with ethyl chloroformate (0.395 mL, 4.03 mmol). The resulting solution was allowed to stir at 70 °C for 3 d and was then quenched by the addition of 1:1 H₂O:CH₂Cl₂ (10 mL). The phases were separated and the aqueous phase extracted with CH₂Cl₂ (3 x 20 mL). The combined organic phases were washed with H₂O and brine, dried (Na₂SO₄), filtered, and the solvent evaporated under reduced pressure to give crude **1-26** (0.350 g) as an orange solid. The crude solid was purified by chromatography on SiO₂ (20% EtOAc in hexanes) to give **1-26** (0.194 g, 0.375 mmol, 59% over 2 steps) as an orange oil: IR (CH₂Cl₂) 3365.80, 2983.18, 1738.22, 1706.37, 1514.40, 1323.26 cm⁻¹; ¹H NMR (DMSO-d₆, 400 MHz, 353 K) δ 9.50 (br s, 1 H), 7.96 (d, 1 H, *J* = 2.4 Hz), 7.77 (d, 1 H, *J* = 8.8 Hz), 7.64 (d, 1 H, *J* = 8.4 Hz), 7.60 (dd, 1 H, *J* = 8.8, 2.4 Hz), 7.48 (d, 1 H, *J* = 8.0 Hz), 7.33-7.26 (m, 7 H), 5.19 (s, 2 H), 5.05 (s, 2 H), 4.15 (q, 2 H, *J* = 7.2 Hz), 1.24 (t, 3 H, *J* = 7.2 Hz); ¹³C NMR (DMSO-d₆, 100 MHz, 353 K) δ 154.2, 152.9, 141.8, 140.0, 136.8, 135.8, 131.8, 130.3, 128.0, 127.9, 127.7, 127.5, 127.1, 124.9 (q, *J* = 3.7 Hz), 123.8 (q, *J* = 270.3 Hz), 123.8, 122.5, 67.0, 60.8, 52.3, 13.8; HRMS (HESI) *m/z* calcd for C₂₅H₂₁N₃O₆F₃ (M-H) 516.1377, found 516.1372.



1-27

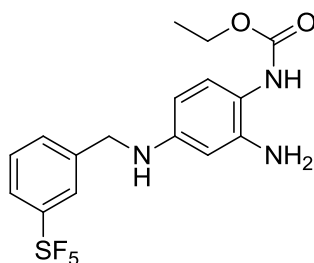
Ethoxy-*N*-[2-nitro-4-((phenylmethoxy)-*N*-{[3-(trifluoromethyl)phenyl]methyl} carbonylamino)phenyl]carboxamide (1-27). A solution of crude **1-23** (0.330 g) and DIPEA (0.545 mL, 3.30 mmol) in 1,4-dioxane (5 mL) at rt was treated dropwise via syringe with ethyl chloroformate (0.160 mL, 1.63 mmol). The resulting solution was allowed to stir at 70 °C for 2 d and was then quenched by the addition of 1:1 H₂O:CH₂Cl₂ (10 mL), the layers were separated and the aqueous phase was extracted with CH₂Cl₂ (2 x 20 mL). The combined organic phases were washed with H₂O (2 x 20 mL) and brine (2 x 10 mL), dried (MgSO₄), filtered, and the solvent evaporated under reduced pressure to give crude **1-27** (0.310 g) as an orange oil. The crude oil was purified by chromatography on SiO₂ (20% EtOAc in hexanes) to give **1-27** (0.113 g) as a yellow oil which was carried on without further purification.



1-5

***N*-[2-amino-4-({[4-(pentafluorothio)phenyl]methyl}amino)phenyl]ethoxycarboxamide (1-5)**. A solution of **1-24** (0.047 g, 0.082 mmol) and 10% Pd/C (0.010 g, 0.009 mmol, 10 mol%) in a mixture of 1,4-dioxane (0.46 mL) and EtOH (0.24 mL) was allowed to stir for 21 h at rt under an H₂ atmosphere (balloon). The reaction mixture was diluted with Et₂O (5 mL) and filtered through a pad of Celite. The organic phase was concentrated under reduced pressure to give crude **1-5** (0.037 g) as an orange oil. The crude oil was purified by chromatography on SiO₂ (50% EtOAc in hexanes) to give **1-5** (0.018 g, 0.044 mmol, 54%) as a light brown solid: Mp 146-147 °C (CH₂Cl₂); IR

(ATR) 3377.56, 2925.72, 1697.84, 1620.85, 1525.67 cm^{-1} ; ^1H NMR (CDCl_3 , 400 MHz) δ 7.70 (d, 2 H, $J = 8.4$ Hz), 7.43 (d, 2 H, $J = 8.4$ Hz), 6.92 (d, 1 H, $J = 8.4$ Hz), 6.02 (dd, 1 H, $J = 8.4$, 2.4 Hz), 5.95 (d, 1 H, $J = 2.4$ Hz), 4.35 (s, 2 H), 4.18 (q, 2 H, $J = 7.2$ Hz), 3.90 (br s, 2 H), 1.28 (t, 3 H, $J = 7.2$ Hz); ^{13}C NMR (CDCl_3 , 100 MHz) δ 155.6, 152.9 (quint., $J = 13.5$ Hz), 147.4, 143.9, 142.2, 128.1, 127.3, 126.4 (quint., $J = 4.0$ Hz), 114.5, 104.5, 100.8, 61.5, 47.6, 14.7; HRMS (HESI) m/z calcd for $\text{C}_{16}\text{H}_{19}\text{N}_3\text{O}_2\text{F}_5\text{S}$ (M+H) 412.1113, found 412.1111.

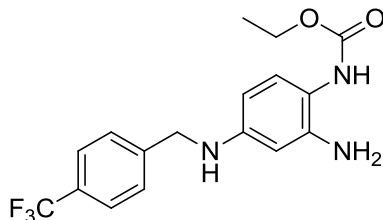


1-6

***N*-[2-Amino-4-**

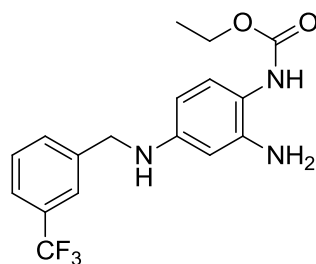
({[3(pentafluorothio)phenyl]methyl}amino)phenyl]ethoxycarboxamide (1-6). A solution of **1-25** (0.050 g, 0.087 mmol) and 10% Pd/C (0.010 g, 0.010 mmol) in 1,4-dioxane (0.46 mL) and EtOH (0.24 mL) was allowed to stir under an H_2 atmosphere (balloon) for 18 h. The reaction mixture was diluted with Et_2O (5 mL) and filtered through a pad of Celite. The solvent was removed under reduced pressure to give crude **1-6** (0.049 g) as an orange oil. The crude residue was purified by chromatography on SiO_2 (50% EtOAc in hexanes) to give **1-6** (0.027 g, 0.066 mmol, 76%) as a light brown oil that solidified on standing: Mp 52-53 $^\circ\text{C}$ (CH_2Cl_2); IR (ATR) 3355.44, 2931.13, 1699.36, 1623.12, 1525.18, 1229.40 cm^{-1} ; ^1H NMR (CDCl_3 , 400 MHz) δ 7.73 (s, 1 H), 7.65 (d, 1 H, $J = 8.0$ Hz), 7.50 (d, 1 H, $J = 7.6$ Hz), 7.42 (app. t, 1 H, $J = 7.8$ Hz), 6.92 (d, 1 H, $J = 8.4$ Hz), 6.04 (dd, 1 H, $J = 8.0$, 2.0 Hz), 5.98 (d, 1 H, $J = 2.0$ Hz), 4.34 (s, 2 H), 4.18

(q, 2 H, $J = 7.1$ Hz), 3.85 (br s, 2 H), 1.28 (t, 3 H, $J = 7.2$ Hz); ^{13}C NMR (CDCl_3 , 175 MHz) δ 155.6, 154.4 (quint., $J = 16.8$ Hz), 147.4, 143.1, 141.1, 130.4, 129.1, 128.0, 124.9 (quint., $J = 4.2$ Hz), 124.8 (quint., $J = 4.4$ Hz), 114.5, 104.5, 100.9, 61.5, 48.1, 14.7; HRMS (HESI) m/z calcd for $\text{C}_{16}\text{H}_{19}\text{N}_3\text{O}_2\text{F}_5\text{S}$ (M+H) 412.1113, found 412.1101.



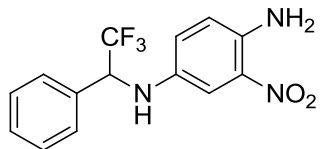
1-7

***N*-[2-Amino-4-((4-(trifluoromethyl)phenyl)methyl)amino)phenyl]ethoxycarboxamide (1-7)**. A solution of **1-26** (0.090 g, 0.174 mmol) and 10% Pd/C (0.018 g, 0.017 mmol) in a mixture of 1,4-dioxane (1 mL) and EtOH (0.50 mL) was allowed to stir at rt for 18 h under an H_2 atmosphere (balloon). The reaction mixture was diluted with Et_2O (5 mL) and filtered through a pad of Celite. The organic phase was concentrated under reduced pressure to give crude **1-7** (0.051 g) as a light brown solid. The crude solid was purified by chromatography on SiO_2 (50% EtOAc in hexanes) to give **1-7** (0.044 g, 0.12 mmol, 72%) as a grey solid: Mp 171-172 $^\circ\text{C}$ (CH_2Cl_2); IR (ATR) 3279.60, 2980.62, 1677.20, 1526.96 cm^{-1} ; ^1H NMR (CDCl_3 , 400 MHz) δ 7.59 (d, 2 H, $J = 8.4$ Hz), 7.46 (d, 2 H, $J = 8.0$ Hz), 6.92 (d, 1 H, $J = 8.4$ Hz), 6.05 (dd, 1 H, $J = 8.4, 2.4$ Hz), 5.98 (d, 1 H, $J = 2.4$ Hz), 4.37 (s, 2 H), 4.19 (q, 2 H, $J = 7.2$ Hz), 4.06 (br s, 1 H), 3.74 (br s, 2 H), 1.28 (t, 3 H, $J = 7.0$ Hz); ^{13}C NMR (CDCl_3 , 100 MHz) δ 155.7, 147.6, 143.9, 143.2, 129.6 (q, $J = 32.0$ Hz), 128.1, 127.5, 125.7 (q, $J = 3.7$ Hz), 124.3 (q, $J = 270.2$ Hz), 114.3, 104.5, 100.6, 61.5, 48.0, 14.8; HRMS (HESI) m/z calcd for $\text{C}_{17}\text{H}_{19}\text{N}_3\text{O}_2\text{F}_3$ (M+H) 354.1424, found 354.1425.



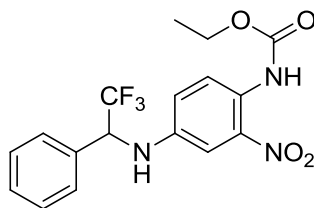
1-8

***N*-[2-Amino-4-((3-(trifluoromethyl)phenyl)methyl)amino)phenyl]ethoxycarboxamide (1-8)**. A suspension of impure **1-27** (0.100 g, 0.193 mmol) and 10% Pd/C (0.020 g, 0.018 mmol, 10 mol%) in 1,4-dioxane (1 mL) and EtOH (0.50 mL) was allowed to stir at rt for 18 h under an H₂ atmosphere (balloon). The reaction mixture was diluted with Et₂O, filtered through a pad of Celite, and the solvent removed under reduced pressure to give crude **1-8** (0.067 g) as a dark brown oil. The crude oil was purified by chromatography on SiO₂ (50% EtOAc in hexanes) to give **1-8** (0.056 g, 0.16 mmol, 24% over 3 steps) as an off-white solid: Mp 103-104 °C (CH₂Cl₂); IR (ATR) 3335.08, 2987.62, 1723.51, 1679.79, 1535.27 cm⁻¹; ¹H NMR (CDCl₃, 400 MHz) δ 7.61 (s, 1 H), 7.53 (app. t, 2 H, *J* = 7.0 Hz), 7.46-7.42 (m, 1 H), 6.92 (d, 1 H, *J* = 8.0 Hz), 6.05 (dd, 1 H, *J* = 8.4, 2.4 Hz), 5.98 (d, 1 H, *J* = 2.4 Hz), 4.34 (s, 2 H), 4.19 (q, 2 H, *J* = 7.2 Hz), 3.76 (br s, 2 H), 1.28 (t, 3 H, *J* = 7.2 Hz); ¹³C NMR (CDCl₃, 100 MHz) δ 155.6, 147.6, 143.2, 140.8, 131.1 (q, *J* = 32.0 Hz), 130.7, 129.2, 128.0, 124.3 (q, *J* = 270.9 Hz), 124.2-124.1 (overlapping q.), 114.3, 104.5, 100.8, 61.5, 48.1, 14.7; HRMS (HESI) *m/z* calcd for C₁₇H₁₉N₃O₂F₃ (M+H) 354.1424, found 354.1421.



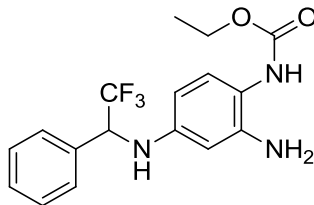
1-29

(4-Amino-3-nitrophenyl)(2,2,2-trifluoro-1-phenylethyl)amine (1-29). A solution of 2-nitro-*p*-phenylenediamine (0.504 g, 3.13 mmol) and PTSA (0.034 g, 0.17 mmol) in toluene (15 mL) at rt was treated with 2,2,2-trifluoroacetophenone (0.544 g, 3.09 mmol) and was stirred at reflux for 24 h with a Dean-Stark trap. The reaction mixture was filtered through a pad of SiO₂ and the solvent evaporated under reduced pressure to give the crude imine (0.170 g), which was suspended in 1,4-dioxane (4 mL) and MeOH (1 mL) and NaBH₄ (0.125 g, 3.27 mmol) was added in 3 portions at 15 minute intervals. The resulting solution was allowed to stir at rt for 3 h. H₂O (25 mL) was added and solution was extracted with CH₂Cl₂ (3 x 20 mL). The organic phase was dried (Na₂SO₄), filtered, and the solvent evaporated under reduced pressure. Further drying under high vacuum gave **1-29** (0.120 g, 0.386 mmol, 12%) as a dark red solid: Mp 126-127 °C (CH₂Cl₂); IR (ATR) 3436.04, 3387.95, 333.42, 1581.30, 1514.40, 1326.05, 1237.64; ¹H NMR (CDCl₃, 400 MHz) δ 7.44-7.38 (m, 5 H), 7.33 (d, 1 H, *J* = 2.8 Hz), 6.89 (dd, 1 H, *J* = 9.2, 2.8 Hz), 6.69 (d, 1 H, *J* = 8.8 Hz), 5.75 (br s, 2 H), 4.84 (m, 1 H), 4.13 (d, 1 H, *J* = 7.6 Hz); ¹³C NMR (CDCl₃, 100 MHz) δ 139.2, 136.6, 133.6, 132.3, 129.51, 129.2, 128.0, 126.0, 125.1 (q, *J* = 280.3 Hz), 120.3, 108.6, 61.4 (q, *J* = 30.0 Hz); HRMS (HESI) *m/z* calcd for C₁₄H₁₃N₃O₂F₃ (M+H) 312.0954, found 312.0953.



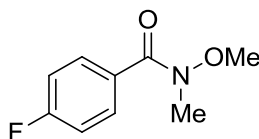
1-31

Ethoxy-*N*-{2-nitro-4-[(2,2,2-trifluoro-1-phenylethyl)amino]phenyl}carboxamide (1-31). A solution of **1-29** (0.060 g, 0.19 mmol) and DIPEA (0.065 mL, 0.39 mmol) in 1,4-dioxane (1.3 mL) at rt was treated dropwise via syringe with ethyl chloroformate (0.020 mL, 0.20 mmol). The resulting solution was allowed to stir at 50 °C for 18 h and was then quenched by the addition of 1:1 H₂O:CH₂Cl₂ (10 mL). The layers were separated and the aqueous phase was extracted with CH₂Cl₂ (3 x 10 mL). The combined organic phases were washed with H₂O (2 x 10 mL) and brine (2 x 10 mL), dried (Na₂SO₄), filtered, and the solvent evaporated under reduced pressure to give crude **1-31** (0.100 g) as an orange-red oil. The crude solid was purified by chromatography on SiO₂ (40-60% CH₂Cl₂ in hexanes) to give **1-31** (0.054 g, 0.14 mmol, 73%) as a red oil: IR (CH₂Cl₂) 3372.96, 2983.93, 1718.95, 1523.09, 1324.06 cm⁻¹; ¹H NMR (CDCl₃, 500 MHz) δ 9.39 (s, 1 H), 8.30 (d, 1 H, *J* = 9.0 Hz), 7.46-7.40 (m, 6 H), 6.98 (dd, 1 H, *J* = 9.5, 2.2 Hz), 4.91 (m, 1 H), 4.56 (br d, 1 H, *J* = 7.0 Hz), 4.22 (q, 2 H, *J* = 7.0 Hz), 1.31 (t, 3 H, *J* = 7.0 Hz); ¹³C NMR (CDCl₃, 125 MHz) δ 153.6, 140.7, 137.0, 133.1, 129.6, 129.3, 128.0, 127.7, 124.9 (q, *J* = 280.5 Hz), 122.7, 122.6, 121.5, 108.8, 61.9, 60.6 (q, *J* = 30.4 Hz), 14.5; HRMS (HESI) *m/z* calcd for C₁₇H₁₇N₃O₄F₃ (M+H) 384.1166, found 384.1163.



1-10

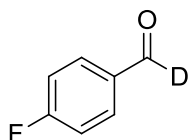
***N*-{2-Amino-4-[(2,2,2-trifluoro-1-phenylethyl)amino]phenyl}ethoxycarboxamide (1-10).** A suspension of **1-31** (0.050 g, 0.13 mmol) and 10% Pd/C (0.014 g, 0.013 mmol) was allowed to stir under an H₂ atmosphere (balloon) for 18 h. The reaction mixture was diluted with Et₂O, filtered through Celite, and the solvent evaporated under reduced pressure to give crude **1-10** (0.066 g) as a gray oil. The crude residue was purified by chromatography on SiO₂ (0-10% EtOAc in CH₂Cl₂) to give **1-10** (0.041 g, 0.12 mmol, 89%) as a clear, colorless oil that solidified upon standing: Mp 51-52 °C (CH₂Cl₂); IR (ATR) 3346.05, 2984.78, 1696.03, 1524.18 cm⁻¹; ¹H NMR (CDCl₃, 400 MHz) δ 7.42-7.37 (m, 5 H), 6.90 (d, 1 H, *J* = 8.0 Hz), 6.05 (app. d, 1 H, *J* = 8.4 Hz), 6.01 (app. s, 1 H), 4.84 (m, 1 H), 4.28 (d, 1 H, *J* = 7.2 Hz), 4.17 (q, 2 H, *J* = 7.1 Hz), 3.72 (br s, 2 H), 1.27 (t, 3 H, *J* = 6.6 Hz); ¹³C NMR (CDCl₃, 100 MHz) δ 155.5, 145.3, 143.0, 134.2, 129.2, 129.0, 128.0, 125.1 (q, *J* = 280.2 Hz), 115.5, 105.2, 102.1, 61.5, 60.7 (q, *J* = 29.8 Hz), 14.7; HRMS (HESI) *m/z* calcd for C₁₇H₁₉N₃O₂F₃ (M+H) 354.1424, found 354.1422.



1-32

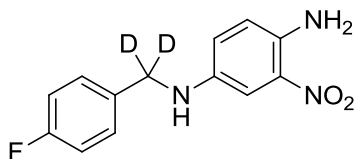
(4-Fluorophenyl)-*N*-methoxy-*N*-methylcarboxamide (1-32).¹ A solution of methoxymethylamine hydrochloride (0.634 g, 6.37 mmol) and Et₃N (0.860 mL, 6.12 mmol) in

CH₂Cl₂ (3.75 mL) at 0 °C was treated dropwise via syringe with 4-fluorobenzoyl chloride (0.370 mL, 3.07 mmol) over 30 min and the resulting solution was allowed to stir at rt for 2 h. The reaction mixture was poured into H₂O and extracted with CH₂Cl₂ (3 x 20 mL). The organic extracts were washed with brine, dried (MgSO₄), and the solvent removed under reduced pressure. Further drying under high vacuum gave crude **1-32** (0.672 g, 2.63 mmol, quant.) which was used without further purification: ¹H NMR (CDCl₃, 400 MHz) δ 7.74 (m, 2 H), 7.08 (m, 2 H), 3.53 (s, 3 H), 3.36 (s, 3 H); HRMS (HESI) *m/z* calcd for C₉H₁₁NO₂F (M+H) 184.0768, found 184.0768.



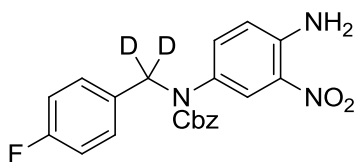
1-33

4-Fluorobenzaldehyde-*d* (1-33). To a solution of **1-33** (0.062 g, 0.338 mmol) in THF (1.9 mL) at -78 °C was added LiAlD₄ (0.018 g, 0.42 mmol) portionwise and the mixture was stirred for 2 h at the same temperature. The reaction mixture was quenched with H₂O at -78 °C, Et₂O was added, and the precipitate removed by filtration through a pad of Celite. The filtrate was washed with H₂O and brine, dried (Na₂SO₄), and concentrated under reduced pressure. Further drying under high vacuum for 1 h gave 0.032 g crude **1-33** as a pale yellow oil which was used without further purification.



1-34

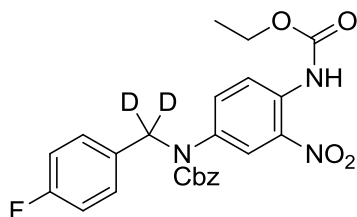
(4-Amino-3-nitrophenyl)[(4-fluorophenyl)methyl]amine- d_2 (1-34). A solution of 2-nitro-*p*-phenylenediamine (0.602 g, 3.73 mmol), PTSA (0.040 g, 0.21 mmol) and crude **1-33** (0.273 g) was heated to reflux with a Dean-Stark trap for 18 h. The solution was filtered through a thin pad of SiO₂ and the solvent evaporated under reduced pressure to give the crude imine (0.328 g) which was suspended in 1,4-dioxane (4 mL) and MeOH (1 mL) and NaBD₄ (0.111 g, 2.60 mmol) was added in 3 portions at 15 minute intervals. The resulting solution was allowed to stir at rt for 3 h and was then quenched with H₂O (25 mL) and filtered to give **1-34** (0.241 g, 0.915 mmol, 42% over 2 steps) as a dark purple powder: Mp 113-114 °C (H₂O); IR (ATR) 3517.22, 3496.96, 3371.18, 1577.41, 1502.47, 1329.45 cm⁻¹; ¹H NMR (CDCl₃, 400 MHz) δ 7.34-7.27 (m, 3 H), 7.28 (d, 1 H, J = 2.4 Hz), 7.03 (t, 2 H, J = 8.6 Hz), 6.84 (dd, 1 H, J = 8.8, 2.4 Hz), 5.75 (br s, 2 H), 3.80 (br s, 1 H); ¹³C NMR (CDCl₃, 100 MHz) δ 162.3 (d, J = 244.0 Hz), 139.4, 138.3, 134.5 (d, J = 3.0 Hz), 132.5, 129.3 (d, J = 8.0 Hz), 125.5, 120.2, 115.7 (d, J = 21.3 Hz), 105.9, 47.7 (t, J = 20.6 Hz); HRMS (HESI) m/z calcd for C₁₃H₁₁D₂N₃O₂F (M+H) 264.1112, found 264.1110.



1-35

***N*-(4-Amino-3-nitrophenyl)-*N*-[(4-fluorophenyl)methyl](phenylmethoxy)carboxamide- d_2 (1-35)**. A solution of **1-34** (0.100 g, 0.380 mmol) and DIPEA (0.095 mL, 0.58 mmol) in 1,4-dioxane (1.9 mL) at rt was treated dropwise via syringe with benzyl chloroformate (0.060 mL, 0.41 mmol). The resulting solution

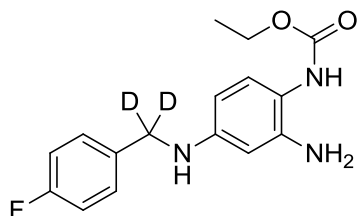
was allowed to stir at rt for 18 h and was then quenched by the addition of 1:1 H₂O:CH₂Cl₂ (10 mL). The layers were separated and the aqueous phase extracted with CH₂Cl₂ (3 x 10 mL). The combined organic phases were washed with H₂O (2 x 10 mL) and brine (2 x 10 mL), dried (Na₂SO₄), filtered, and the solvent evaporated under reduced pressure to give crude **1-35** (0.220 g) as an orange-yellow oil which was used without further purification.



1-36

Ethoxy-N-(4-{N-[(4-fluorophenyl)methyl](phenylmethoxy)carbonylamino}-2-nitrophenyl)carboxamide-*d*₂ (1-36). A solution of crude **1-35** (0.220 g) and DIPEA (0.190 mL, 1.15 mmol) in 1,4-dioxane (3.5 mL) at rt was treated dropwise via syringe with ethyl chloroformate (0.090 mL, 0.92 mmol). The resulting solution was allowed to stir at 70 °C for 2 d and was then quenched by the addition of 1:1 H₂O:CH₂Cl₂ (20 mL). The layers were separated and the aqueous phase extracted with CH₂Cl₂ (2 x 10 mL). The combined organic phases were washed with 1 M aq. HCl (2 x 10 mL) and brine (2 x 10 mL), dried (MgSO₄), filtered, and the filtrate concentrated under reduced pressure. Further drying under high vacuum gave crude **1-36** (0.320 g) as an orange-yellow solid. The crude solid was purified by chromatography on SiO₂ (20% EtOAc in hexanes) to give **1-36** (0.100 g, 0.213 mmol, 56%) as a yellow oil: IR (CH₂Cl₂) 3364.46, 2981.47, 1738.36, 1702.40, 1509.76, 1331.36; ¹H NMR (CDCl₃, 400 MHz) δ 9.77 (s, 1 H), 8.51 (d, 1 H, *J* = 8.8 Hz), 7.99 (br s, 1 H), 7.36-7.30 (m, 4 H), 7.27-7.25 (m, 2 H), 7.17-7.13 (m, 2 H), 6.96 (tt, 2 H, *J* = 8.6, 2.3 Hz), 5.19 (s, 2 H), 4.26 (q, 2 H, *J* = 7.0 Hz), 1.34 (t, 3 H, *J* =

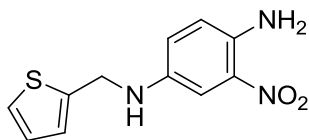
7.0 Hz); ^{13}C NMR (CDCl_3 , 100 MHz) δ 162.4 (d, $J = 245.0$ Hz), 155.2, 153.1, 136.0, 135.7, 134.7, 134.0, 132.6 (d, $J = 3.2$ Hz), 129.7, 128.7, 128.4, 128.1, 123.9, 121.1, 115.7 (d, $J = 21.3$ Hz), 68.1, 62.2, 52.8 (br), 14.5; HRMS (HESI) m/z calcd for $\text{C}_{24}\text{H}_{19}\text{D}_2\text{N}_3\text{O}_6\text{F}$ (M-H) 468.1534, found 468.1545.



1-9

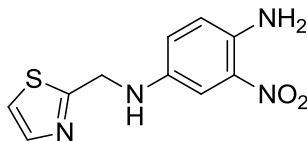
***N*-(2-Amino-4-[[4-fluorophenyl)methyl]amino]phenyl)ethoxycarboxamide- d_2 (**1-9**).**

A suspension of **1-36** (0.095 g, 0.196 mmol) and 10% Pd/C (0.022 g, 0.020 mmol) in 1,4-dioxane (1.1 mL) and EtOH (0.60 mL) was allowed to stir at rt under an H_2 atmosphere (balloon) for 18 h. The solution was diluted with Et_2O (5 mL), filtered through a pad of Celite, and the solvent evaporated under reduced pressure to give crude **1-9** (0.078 g) as a light brown oil. The crude residue was purified by chromatography on SiO_2 (55% EtOAc in hexanes) to give **1-9** (0.045 g, 0.147 mmol, 75%) as a light brown solid: Mp 142-143 $^\circ\text{C}$ (CH_2Cl_2); IR (ATR) 3394.70, 3342.61, 2987.36, 1675.57, 1506.24 cm^{-1} ; ^1H NMR (CDCl_3 , 400 MHz) δ 7.32 – 7.28 (m, 2 H), 7.01 (app. t, 2 H, $J = 8.6$ Hz), 6.91 (d, 1 H, $J = 8.4$ Hz), 6.04 (dd, 1 H, $J = 8.4, 2.4$ Hz), 5.98 (d, 1 H, $J = 2.4$ Hz), 4.18 (q, 2 H, $J = 7.0$ Hz), 3.78 (br s, 2 H), 1.28 (t, 3 H, $J = 7.0$ Hz); ^{13}C NMR (CDCl_3 , 100 MHz) 162.1 (d, $J = 243.0$ Hz), 155.7, 147.8, 143.1, 135.1 (d, $J = 3.0$ Hz), 129.0 (d, $J = 8.0$ Hz), 128.0, 115.5 (d, $J = 21.2$ Hz), 114.1, 104.4, 100.8, 61.5, 47.1 (t, $J = 20.6$ Hz), 14.7; HRMS (HESI) m/z calcd for $\text{C}_{16}\text{H}_{17}\text{D}_2\text{N}_3\text{O}_2\text{F}$ (M+H) 306.1581, found 306.1584.



1-37

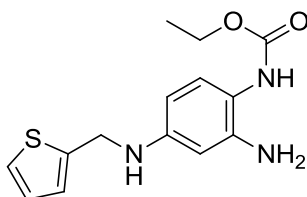
(4-Amino-3-nitrophenyl)(2-thienylmethyl)amine (1-37). A solution of thiophene-2-carboxaldehyde (0.125 mL, 1.34 mmol), 2-nitro-*p*-phenylenediamine (0.210 g, 1.30 mmol), PTSA (0.035 g, 0.18 mmol), and 4 Å mol. sieves (1.063 g) in CH₂Cl₂ (3.1 mL) and MeOH (3.1 mL) was allowed to stir at rt for 5 h. The resulting solution was filtered through Celite and the solvent removed under reduced pressure to give a dark brown solid that was dissolved in CH₂Cl₂ (20 mL), filtered through a thin pad of SiO₂ eluting with the same solvent, and concentrated under reduced pressure to give crude imine (0.250 g) as a bright orange solid. The solid was suspended in 1,4-dioxane (1.5 mL) and MeOH (0.50 mL), NaBH₄ (0.070 g, 1.83 mmol) was added in 3 portions at 15 min intervals, and the resulting solution was allowed to stir at rt for 20 h. The reaction mixture was quenched by the addition of 1:1 H₂O:CH₂Cl₂ (30 mL). The layers were separated and the aqueous layer was extracted with CH₂Cl₂ (3 x 10 mL). The combined organic layers were washed with H₂O (2 x 10 mL) and brine (2 x 10 mL), dried (Na₂SO₄), filtered, and the solvent evaporated under reduced pressure. Further drying under high vacuum at 50 °C gave **1-37** (0.230 g, 0.923 mmol, 71%) as a dark red solid: Mp 103-105 °C (CH₂Cl₂); IR (ATR) 3506.46, 3380.50, 3115.96, 1576.61, 1518.86, 1332.92 cm⁻¹; ¹H NMR (CDCl₃, 400 MHz) δ 7.37 (d, 1 H, *J* = 2.8 Hz), 7.23 (dd, 1 H, *J* = 4.8, 1.2 Hz), 7.03-7.02 (m, 1 H), 6.97 (dd, 1 H, *J* = 5.2, 3.6 Hz), 6.88 (dd, 1 H, *J* = 8.8, 2.8 Hz), 6.71 (d, 1 H, *J* = 8.8 Hz), 5.74 (br s, 2 H), 4.48 (s, 2 H), 3.83 (br s, 2 H); ¹³C NMR (CDCl₃, 100 MHz) δ 142.2, 139.0, 138.5, 132.6, 127.1, 125.6, 125.6, 125.0, 120.2, 106.6, 44.2; HRMS (HESI) *m/z* calcd for C₁₁H₁₂N₃O₂S (M+H) 250.0645, found 250.0644.



1-39

(4-Amino-3-nitrophenyl)(1,3-thiazol-2-ylmethyl)amine (1-39). A solution of 2-thiazolecarboxaldehyde (0.115 mL, 1.27 mmol), 2-nitro-*p*-phenylenediamine (0.209 g, 1.30 mmol), PTSA (0.025 g, 0.13 mmol), and 4 Å mol. sieves (1.15 g) in CH₂Cl₂ (3.1 mL) and MeOH (3.1 mL) was allowed to stir for 18 h at rt. The resulting solution was filtered through Celite and the solvent removed under reduced pressure to give a dark brown solid. This solid was suspended in CH₂Cl₂ (20 mL), filtered through a thin pad of SiO₂ eluting with the same solvent, and the solvent removed under reduced pressure to give crude imine (0.205 g) as a bright orange solid. The solid was suspended in 1,4-dioxane (2 mL) and MeOH (0.75 mL), NaBH₄ (0.035 g, 0.92 mmol) was added in a single portion, and the resulting solution was allowed to stir at rt for 8 h. The reaction mixture was quenched by the addition of 1:1 H₂O:CH₂Cl₂ (15 mL). The layers were separated and the aqueous layer was extracted with CH₂Cl₂ (3 x 10 mL). The combined organic layers were washed with H₂O (2 x 10 mL) and brine (2 x 10 mL), dried (Na₂SO₄), filtered, and the solvent evaporated under reduced pressure. Further drying under high vacuum at 50 °C overnight gave **1-39** (0.194 g, 0.775 mmol, 61%) as a dark red solid: Mp 161-162 °C (CH₂Cl₂); IR (ATR) 3469.82, 3380.19, 3349.79, 1584.11, 1518.80, 1384.29, 1330.62 cm⁻¹; ¹H NMR (DMSO-d₆, 500 MHz) δ 7.74 (d, 1 H, *J* = 3.0 Hz), 7.58 (d, 1 H, *J* = 3.0 Hz), 7.04 (br s, 2 H), 7.02 (d, 1 H, *J* = 3.0 Hz), 6.99 (d, 1 H, *J* = 2.5 Hz), 6.90 (d, 1 H, *J* = 9.0 Hz), 6.39 (t, 1 H, *J* = 6.0 Hz), 4.54 (d, 2 H, *J* = 6.0 Hz); ¹³C NMR (DMSO-d₆, 125 MHz) δ 171.8, 142.4, 140.1, 138.2,

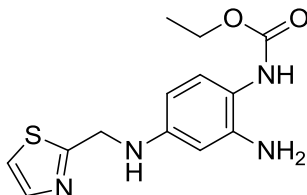
129.9, 126.5, 120.4, 119.9, 103.0, 45.6; HRMS (HESI) m/z calcd for $C_{10}H_{11}N_4O_2S$ (M+H) 251.0597, found 251.0595.



1-11

***N*-(2-Amino-4-[(2-thienylmethyl)amino]phenyl)ethoxycarboxamide (1-11).** A suspension of **1-37** (0.104 g, 0.334 mmol, 80% purity) and 10% Pd/C (0.035 g, 0.032 mmol) in 1,4-dioxane (1.7 mL) and EtOH (0.70 mL) was allowed to stir at rt for 16 h under an H_2 atmosphere. The reaction mixture was diluted with Et_2O , filtered through a pad of Celite, and the solvent evaporated under reduced pressure. Further drying under high vacuum gave the crude aryl triamine (0.093 g) as a dark yellow oil. A solution of crude aryl triamine (0.093 g) and Et_3N (0.080 mL, 0.57 mmol) in CH_2Cl_2 (1.2 mL) at rt was treated dropwise via syringe over 15 min with a solution of **1-41** (0.050 g, 0.21 mmol) in CH_2Cl_2 (1.2 mL). The resulting solution was allowed to stir at rt for 18 h, the solvent was evaporated under reduced pressure, the crude residue dissolved in EtOAc (20 mL), and washed with sat. aq. $NaHCO_3$ (5 x 10 mL). The aqueous washes were extracted with EtOAc (2 x 20 mL) and the combined organic phases were dried ($MgSO_4$), filtered, and the solvent evaporated under reduced pressure to give crude **1-11** (0.200 g) as a brown-green oil. The crude residue was purified by chromatography on SiO_2 (5-10% EtOAc in CH_2Cl_2) to give **1-11** (0.037 g, 0.13 mmol, 60%) as a gray oil that solidified upon standing: Mp 95-96 °C (CH_2Cl_2); IR (ATR) 3403.37, 3287.93, 1677.01, 1518.63 cm^{-1} ; 1H NMR ($CDCl_3$, 500 MHz) δ 7.20 (dd, 1 H, $J = 5.0, 1.5$ Hz), 6.99 (app. d, 1 H, $J = 2.5$ Hz), 6.96 (dd, 1 H,

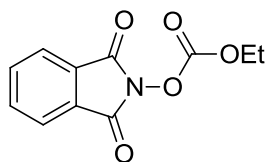
$J = 5.0, 3.5$ Hz), 6.93 (d, 1 H, $J = 8.5$ Hz), 6.09 (dd, 1 H, $J = 8.3, 2.5$ Hz), 6.04 (d, 1 H, $J = 2.5$ Hz), 4.44 (s, 2 H), 4.19 (q, 2 H, $J = 7.0$ Hz), 3.82 (br s, 3 H), 1.28 (t, 3 H, $J = 6.5$ Hz); ^{13}C NMR (CDCl_3 , 125 MHz) δ 155.6, 147.4, 143.1, 127.8, 127.0, 125.1, 124.7, 114.5, 104.7, 101.2, 61.5, 43.7, 14.7; HRMS (HESI) m/z calcd for $\text{C}_{14}\text{H}_{18}\text{N}_3\text{O}_2\text{S}$ ($\text{M}+\text{H}$) 292.1120, found 292.1109.



1-12

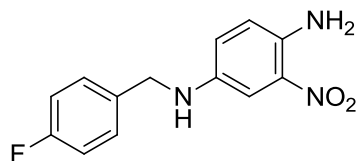
N-{2-Amino-4-[(1,3-thiazol-2-ylmethyl)amino]phenyl}ethoxycarboxamide (**1-12**). A suspension of **1-39** (0.072 g, 0.29 mmol) and Pd/C (0.028 g, 0.026 mmol) was allowed to stir under an H_2 atmosphere (balloon) for 18 h. The reaction mixture was diluted with Et_2O (10 mL) and filtered through a pad of Celite. The solvent was removed under reduced pressure to give the crude aryl triamine (0.076 g) as a dark red oil which was used without further purification. A solution of the crude aryl triamine (0.076 g) and Et_3N (0.075 mL, 0.53 mmol) in CH_2Cl_2 (1.00 mL) at rt was treated dropwise via syringe over 10 min with a solution of **1-41** (0.061 g, 0.26 mmol) in CH_2Cl_2 (1.10 mL). The resulting solution was allowed to stir for 18 h, the solvent was evaporated under reduced pressure, the crude residue dissolved in EtOAc (20 mL), and washed with sat aq. NaHCO_3 (4 x 20 mL) until the washes were clear. The aqueous washes were extracted with EtOAc (2 x 20 mL) and the combined organic fractions were washed with H_2O (2 x 20 mL) and brine (2 x 20 mL), dried (MgSO_4), filtered, and the solvent evaporated under reduced pressure to give crude **1-12** (0.060 g) as a brown-red oil. The crude residue was purified by chromatography on SiO_2 (70% EtOAc in hexanes) to give **1-12** (0.045 g, 0.15 mmol, 59%

over 2 steps) as a blue-green oil that solidified upon standing: Mp 46-47 °C (CH₂Cl₂); IR (CH₂Cl₂) 3352.87, 2981.33, 1696.90, 1621.12, 1523.21 cm⁻¹; ¹H NMR (CDCl₃, 400 MHz) δ 7.72 (d, 1 H, *J* = 3.2 Hz), 7.24 (d, 1 H, *J* = 3.2 Hz), 6.91 (d, 1 H, *J* = 8.4 Hz), 6.16 (br s, 1 H), 6.08 (dd, 1 H, *J* = 8.4, 2.4 Hz), 6.02 (d, 1 H, *J* = 2.4 Hz), 4.59 (s, 2 H), 4.17 (q, 2 H, *J* = 7.2 Hz), 3.81 (br s, 2 H), 1.27 (t, 3 H, *J* = 6.8 Hz); ¹³C NMR (CDCl₃, 400 MHz) δ 171.6, 155.7, 146.8, 143.1, 142.7, 127.9, 119.2, 114.8, 104.7, 101.2, 61.5, 46.5, 14.7; HRMS (HESI) *m/z* calcd for C₁₃H₁₇N₄O₂S (M+H) 293.1067, found 293.1063.



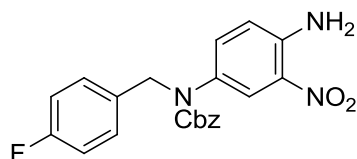
1-41

Ethyl (1,3-dioxobenzo[c]azolidin-2-yl)oxyformate (1-41).¹¹⁵ A suspension of diphthalimidyl carbonate (0.382 g, 1.08 mmol) and EtOH (0.065 mL, 1.1 mmol) in THF (2.5 mL) was treated with Et₃N (0.150 mL, 1.07 mmol). Upon addition of base, the suspension turned yellow progressing to orange over 30 min. The reaction mixture was stirred for 5 h and the solvent evaporated. The residue was dissolved in EtOAc (25 mL) and washed with sat. aq. NaHCO₃ (5 x 10 mL) until the organic layer became clear. The combined aqueous washings were extracted with EtOAc (2 x 20 mL). The combined organic layers were dried (MgSO₄), filtered, and the solvent evaporated under reduced pressure. Further drying under high vacuum gave **1-41** (0.230 g, 0.978 mmol, 90%) as a light yellow solid: ¹H NMR (CDCl₃, 300 MHz) δ 7.90-7.84 (m, 2 H), 7.81-7.76 (m, 2 H), 4.40 (q, 2 H, *J* = 7.2 Hz), 1.40 (t, 3 H, *J* = 7.2 Hz); ¹³C NMR (CDCl₃, 75 MHz) δ 161.6, 152.4, 135.0, 128.8, 124.1, 67.7, 14.1.



1-2

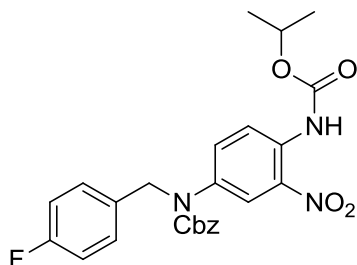
(4-Amino-3-nitrophenyl)[(4-fluorophenyl)methyl]amine (1-2). A solution of 2-nitro-*p*-phenylenediamine (0.998 g, 6.19 mmol) and 3 Å mol. sieves (3.00 g) in xylenes (30 mL) was heated to 90 °C and treated with 4-fluorobenzaldehyde (0.690 mL, 6.27 mmol). The resulting solution was allowed to stir for 20 h, filtered through a short pad of SiO₂, allowed to cool for 6 h, and the solid precipitate filtered off to give the crude imine (0.719 g), that was dissolved in 1,4-dioxane (4 mL) and MeOH (1 mL) and NaBH₄ (0.157 g, 4.11 mmol) was added in 3 batches at 15 min intervals. The solution was stirred for 10 h, quenched with H₂O (25 mL), and the solid filtered to give **1-2** (0.573 g, 2.19 mmol, 35%): Mp 113-114 °C; IR (ATR) 3517.98, 3497.88, 3395.77, 3372.60, 1578.67, 1503.24, 1406.73, 1329.96 cm⁻¹; ¹H NMR (CDCl₃, 400 MHz) δ 7.33 (app. dd, 2 H, *J* = 5.4, 2.2 Hz), 7.30 (d, 1 H, *J* = 2.8 Hz), 7.04 (app. t, 2 H, *J* = 8.6 Hz), 6.84 (dd, 1 H, *J* = 8.8, 2.8 Hz), 6.70 (d, 1 H, *J* = 8.8 Hz), 5.73 (br s, 2 H), 4.26 (d, 2 H, *J* = 4.0 Hz); ¹³C NMR (CDCl₃, 100 MHz) δ 162.3 (d, *J* = 245.0 Hz), 139.4, 138.3, 134.6 (d, *J* = 2.9 Hz), 132.6, 129.4 (d, *J* = 8.0 Hz), 125.4, 120.2, 115.7 (d, *J* = 22.0 Hz), 106.1, 48.4; HRMS (HESI) *m/z* calcd for C₁₃H₁₃N₃O₂F (M+H) 262.0986, found 262.0981.



1-42

***N*-(4-Amino-3-nitrophenyl)-*N*-**

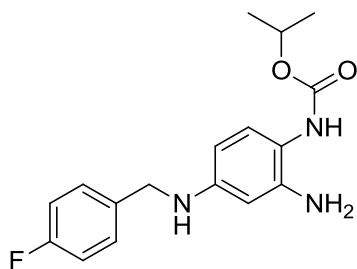
[(4fluorophenyl)methyl](phenylmethoxy)carboxamide (1-42). A solution of **1-2** (0.207 g, 0.792 mmol) and DIPEA (0.140 mL, 0.848 mmol) in 1,4-dioxane (4 mL) at rt was treated dropwise via syringe with benzyl chloroformate (0.120 mL, 0.819 mmol). The resulting solution was allowed to stir at rt for 5 h and was then quenched with 1:1 H₂O:CH₂Cl₂ (6.5 mL). The phases were separated and the aqueous phase extracted with CH₂Cl₂ (3 x 5 mL). The combined organic phases were washed with brine, dried (Na₂SO₄), filtered, and the solvent evaporated under reduced pressure to give crude **1-42** (0.420 g) as an orange oil which was used without further purification.



1-43

***N*-(4-{*N*-[(4-Fluorophenyl)methyl](phenylmethoxy)carbonylamino}-2-nitrophenyl)(methylethoxy)carboxamide (1-43)**. A solution of crude **1-42** (0.415 g) and DIPEA (0.390 mL, 2.36 mmol) in 1,4-dioxane (6.00 mL) at rt was treated dropwise via syringe with a solution of isopropyl chloroformate in toluene (1.95 mL, 1.95 mmol, 1.0 M). The resulting solution was allowed to stir at 70 °C for 2 d and was then quenched by the addition of 1:1 H₂O: CH₂Cl₂ (10 mL), the layers were separated, and the aqueous phase extracted with CH₂Cl₂ (3 x 10 mL). The combined organic phases were washed with water and brine, dried (MgSO₄), filtered, and concentrated under reduced pressure to give crude **1-43** (0.410 g) as a dark orange oil. The crude

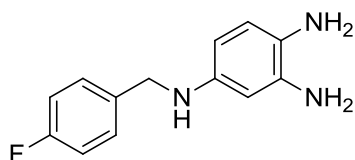
oil was purified by chromatography on SiO₂ (10% EtOAc in hexanes) to give **1-43** (0.097 g) as a yellow oil along with recovered starting material (0.140 g). The starting material was recycled through the reaction procedure again to give **1-43** (0.050 g, 0.147 g total, 0.305 mmol, 39% over two steps) as a yellow oil: IR (CH₂Cl₂) 3367.42, 2982.20, 1735.01, 1705.36, 1510.64, 1338.30 cm⁻¹; ¹H NMR (CDCl₃, 400 MHz) δ 9.72 (s, 1 H), 8.52 (d, 1 H, *J* = 8.8 Hz), 7.98 (br s, 1 H), 7.36-7.25 (m, 5 H), 7.15 (app. t, 2 H, *J* = 6.8 Hz), 6.96 (t, 2 H, *J* = 8.8 Hz), 5.19 (s, 2 H), 5.08-4.96 (m, 2 H), 4.84 (s, 2 H), 1.32 (d, 6 H, *J* = 6.4 Hz); ¹³C NMR (CDCl₃, 100 MHz) δ 162.4 (d, *J* = 245.0 Hz), 155.3, 152.8, 136.0, 135.7, 134.7, 134.2, 132.8 (d, *J* = 3.2 Hz), 129.8, 128.7, 128.4, 128.1, 124.0, 121.1, 115.8 (d, *J* = 21.3 Hz); HRMS (HESI) *m/z* calcd for C₂₅H₂₄N₃O₆F (M-H) 480.1565, found 480.1575.



1-44

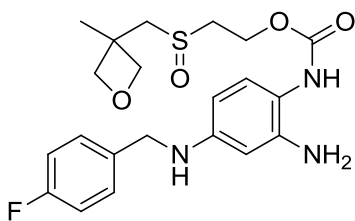
***N*-(2-Amino-4-[[4-fluorophenyl]methyl]amino}phenyl)(methylethoxy)carboxamide (1-44)**. A suspension of **1-43** (0.049 g, 0.10 mmol) and 10% Pd/C (0.013 g, 0.012 mmol, 10 mol%) in 1,4-dioxane (0.60 mL) and EtOH (0.30 mL) was allowed to stir at rt for 18 h under an H₂ atmosphere (balloon). The reaction mixture was diluted with Et₂O (5 mL), filtered through Celite, and the solvent evaporated under reduced pressure to give crude **1-43** (0.033 g) as a brown oil. The crude oil was purified by chromatography on SiO₂ (50% EtOAc in hexanes) to

give **1-43** (0.024 g, 0.076 mmol, 74%) as an off-white solid: Mp 171-172 °C (CH₂Cl₂); IR (ATR) 3396.44, 3342.93, 3289.29, 2981.70, 1674.75; ¹H NMR (CDCl₃, 400 MHz) δ 7.31 (app. dd, 2 H, *J* = 8.4, 5.6 Hz), 7.01 (app. t, 2 H, *J* = 10.2 Hz), 6.92 (d, 1 H, *J* = 8.0 Hz), 6.06 (dd, 1 H, *J* = 8.4, 2.4 Hz), 6.00 (d, 1 H, *J* = 2.4 Hz), 4.97 (m, 1 H), 4.25 (s, 2 H), 3.81 (br s, 2 H), 1.27 (d, 6 H, *J* = 6.4 Hz); ¹³C NMR (CDCl₃, 100 MHz) δ 162.2 (d, *J* = 244.0 Hz), 155.3, 147.7, 143.1, 135.3 (d, *J* = 2.9 Hz), 129.1 (d, *J* = 7.9 Hz), 127.8, 115.6 (d, *J* = 21.2 Hz), 114.4, 104.5, 100.8, 68.9, 47.8, 22.3; HRMS (HESI) *m/z* calcd for C₁₇H₂₁N₃O₂F (M-H) 318.1612, found 318.1611.



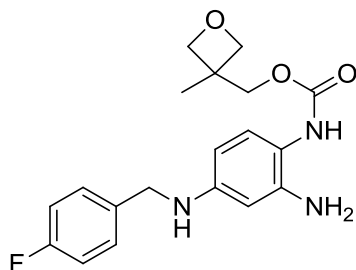
1-45

(3,4-Diaminophenyl)[(4-fluorophenyl)methyl]amine (1-45). A suspension of **1-2** (0.101 g, 0.321 mmol) and 10% Pd/C (0.035 g, 0.032 mmol) in 1,4-dioxane (1.6 mL) and EtOH (0.80 mL) was allowed to stir at rt under an H₂ atmosphere (balloon) for 18 h. The reaction mixture was diluted with Et₂O (10 mL), filtered through a pad of celite, and the solvent evaporated under reduced pressure. Further drying under high vacuum gave crude **1-45** (0.077 g) as a brown oil which was used without further purification.



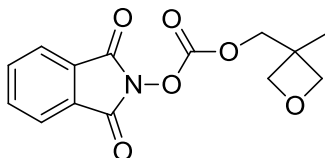
1-14

***N*-(2-Amino-4-[[*(4*-fluorophenyl)methyl]amino]phenyl){2-[(3-methyloxetan-3-yl)sulfinyl] ethoxy}carboxamide (1-14).** A solution of crude **1-45** (0.062 g, 0.27 mmol) and Et₃N (0.070 mL, 0.50 mmol) in CH₂Cl₂ (1.00 mL) was treated dropwise via syringe over 10 min with a solution of crude **1-47** (0.095 g, 0.26 mmol) in CH₂Cl₂ (1.00 mL). The resulting solution was allowed to stir for 18 h at rt, the solvent was evaporated under reduced pressure, the residue dissolved in EtOAc (20 mL), and washed with sat. aq. NaHCO₃ (3 x 10 mL). The combined aqueous layers were extracted with EtOAc (2 x 20 mL) and the combined organic layers were dried (MgSO₄), filtered, and the solvent evaporated under reduced pressure to give crude **1-14** (0.090 g) as a dark green oil. The crude residue was purified by chromatography on SiO₂ (3-5% MeOH in CH₂Cl₂) to give **1-14** (0.041 g, 0.094 mmol, 39% over two steps) as a light brown oil: IR (CH₂Cl₂) 3362.88, 2256.98, 1712.79, 1619.15, 1525.30, 1508.32 cm⁻¹; ¹H NMR (DMSO-d₆, 500 MHz, 323 K) δ 7.99 (br s, 1 H), 7.38-7.35 (m, 2 H), 7.09 (t, 2 H, *J* = 8.8 Hz), 6.73 (d, 1 H, *J* = 8.5 Hz), 5.99 (d, 1 H, *J* = 2.0 Hz), 5.88 (dd, 1 H, *J* = 8.5, 2.5 Hz), 5.56 (s, 1 H), 4.64 (d, 1 H, *J* = 5.5 Hz), 4.55 (d, 1 H, *J* = 5.5 Hz), 4.45-4.31 (m, 5 H), 4.24 (d, 1 H, *J* = 6.0 Hz), 4.19 (d, 2 H, *J* = 4.5 Hz), 3.19-3.13 (m, 2 H), 3.03-3.00 (m, 2 H), 1.49 (s, 3 H); ¹³C NMR (DMSO-d₆, 125 MHz, 323 K) δ 160.7 (d, *J* = 240.0 Hz), 154.2, 147.1, 143.2, 136.4, 128.5 (d, *J* = 7.5 Hz), 126.9, 114.3 (d, *J* = 21.3 Hz), 112.7, 101.7, 98.9, 90.0, 80.6, 59.8, 56.7, 51.7, 45.9, 37.6, 23.0; HRMS (HESI) *m/z* calcd for C₂₁H₂₇N₃O₄FS (M+H) 436.1701, found 436.1698.



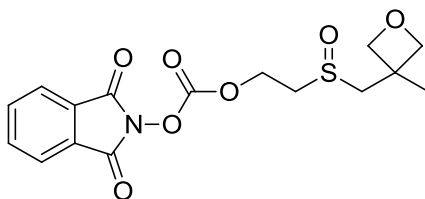
1-15

***N*-(2-Amino-4-[[*(*4-fluorophenyl)methyl]amino]phenyl)[(3-methyloxetan-3-yl)methoxy] carboxamide (1-15).** A solution of crude **1-45** (0.077 g) and Et₃N (0.090 mL, 0.64 mmol) in CH₂Cl₂ (1.30 mL) at rt was treated dropwise via syringe over 15 min with a solution of **1-46** (0.101 g, 0.347 mmol) in CH₂Cl₂ (1.30 mL). The resulting solution was allowed to stir for 18 h, the solvent was evaporated under reduced pressure, the crude residue dissolved in EtOAc (20 mL), and washed with sat. aq. NaHCO₃ (3 x 10 mL). The combined aqueous washes were extracted with EtOAc (2 x 20 mL) and the combined organic layers were dried (MgSO₄), filtered, and the solvent evaporated under reduced pressure to give crude **1-15** (0.110 g) as an olive green oil. The crude oil was purified by chromatography on SiO₂ (40-50% EtOAc in hexanes) to give **1-15** (0.033 g, 0.092 mmol, 29% over 2 steps) as a dark brown oil; IR (CH₂Cl₂) 3346.52, 2960.42, 2876.96, 1701.71, 1619.50, 1524.48, 1508.10 cm⁻¹; ¹H NMR (CDCl₃, 400 MHz) δ 7.30 (dd, 2 H, *J* = 8.2, 5.4 Hz), 7.02 (app. t, 2 H, *J* = 8.6 Hz), 6.93 (d, 1 H, *J* = 7.6 Hz), 6.21 (br s, 1 H), 6.06 (d, 1 H, *J* = 8.4 Hz), 6.00 (s, 1 H), 4.58 (app. br s, 2 H), 4.39 (app. br s, 2 H), 4.25 (s, 2 H), 4.20 (s, 2 H), 3.80 (br s, 3 H), 1.35 (s, 3 H); ¹³C NMR (CDCl₃, 100 MHz) δ 161.2 (d, *J* = 243.0 Hz), 155.5, 147.9, 143.1, 135.2 (d, *J* = 3.0 Hz), 129.0 (d, *J* = 8.0 Hz), 127.9, 115.6 (d, *J* = 21.0 Hz), 113.9, 104.6, 100.8, 79.6, 69.4, 47.7, 39.5, 21.3; HRMS (HESI) *m/z* calcd for C₁₉H₂₃N₃O₃F (M+H) 360.1723, found 360.1712.



1-46

(3-Methyloxetan-3-yl)methyl (1,3-dioxobenzo[c]azolidin-2-yloxy)formate (1-46). A suspension of diphthalimidyl carbonate (0.381 g, 1.08 mmol) and 3-methyl-3-oxetanemethanol (0.110 mL, 1.08 mmol) in THF (5 mL) was treated with Et₃N (0.160 mL, 1.14 mmol). Upon addition of base, the suspension turned yellow progressing to orange over 2 h. The reaction mixture was stirred for 14 h and the solvent was evaporated under reduced pressure. The residue was dissolved in EtOAc (25 mL) and washed with sat. aq. NaHCO₃ (5 x 10 mL) until the organic layer became clear. The combined aqueous washings were extracted with EtOAc (2 x 20 mL). The combined organic layers were dried (MgSO₄), filtered, and the solvent evaporated under reduced pressure. Further drying under high vacuum gave **1-46** (0.255 g, 0.876 mmol, 81%) as a clear, light yellow oil: IR (CH₂Cl₂) 2965.43, 2875.74, 1811.79, 1788.73, 1741.98 cm⁻¹; ¹H NMR (CDCl₃, 400 MHz) δ 7.91-7.88 (m, 2 H), 7.81-7.79 (m, 2 H), 4.54 (d, 2 H, *J* = 6.4 Hz), 4.47 (s, 2 H), 4.43 (d, 2 H, *J* = 6.0 Hz), 1.41 (s, 3 H); ¹³C NMR (CDCl₃, 100 MHz) 161.5, 152.7, 135.1, 128.8, 124.3, 79.1, 75.4, 39.5, 20.8; HRMS (HESI) *m/z* calcd for C₁₄H₁₄NO₆ (M+H) 292.0816, found 292.0819.

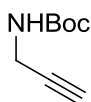


1-47

2-[[3-(3-Methyloxetan-3-yl)methyl]sulfinyl]ethyl (1,3-dioxobenzo[c]azolidin-2-yloxy)formate (1-47).² A suspension of diphthalimidyl carbonate (0.380 g, 1.08 mmol) and MMS-350 sulfoxide alcohol (0.195 g, 1.09 mmol) in THF (5 mL) was treated with Et₃N (0.145 mL, 1.03 mmol). Upon addition of base, the suspension turned yellow, eventually progressing to

a clear orange solution after 20 min. The reaction mixture was stirred 2 h, and the solvent was evaporated. The residue was dissolved in EtOAc (25 mL) and washed with saturated aqueous NaHCO₃ (5 x 3 mL) until the organic layer became clear. The combined aqueous washings were extracted with EtOAc (2 x 10 mL). The combined organics were dried (MgSO₄) and the solvent evaporated under reduced pressure to give **1-47** (0.265 g, 0.721 mmol, 66%) as a foaming solid which was used without further purification.

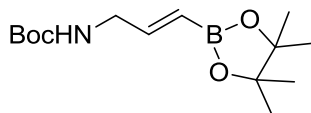
3.3 CHAPTER 2 EXPERIMENTAL PART



2-32

(tert-butoxy)-N-prop-2-ynylcarboxamide (2-32).¹⁰⁹ A solution of propargylamine (4.00 mL, 57.7 mmol) in CH₂Cl₂ (110 mL) at 0 °C was treated dropwise via syringe over 15 min with a solution of Boc₂O (12.75 g, 57.84 mmol) in CH₂Cl₂ (5 mL). The resulting solution was allowed to stir for 2 h at 0 °C and the solvent was removed under reduced pressure. Further drying under high vacuum gave crude **2-32** as an orange oil. The crude oil was purified by chromatography on SiO₂ (10% EtOAc in hexanes) to give **2-32** (7.641 g, 49.24 mmol, 85%) as a white, crystalline solid: Mp 39-41 °C; IR 3320.16, 3290.77, 2980.70, 1679.97, 1524.58 cm⁻¹; ¹H NMR (CDCl₃,

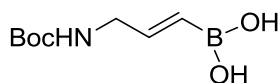
300 MHz) δ 4.82 (br s, 1 H), 3.89 (d, 2 H, $J = 3.3$ Hz), 2.19 (t, 1 H, $J = 2.6$ Hz), 1.42 (s, 9 H); ^{13}C NMR (CDCl_3 , 400 MHz) δ 155.4, 80.2, 80.1, 71.3, 30.5, 28.4.



2-33

(*E*)-tert-Butyl (3-(4,4,5,5-tetramethyl-1,3,2-dioxaborolan-2-yl)allyl)carbamate (2-33).

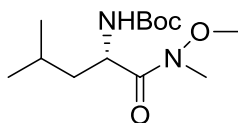
A solution of **2-32** (5.02 g, 19.5 mmol) in THF (9.6 mL) at 0 °C was treated dropwise via syringe with pinacolborane (3.30 mL, 22.5 mmol) and the resulting solution was allowed to stir for 5 min. The reaction mixture was transferred via syringe to a flask containing Schwartz's reagent (0.540 g, 2.09 mmol) at 0 °C. The solution was allowed to stir at 50 °C for 22 h before being quenched with H₂O (50 mL). The mixture was extracted with Et₂O (2 x 75 mL) and the organic phase washed with H₂O (2 x 15 mL), dried (MgSO₄), filtered, and the solvent evaporated under reduced pressure to give crude **2-33** (5.91 g, 107% by mass) as a pale yellow solid-oil mixture which was used without further purification.



2-34

(*E*)-(3-((tert-butoxycarbonyl)amino)prop-1-en-1-yl)boronic acid (2-34). A suspension of crude **2-33** (3.419 g), NaIO₄ (4.47 g, 20.9 mmol), and NH₄OAc (1.86 g, 24.1 mmol) in 1:1 acetone:H₂O (110 mL) was allowed to stir for 18 h at rt. The slurry was diluted

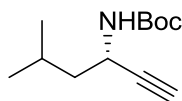
with EtOAc (100 mL) and H₂O (100 mL), the layers were separated, and the organic phase washed with H₂O (3 x 30 mL). The organic layer was washed with brine (2 x 30 mL), dried (MgSO₄), filtered, and the solvent evaporated under reduced pressure. The crude residue was crystallized from CH₂Cl₂ (20 mL) to give **2-34** (1.299 g, 6.462 mmol, 54% over 2 steps) as a white crystalline solid: Mp 113-117 °C (CH₂Cl₂); IR (ATR) 3294.50, 2981.18, 1685.52, 1641.37, 1520.45 cm⁻¹; ¹H NMR (acetone-d₆, 400 MHz) δ 6.73 (br s, 2 H), 6.50 (dt, 1 H, *J* = 18.0, 4.8 Hz), 6.08 (br s, 1 H), 5.54 (app. d, 1 H, *J* = 18.0 Hz), 3.74 (t, 2 H, *J* = 4.8 Hz), 1.41 (s, 9 H); ¹³C NMR (acetone-d₆, 100 MHz) δ 156.5, 148.0, 123.8 (br), 78.6, 44.7, 28.6; HRMS (HESI) *m/z* calcd for C₄H₈BNO₄ (M-C₄H₉+H) 146.0619, found 146.0618.



2-35

(S)-tert-Butyl (1-(methoxy(methyl)amino)-4-methyl-1-oxopentan-2-yl)carbamate (2-35).^{112a} To a solution of *N*-Boc-*L*-leucine (3.13 g, 13.3 mmol), BOP (5.70 g, 12.9 mmol), and DIPEA (5.50 mL, 33.3 mmol) in CH₂Cl₂ (130 mL) was added *N,O*-dimethylhydroxylamine hydrochloride (1.74 g, 17.5 mmol) and the resulting solution was allowed to stir at rt for 36 h. The reaction mixture was diluted with EtOAc (50 mL) and washed consecutively with 1 M aq. HCl (2 x 100 mL), sat. aq. NaHCO₃ (100 mL), and brine (100 mL). The organic phase was dried (MgSO₄), filtered, and the solvent removed under reduced pressure to give crude **2-35** (6.46 g) as a clear gel. The crude gel was purified by chromatography on SiO₂ (20% EtOAc in hexanes) to give **2-35** (3.35 g, 12.2 mmol, 95%) as a clear, colorless oil: [α]_D -9.1 (*c* 1.0, CHCl₃); ¹H NMR (CDCl₃, 300 MHz) δ 5.06 (d, 1 H, *J* = 9.0 Hz), 4.64 (br. s, 1 H), 3.71 (s, 3 H), 3.12 (s, 3 H), 1.71-

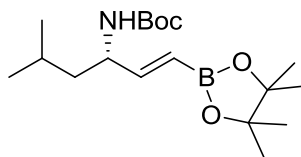
1.56 (m, 1 H), 1.35 (app. s, 12 H), 0.88 (d, 3 H, $J = 6.6$ Hz), 0.85 (d, 3 H, $J = 6.9$ Hz); ^{13}C NMR (CDCl_3 , 75 MHz) δ 173.9, 155.6, 79.4, 61.5, 49.0, 42.1, 32.2, 28.4, 24.7, 23.3, 21.6.



2-36

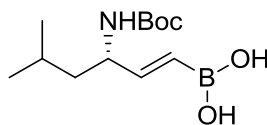
N-[(1*S*)-1-(2-Methylpropyl)prop-2-ynyl](*tert*-butoxy)carboxamide (**2-36**).^{112b} A solution of **2-35** (3.55 g, 12.9 mmol) in Et_2O (85 mL) at 0 °C was treated dropwise via syringe with LiAlH_4 (15.50 mL, 15.50 mmol, 1.0 M in Et_2O). The resulting solution was allowed to stir at the same temperature for 2 h, then for 2 h at rt, and was then quenched by the dropwise addition of 5% aq. KHSO_4 (15 mL). H_2O (100 mL) was added, the phases were separated, and the aqueous phase extracted with Et_2O (3 x 100 mL). The combined organic phases were dried (MgSO_4), filtered, and the solvent was evaporated under reduced pressure to give crude amino aldehyde (3.42 g). The crude residue was dissolved in MeOH (35 mL) and added via syringe to a solution of K_2CO_3 (5.62 g, 39.9 mmol) and the Ohira-Bestmann reagent (3.82 g, 19.7 mmol) in MeCN (175 mL). The resulting solution was allowed to stir at rt for 18 h and the solvent was removed under reduced pressure. Et_2O (150 mL) and H_2O (150 mL) were added and the layers separated. The aqueous phase was extracted with Et_2O (3 x 100 mL) and the combined organic phases were dried (MgSO_4), filtered, and the solvent evaporated under reduced pressure to give crude **2-36** (2.71 g) as an orange oil. The crude residue was purified by chromatography on SiO_2 (10% EtOAc in hexanes) to give **2-36** (1.771 g, 8.381 mmol, 65%) as a clear, colorless oil: ^1H NMR (CDCl_3 , 400 MHz) δ 4.63 (br. s, 1 H), 4.44 (br. d, 1 H, $J = 6.4$ Hz), 2.25 (d, 1 H, $J = 2.4$

Hz), 1.80 (app. hept., 1 H, $J = 6.8$ Hz), 1.59 (s, 1 H), 1.52 (t, 2 H, $J = 7.6$ Hz), 1.45 (s, 9 H), 0.94 (d, 3 H, $J = 6.4$ Hz), 0.93 (d, 3 H, $J = 6.8$ Hz).



2-37

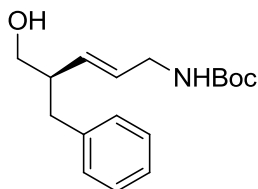
N-[(*2E*)(*1S*)-1-(2-Methylpropyl)-3-(4,4,5,5-tetramethyl(1,3,2-dioxaborolan-2-yl))prop-2-enyl](*tert*-butoxy)carboxamide (**2-37**). A solution of **2-36** (0.970 g, 4.59 mmol) in THF (2.5 mL) was treated dropwise via syringe with pinacolborane (0.775 mL, 5.34 mmol) and the resulting solution was allowed to stir for 5 min. The reaction mixture was transferred via syringe to a flask containing Schwartz's reagent (0.192 g, 0.745 mmol) at 0 °C. The solution was allowed to stir at 50 °C for 22 h before being quenched with H₂O (5 mL). The mixture was extracted with Et₂O (3 x 50 mL), washed with H₂O (2 x 50 mL), dried (MgSO₄), filtered, and the solvent evaporated under reduced pressure to give crude **2-37** (1.47 g, 94% by mass) as a yellow oil which was used without further purification.



2-38

(*S,E*)-3-((*tert*-Butoxycarbonyl)amino)-5-methylhex-1-en-1-ylboronic acid (**2-38**). A suspension of crude **2-38** (3.05 g), NaIO₄ (3.65 g, 17.1 mmol) and NH₄OAc (1.37 g, 17.8 mmol) in 1:1 acetone:H₂O (84 mL) was allowed to stir for 24 h at rt. The slurry was diluted with EtOAc (50 mL) and H₂O (50 mL), the layers separated, and the organic phase extracted with

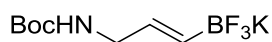
brine (3 x 30 mL). The organic layer was dried (MgSO₄), filtered, and the solvent evaporated under reduced pressure. The crude residue was crystallized from CH₂Cl₂ (20 mL) at -20 °C to give **2-38** (1.214 g, 4.721 mmol, 56%) as a white, crystalline solid: [α]_D -17.3 (*c* 1.0, MeOH); Mp 103-108 (decomp., CH₂Cl₂); IR (ATR) 3313.01, 2958.25, 2935.58, 1686.86, 1367.37, 1165.78 cm⁻¹; ¹H NMR (acetone-d₆, 400 MHz) δ 6.74 (br. s, 2 H), 6.46 (dd, 1 H, *J* = 18.0, 6.0 Hz), 5.87 (d, 1 H, *J* = 8.4 Hz), 5.52 (dd, 1 H, *J* = 17.6, 1.0 Hz), 4.19 (app. br. s, 1 H), 1.69 (hept., 1 H, *J* = 6.8 Hz), 1.45-1.29 (m, 11 H), 0.92 (d, 3 H, *J* = 6.4 Hz), 0.91 (d, 3 H, *J* = 6.8 Hz); ¹³C NMR (acetone-d₆, 100 MHz) δ 156.1, 152.2, 122.8, 78.4, 52.9, 44.8, 28.7, 25.5, 23.2, 22.4; HRMS (HESI) *m/z* calcd for C₈H₁₇BNO₄ (M-C₄H₈+H) 202.1245, found 202.1244.



2-42

***N*-[(2*E*)(4*R*)-5-Hydroxy-4-benzylpent-2-enyl](*tert*-butoxy)carboxamide (2-43).** To a solution of methyl boronic acid (0.030 g, 0.49 mmol), **2-34** (0.091 g, 0.45 mmol), **2-40** TFA salt (0.026 g, 0.072 mmol), and molecular sieves (4 Å beads, 0.230 g) in EtOAc (7 mL) was added hydrocinnamaldehyde (0.050 mL, 0.359 mmol) and copper acetate (0.014 g, 0.076 mmol). The headspace was purged with a gentle stream of O₂ for 1 min and the reaction mixture was allowed to stir under an atmosphere of O₂ (balloon) for 48 h at rt. The solution turned blue to green during this time. The reaction mixture was diluted with 10% EtOH in CH₂Cl₂ (10 mL), the solution was cooled to -78 °C, NaBH₄ (0.101 g, 2.62 mmol) was added in one portion, and the

resulting mixture was allowed to stir for 30 min at the same temperature before warming to rt over 1 h. The reaction mixture was poured into half saturated NH₄Cl (20 mL) at 0 °C and allowed to warm to rt over 30 min while stirring. The layers were separated and the aqueous phase extracted with CH₂Cl₂ (3 x 30 mL). The organic phases were dried (MgSO₄), filtered, and the solvent evaporated under reduced pressure to give crude **2-42** (0.060 g) as a clear, colorless oil. The crude residue was purified by chromatography on SiO₂ (50% Et₂O in hexanes) to give **2-42** (0.022 g, 0.076 mmol, 33%) as a clear, colorless oil: [α]_D -14.6 (*c* 0.50, CHCl₃); IR (CH₂Cl₂) 3341.12, 2976.54, 2923.64, 1687.16 cm⁻¹; ¹H NMR (CDCl₃, 400 MHz) δ 7.29-7.25 (m, 2 H), 7.20-7.13 (m, 3 H), 5.48 (app d, 2 H, *J* = 4.0 Hz), 4.54 (br s, 1 H), 3.66 (app br s, 2 H), 3.59 (dd, 1 H, *J* = 10.8, 4.8 Hz), 3.46 (dd, 1 H, *J* = 10.6, 7.6 Hz); 2.73 (dd, 1 H, *J* = 13.2, 6.8 Hz), 2.65-2.59 (m, 1H), 2.56-2.51 (m, 1 H), 1.44 (s, 9 H); ¹³C NMR (CHCl₃, 100 MHz) δ 155.9, 139.8, 133.2, 129.5, 129.3, 128.4, 126.2, 79.6, 65.1, 46.9, 42.7, 37.7, 28.5; HRMS (HESI) *m/z* calcd for C₁₇H₂₅NO₃ (M+Na) 314.1732, found 314.1724.



2-43

(E)-3-((tert-Butoxycarbonyl)amino)prop-1-en-1-yltrifluoroborate (2-43). A solution of **2-34** (3.21 g) in MeOH (21 mL) was treated dropwise via syringe with sat. aq. KHF₂ (0.842 g, 52.2 mmol) at rt over 5 min and the resulting solution was allowed to stir at rt for 2 h. The solvent was removed under reduced pressure and the residue dried under high vacuum overnight. Extraction of the solid residue with acetone (3 x 50 mL) followed by concentration under reduced pressure, addition of Et₂O (100 mL) and filtration gave **2-43** (1.723 g, 6.549 mmol, 63%) as a white, crystalline solid: Mp 129-131 °C (acetone/Et₂O); IR (ATR) 3355.79, 2978.67,

2933.66, 1676.59, 1648.34, 1521.86 cm^{-1} ; ^1H NMR (acetone- d_6 , 400 MHz) δ 5.68 (dt, 2 H, $J = 17.6, 5.2$ Hz), 5.53-5.48 (m, 1 H), 3.56 (app. s, 2 H), 1.40 (s, 9 H); ^{13}C NMR (acetone- d_6 , 100 MHz) δ 156.6, 132.7, 78.2, 45.8, 28.7; HRMS (HESI) m/z calcd for $\text{C}_8\text{H}_{14}\text{O}_2\text{NBF}_3$ (M-K) 224.1063, found 224.1064.

4.0 BIBLIOGRAPHY

1. Langguth, B.; Kreuzer, P. M.; Kleinjung, T.; De Ridder, D., Tinnitus: Causes and clinical management. *Lancet Neurol.* **2013**, *12* (9), 920-930.
2. (a) Krog, N. H.; Engdahl, B.; Tambs, K., The association between tinnitus and mental health in a general population sample: Results from the HUNT Study. *J. Psychosom. Res.* **2010**, *69* (3), 289-298; (b) Axelsson, A.; Ringdahl, A., Tinnitus—a study of its prevalence and characteristics. *Brit. J. Audiol.* **1989**, *23* (1), 53-62; (c) Shargorodsky, J.; Curhan, G. C.; Farwell, W. R., Prevalence and characteristics of tinnitus among US adults. *Am. J. Med.* *123* (8), 711-718; (d) Khedr, E. M.; Ahmed, M. A.; Shawky, O. A.; Mohamed, E. S.; El Attar, G. S.; Mohammad, K. A., Epidemiological study of chronic tinnitus in Assiut, Egypt. *Neuroepidemiology* **2010**, *35* (1), 45-52; (e) Xu, X.; Bu, X.; Zhou, L.; Xing, G.; Liu, C.; Wang, D., An epidemiologic study of tinnitus in a population in Jiangsu Province, China. *J. Am. Acad. Audiol.* **2011**, *22* (9), 578-585.
3. Helfer, T. M., Noise-induced hearing injuries, active component, U.S. Armed Forces, 2007-2010. *MSMR* **2011**, *18* (6), 7-10.
4. von der Behrens, W., Animal models of subjective tinnitus. *Neural Plast.* **2014**, *2014*, 13.
5. Weissman, J. L.; Hirsch, B. E., Imaging of Tinnitus: A review. *Radiology* **2000**, *216* (2), 342-349.
6. Plinkert, P. K.; Gitter, A. H.; Zenner, H. P., Tinnitus associated spontaneous otoacoustic emissions: active outer hair cell movements as common origin? *Acta Otolaryngol.* **1990**, *110* (5-6), 342-347.
7. Weisz, N.; Hartmann, T.; Dohrmann, K.; Schlee, W.; Norena, A., High-frequency tinnitus without hearing loss does not mean absence of deafferentation. *Hearing Res.* **2006**, *222* (1-2), 108-114.
8. Job, A.; Raynal, M.; Kossowski, M., Susceptibility to tinnitus revealed at 2 kHz range by bilateral lower DPOAEs in normal hearing subjects with noise exposure. *Audiol. Neurotol.* **2007**, *12* (3), 137-144.

9. Yang, S.; Weiner, B. D.; Zhang, L. S.; Cho, S.-J.; Bao, S., Homeostatic plasticity drives tinnitus perception in an animal model. *Proc. Natl. Acad. Sci. U. S. A.* **2011**, *108* (36), 14974-14979.
10. Brozoski, T.; Wisner, K.; Sybert, L.; Bauer, C., Bilateral dorsal cochlear nucleus lesions prevent acoustic-trauma induced tinnitus in an animal model. *J. Assoc. Res. Otolaryngol.* **2012**, *13* (1), 55-66.
11. Li, S.; Choi, V.; Tzounopoulos, T., Pathogenic plasticity of Kv7.2/3 channel activity is essential for the induction of tinnitus. *Proc. Natl. Acad. Sci. U. S. A.* **2013**, *110* (24), 9980-9985.
12. Cima, R. F. F.; Maes, I. H.; Joore, M. A.; Scheyen, D. J. W. M.; El Refaie, A.; Baguley, D. M.; Anteunis, L. J. C.; van Breukelen, G. J. P.; Vlaeyen, J. W. S., Specialised treatment based on cognitive behaviour therapy versus usual care for tinnitus: a randomised controlled trial. *The Lancet* **2012**, *379* (9830), 1951-1959.
13. Schaette, R.; König, O.; Hornig, D.; Gross, M.; Kempster, R., Acoustic stimulation treatments against tinnitus could be most effective when tinnitus pitch is within the stimulated frequency range. *Hearing Res.* **2010**, *269* (1-2), 95-101.
14. McNeill, C.; Távora-Vieira, D.; Alnafjan, F.; Searchfield, G. D.; Welch, D., Tinnitus pitch, masking, and the effectiveness of hearing aids for tinnitus therapy. *Int. J. Audiol.* **2012**, *51* (12), 914-919.
15. Kleinjung, T.; Steffens, T.; Strutz, J.; Langguth, B., Curing tinnitus with a cochlear implant in a patient with unilateral sudden deafness: a case report. *Cases J.* **2009**, *2* (1), 7462.
16. Trellakis, S.; Lautermann, J.; Lehnerdt, G., Lidocaine: Neurobiological targets and effects on the auditory system. In *Prog. Brain Res.*, B. Langguth, G. H. T. K. A. C.; Møller, A. R., Eds. Elsevier: 2007; Vol. Volume 166, pp 303-322.
17. Carlijn, E.; Rynja, S.; van Zanten, G.; Rovers, M., Anticonvulsants for tinnitus. *Cochrane Database Syst. Rev.* **2011**, *7*, CD007960.
18. Hodgkin, A. L.; Huxley, A. F., A quantitative description of membrane current and its application to conduction and excitation in nerve. *J. Physiol.* **1952**, *117* (4), 500-544.
19. Behrends, J. C., Evolution of the ion channel concept: The historical perspective. *Chem. Rev.* **2012**, *112* (12), 6218-6226.
20. MacKinnon, R., Determination of the subunit stoichiometry of a voltage-activated potassium channel. *Nature* **1991**, *350* (6315), 232-235.
21. Abbott, G. W.; Sesti, F.; Splawski, I.; Buck, M. E.; Lehmann, M. H.; Timothy, K. W.; Keating, M. T.; Goldstein, S. A. N., MiRP1 forms IKr potassium channels with HERG and is associated with cardiac arrhythmia. *Cell* **1997**, *97* (2), 175-187.

22. Barhanin, J.; Lesage, F.; Guillemare, E.; Fink, M.; Lazdunski, M.; Romey, G., KvLQT1 and IsK (minK) proteins associate to form the IKS cardiac potassium current. *Nature* **1996**, *384* (6604), 78-80.
23. Jiang, Y.; Lee, A.; Chen, J.; Ruta, V.; Cadene, M.; Chait, B. T.; MacKinnon, R., X-ray structure of a voltage-dependent K⁺ channel. *Nature* **2003**, *423* (6935), 33-41.
24. (a) Seoh, S.-A.; Sigg, D.; Papazian, D. M.; Bezanilla, F., Voltage-sensing residues in the S2 and S4 segments of the Shaker K⁺ channel. *Neuron* **1996**, *16* (6), 1159-1167; (b) Aggarwal, S. K.; MacKinnon, R., Contribution of the S4 segment to gating charge in the Shaker K⁺ channel. *Neuron* **1996**, *16* (6), 1169-1177.
25. (a) Larsson, H. P.; Baker, O. S.; Dhillon, D. S.; Isacoff, E. Y., Transmembrane movement of the Shaker K⁺ channel S4. *Neuron* *16* (2), 387-397; (b) Baker, O. S.; Larsson, H. P.; Mannuzzu, L. M.; Isacoff, E. Y., Three transmembrane conformations and sequence-dependent displacement of the S4 domain in Shaker K⁺ channel gating. *Neuron* *20* (6), 1283-1294.
26. Jiang, Y.; Lee, A.; Chen, J.; Cadene, M.; Chait, B. T.; MacKinnon, R., Crystal structure and mechanism of a calcium-gated potassium channel. *Nature* **2002**, *417* (6888), 515-522.
27. (a) Yellen, G.; Jurman, M. E.; Abramson, T.; MacKinnon, R., Mutations affecting internal TEA blockade identify the probable pore-forming region of a K⁺ channel. *Science* **1991**, *251* (4996), 939-942; (b) Heginbotham, L.; Lu, Z.; Abramson, T.; MacKinnon, R., Mutations in the K⁺ channel signature sequence. *Biophys. J.* **1994**, *66* (4), 1061-1067.
28. Brown, D. A.; Adams, P. R., Muscarinic suppression of a novel voltage-sensitive K⁺ current in a vertebrate neurone. *Nature* **1980**, *283* (5748), 673-676.
29. Wang, H.-S.; Pan, Z.; Shi, W.; Brown, B. S.; Wymore, R. S.; Cohen, I. S.; Dixon, J. E.; McKinnon, D., KCNQ2 and KCNQ3 potassium channel subunits: Molecular correlates of the M-channel. *Science* **1998**, *282* (5395), 1890-1893.
30. Hadley, J. K.; Passmore, G. M.; Tatulian, L.; Al-Qatari, M.; Ye, F.; Wickenden, A. D.; Brown, D. A., Stoichiometry of expressed KCNQ2/KCNQ3 potassium channels and subunit composition of native ganglionic M channels deduced from block by tetraethylammonium. *J. Neurosci.* **2003**, *23* (12), 5012-5019.
31. Hedley, P. L.; Jørgensen, P.; Schlamowitz, S.; Wangari, R.; Moolman-Smook, J.; Brink, P. A.; Kanters, J. K.; Corfield, V. A.; Christiansen, M., The genetic basis of long QT and short QT syndromes: A mutation update. *Hum. Mutat.* **2009**, *30* (11), 1486-1511.
32. Ferron, G. M.; Patat, A.; Parks, V.; Rolan, P.; Troy, S. M., Lack of pharmacokinetic interaction between retigabine and phenobarbitone at steady-state in healthy subjects. *Br. J. Clin. Pharmacol.* **2003**, *56* (1), 39-45.

33. Schuster, G.; Schwarz, M.; Block, F.; Pergande, G.; Schmidt, W. J., Flupirtine: A review of its neuroprotective and behavioral properties. *CNS Drug Rev.* **1998**, *4* (2), 149-164.
34. Schwarz, M.; Nolden-Koch, M.; Purr, J.; Pergande, G.; Block, F., Antiparkinsonian effect of flupirtine in monoamine-depleted rats. *J. Neural Transm.* **1996**, *103* (5), 581-590.
35. Splinter, M. Y., Ezogabine (retigabine) and its role in the treatment of partial-onset seizures: A review. *Clin. Ther.* **2012**, *34* (9), 1845-1856.e1.
36. Rogawski, M. A., Diverse mechanisms of antiepileptic drugs in the development pipeline. *Epilepsy Res.* **2006**, *69* (3), 273-294.
37. Gunthorpe, M. J.; Large, C. H.; Sankar, R., The mechanism of action of retigabine (ezogabine), a first-in-class K⁺ channel opener for the treatment of epilepsy. *Epilepsia* **2012**, *53* (3), 412-424.
38. (a) Main, M. J.; Cryan, J. E.; Dupere, J. R. B.; Cox, B.; Clare, J. J.; Burbidge, S. A., Modulation of KCNQ2/3 potassium channels by the novel anticonvulsant retigabine. *Mol. Pharmacol.* **2000**, *58* (2), 253-262; (b) Rundfeldt, C.; Netzer, R., The novel anticonvulsant retigabine activates M-currents in Chinese hamster ovary-cells transfected with human KCNQ2/3 subunits. *Neurosci. Lett.* **2000**, *282* (1-2), 73-76.
39. Lange, W.; Geißendörfer, J.; Schenzer, A.; Grötzinger, J.; Seebohm, G.; Friedrich, T.; Schwake, M., Refinement of the binding site and mode of action of the anticonvulsant retigabine on KCNQ K⁺ channels. *Mol. Pharmacol.* **2009**, *75* (2), 272-280.
40. Porter, R. J.; Partiot, A.; Sachdeo, R.; Nohria, V.; Alves, W. M.; on behalf of the 205 Study, G., Randomized, multicenter, dose-ranging trial of retigabine for partial-onset seizures. *Neurology* **2007**, *68* (15), 1197-1204.
41. Dieter, H.-R.; Engel, J.; Kutscher, B.; Polymeropoulos, E.; Szelenyi, S.; Nickel, B. 1,2,4-Triaminobenzene derivatives and process for their preparation. July 31, 1996.
42. Blackburn-Munro, G.; Dalby-Brown, W.; Mirza, N. R.; Mikkelsen, J. D.; Blackburn-Munro, R. E., Retigabine: Chemical synthesis to clinical application. *CNS Drug Rev.* **2005**, *11* (1), 1-20.
43. Mandal, A. K.; Ranbhan, K. j.; Saxena, S.; Gaikwad, S. R. Process for the preparation of retigabine of the formula I and pharmaceutically acceptable salts thereof. 2013.
44. Tompson, D. J.; Crean, C. S., Clinical pharmacokinetics of retigabine/ezogabine. *Curr. Clin. Pharmacol.* **2013**, *8* (4), 319-331.
45. Hermann, R.; Ferron, G. M.; Erb, K.; Knebel, N.; Ruus, P.; Paul, J.; Richards, L.; Cnota, H.-P.; Troy, S., Effects of age and sex on the disposition of retigabine. *Clin. Pharmacol. Ther.* **2003**, *73* (1), 61-71.

46. Łuszczki, J., Third-generation antiepileptic drugs: mechanisms of action, pharmacokinetics and interactions. *Pharmacol. Rep.* **2009**, *61* (2), 197-216.
47. Large, C. H.; Sokal, D. M.; Nehlig, A.; Gunthorpe, M. J.; Sankar, R.; Crean, C. S.; VanLandingham, K. E.; White, H. S., The spectrum of anticonvulsant efficacy of retigabine (ezogabine) in animal models: Implications for clinical use. *Epilepsia* **2012**, *53* (3), 425-436.
48. Hiller, A.; Nguyen, N.; Strassburg, C. P.; Li, Q.; Jainta, H.; Pechstein, B.; Ruus, P.; Engel, J.; Tukey, R. H.; Kronbach, T., Retigabine *N*-glucuronidation and its potential role in enterohepatic circulation. *Drug Metab. Dispos.* **1999**, *27* (5), 605-612.
49. Ferron, G. M.; Paul, J.; Fruncillo, R.; Richards, L.; Knebel, N.; Getsy, J.; Troy, S., Multiple-dose, linear, dose-proportional pharmacokinetics of retigabine in healthy volunteers. *J. Clin. Pharmacol.* **2002**, *42* (2), 175-182.
50. Hermann, R.; Knebel, N.; Niebch, G.; Richards, L.; Borlak, J.; Locher, M., Pharmacokinetic interaction between retigabine and lamotrigine in healthy subjects. *Eur. J. Clin. Pharmacol.* **2003**, *58* (12), 795-802.
51. Mittapalli, G. K.; Roberts, E., Structure activity relationships of novel antiepileptic drugs. *Curr. Med. Chem.* **2014**, *21* (6), 722-754.
52. (a) Bak-Jensen, H.; Hertel, K. P. Use of KCNQ potassium channel openers for reducing symptoms or treating disorders or conditions wherein the dopaminergic system is disrupted. 2007; (b) Rottlaender, M.; Ritzen, A. 1,2,4-Triaminobenzene derivatives useful for treating disorders of the central nervous system. 2004.
53. Jean-Michel, V.; MArtha, D. I. R.; Huanming, C.; Jim Zhen, W.; Gary Lee, L.; Lan Wayne, C. Preparation of 4-(*N*-azacycloalkyl)anilides as potassium channel modulators. 2011.
54. Amato, G.; Roeloffs, R.; Rigdon, G. C.; Antonio, B.; Mersch, T.; McNaughton-Smith, G.; Wickenden, A. D.; Fritch, P.; Suto, M. J., *N*-Pyridyl and pyrimidine benzamides as KCNQ2/Q3 potassium channel openers for the treatment of epilepsy. *ACS Med. Chem. Lett.* **2011**, *2* (6), 481-484.
55. Hu, H.-n.; Zhou, P.-z.; Chen, F.; Li, M.; Nan, F.-j.; Gao, Z.-b., Discovery of a retigabine derivative that inhibits KCNQ2 potassium channels. *Acta Pharmacol. Sin.* **2013**, *34* (10), 1359-1366.
56. (a) Xiao, J.; Weisblum, B.; Wipf, P., Electrostatic versus steric effects in peptidomimicry: Synthesis and secondary structure analysis of Gramicidin S analogues with (*E*)-alkene peptide isosteres. *J. Am. Chem. Soc.* **2005**, *127* (16), 5742-5743; (b) Wipf, P.; Mo, T.; Geib, S. J.; Caridha, D.; Dow, G. S.; Gerena, L.; Roncal, N.; Milner, E. E., Synthesis and biological evaluation of the first pentafluorosulfanyl analogs of mefloquine. *Org. Biomol. Chem.* **2009**, *7* (20), 4163-4165; (c) Mo, T.; Mi, X.; Milner, E. E.; Dow, G. S.; Wipf, P., Synthesis of an

8-pentafluorosulfanyl analog of the antimalarial agent mefloquine. *Tetrahedron Lett.* **2010**, *51* (39), 5137-5140.

57. Skoda, E. M.; Sacher, J. R.; Kazancioglu, M. Z.; Saha, J.; Wipf, P., An uncharged oxetanyl sulfoxide as a covalent modifier for improving aqueous solubility. *ACS Med. Chem. Lett.* **2014**, *5* (8), 900-904.

58. Sprachman, M. M.; Wipf, P., A bifunctional dimethylsulfoxide substitute enhances the aqueous solubility of small organic molecules. *ASSAY Drug Dev. Technol.* **2012**, *10* (3), 269-277.

59. Burkhard, J. A.; Wuitschik, G.; Rogers-Evans, M.; Müller, K.; Carreira, E. M., Oxetanes as versatile elements in drug discovery and synthesis. *Angew. Chem. Int. Ed.* **2010**, *49* (48), 9052-9067.

60. Purser, S.; Moore, P. R.; Swallow, S.; Gouverneur, V., Fluorine in medicinal chemistry. *Chem. Soc. Rev.* **2008**, *37* (2), 320-330.

61. John, T. W., Applications of pentafluorosulfanyl substitution in life sciences research. In *Fluorine in Pharmaceutical and Medicinal Chemistry*, IMPERIAL COLLEGE PRESS: 2012; Vol. Volume 6, pp 175-207.

62. Calculated using Advanced Chemistry Development (ACD/Labs) Software V11.02 (© 1994-2014 ACD/Labs).

63. Goff, J. P.; Shields, D. S.; Wang, H.; Skoda, E. M.; Sprachman, M. M.; Wipf, P.; Garapati, V. K.; Atkinson, J.; London, B.; Lazo, J. S.; Kagan, V.; Epperly, M. W.; Greenberger, J. S., Evaluation of potential ionizing irradiation protectors and mitigators using clonogenic survival of human umbilical cord blood hematopoietic progenitor cells. *Exp. Hematol.* **2013**, *41* (11), 957-966.

64. Brickel, N.; Gandhi, P.; VanLandingham, K.; Hammond, J.; DeRossett, S., The urinary safety profile and secondary renal effects of retigabine (ezogabine): A first-in-class antiepileptic drug that targets KCNQ (Kv7) potassium channels. *Epilepsia* **2012**, *53* (4), 606-612.

65. (a) Levin, V. V.; Dilman, A. D.; Belyakov, P. A.; Struchkova, M. I.; Tartakovsky, V. A., Nucleophilic trifluoromethylation of imines under acidic conditions. *Eur. J. Org. Chem.* **2008**, *31*, 5226-5230; (b) Prakash, G. K. S.; Mandal, M.; Olah, G. A., Nucleophilic trifluoromethylation of *N*-tosyl aldimines. *Synlett* **2001**, *01*, 0077-0078.

66. Allendörfer, N.; Sudau, A.; Bräse, S., Expedient trimethylaluminium-promoted one-pot synthesis of functional heteroaromatic and carbocyclic trifluoroethylamines. *Adv. Synth. Cat.* **2010**, *352* (16), 2815-2824.

67. Gallagher, T. F.; Seibel, G. L.; Kassis, S.; Laydon, J. T.; Blumenthal, M. J.; Lee, J. C.; Lee, D.; Boehm, J. C.; Fier-Thompson, S. M.; Abt, J. W.; Soreson, M. E.; Smietana, J. M.; Hall,

R. F.; Garigipati, R. S.; Bender, P. E.; Erhard, K. F.; Krog, A. J.; Hofmann, G. A.; Sheldrake, P. L.; McDonnell, P. C.; Kumar, S.; Young, P. R.; Adams, J. L., Regulation of stress-induced cytokine production by pyridinylimidazoles; Inhibition of CSBP kinase. *Bioorg. Med. Chem.* **1997**, *5* (1), 49-64.

68. Chang, M.; Liu, S.; Huang, K.; Zhang, X., Direct catalytic asymmetric reductive amination of simple aromatic ketones. *Org. Lett.* **2013**, *15* (17), 4354-4357.

69. Takeda, K.; Ayabe, A.; Suzuki, M.; Konda, Y.; Harigaya, Y., An improved method for the synthesis of active esters of *N*-protected amino acids and subsequent synthesis of dipeptides. *Synthesis* **1991**, *1991* (09), 689-691.

70. Li, H.; Chen, C.-y.; Balsells Padros, J., Highly efficient carbamate formation from alcohols and hindered amino acids or esters using *N,N'*-disuccinimidyl carbonate (DSC). *Synlett* **2011**, *2011* (10), 1454-1458.

71. Mack, R. A.; St. Georgiev, V.; Wu, E. S. C.; Matz, J. R., Synthesis of some novel 1,3-dihydro-2*H*-benzimidazol-2-ylidenes. *J. Org. Chem.* **1993**, *58* (22), 6158-6162.

72. Matzner, M.; Kurkky, R. P.; Cotter, R. J., The chemistry of chloroformates. *Chem. Rev.* **1964**, *64* (6), 645-687.

73. Harman, D., Aging: A theory based on free radical and radiation chemistry. *J. Gerontol.* **1956**, *11* (3), 298-300.

74. Balaban, R. S.; Nemoto, S.; Finkel, T., Mitochondria, oxidants, and aging. *Cell* **2005**, *120* (4), 483-495.

75. Sheu, S.-S.; Nauduri, D.; Anders, M. W., Targeting antioxidants to mitochondria: A new therapeutic direction. *BBA-Mol. Basis Dis.* **2006**, *1762* (2), 256-265.

76. Frantz, M.-C.; Wipf, P., Mitochondria as a target in treatment. *Environ. Mol. Mutagen.* **2010**, *51* (5), 462-475.

77. Hamanaka, R. B.; Chandel, N. S., Mitochondrial reactive oxygen species regulate hypoxic signaling. *Curr. Opin. Cell Biol.* **2009**, *21* (6), 894-899.

78. Jiang, J.; Kurnikov, I.; Belikova, N. A.; Xiao, J.; Zhao, Q.; Amoscato, A. A.; Braslau, R.; Studer, A.; Fink, M. P.; Greenberger, J. S.; Wipf, P.; Kagan, V. E., Structural requirements for optimized delivery, inhibition of oxidative stress, and antiapoptotic activity of targeted nitroxides. *J. Pharm. Exp. Ther.* **2007**, *320* (3), 1050-1060.

79. Hoye, A. T.; Davoren, J. E.; Wipf, P.; Fink, M. P.; Kagan, V. E., Targeting mitochondria. *Acc. Chem. Res.* **2008**, *41* (1), 87-97.

80. Zhao, K.; Zhao, G.-M.; Wu, D.; Soong, Y.; Birk, A. V.; Schiller, P. W.; Szeto, H. H., Cell-permeable peptide antioxidants targeted to inner mitochondrial membrane inhibit mitochondrial swelling, oxidative cell death, and reperfusion injury. *J. Biol. Chem.* **2004**, *279* (33), 34682-34690.
81. Wipf, P.; Xiao, J.; Jiang, J.; Belikova, N. A.; Tyurin, V. A.; Fink, M. P.; Kagan, V. E., Mitochondrial targeting of selective electron scavengers: Synthesis and biological analysis of hemigramicidin–TEMPO conjugates. *J. Am. Chem. Soc.* **2005**, *127* (36), 12460-12461.
82. Hull, S. E.; Karlsson, R.; Main, P.; Woolfson, M. M.; Dodson, E. J., The crystal structure of a hydrated gramicidin S-urea complex. *Nature* **1978**, *275* (5677), 206-207.
83. Schmidt, G. M.; Hodgkin, D. C.; Oughton, B. M., A crystallographic study of some derivatives of gramicidin S. *Biochem. J.* **1957**, *65* (4), 744-750.
84. Xun, Z.; Rivera-Sánchez, S.; Ayala-Peña, S.; Lim, J.; Budworth, H.; Skoda, Erin M.; Robbins, Paul D.; Niedernhofer, Laura J.; Wipf, P.; McMurray, Cynthia T., Targeting of XJB-5-131 to mitochondria suppresses oxidative DNA damage and motor decline in a mouse model of Huntington's disease. *Cell Rep.* **2012**, *2* (5), 1137-1142.
85. Macias, C. A.; Chiao, J. W.; Xiao, J.; Arora, D. S.; Tyurina, Y. Y.; Delude, R. L.; Wipf, P.; Kagan, V. E.; Fink, M. P., Treatment with a novel hemigramicidin-TEMPO conjugate prolongs survival in a rat model of lethal hemorrhagic shock. *Ann. Surg.* **2007**, *245* (2), 305-314.
86. Frantz, M.-C. I.; Pierce, J. G.; Pierce, J. M.; Kangying, L.; Qingwei, W.; Johnson, M.; Wipf, P., Large-scale asymmetric synthesis of the bioprotective agent JP4-039 and analogs. *Org. Lett.* **2011**, *13* (9), 2318-2321.
87. (a) Goff, J. P.; Epperly, M. W.; Dixon, T.; Wang, H.; Franicola, D.; Shields, D.; Wipf, P.; Li, S.; Gao, X.; Greenberger, J. S., Radiobiologic effects of GS-nitroxide (JP4-039) on the hematopoietic syndrome. *In Vivo* **2011**, *25* (3), 315-323; (b) Rajagopalan, M. S.; Gupta, K.; Epperly, M. W.; Franicola, D.; Zhang, X.; Wang, H.; Zhao, H.; Tyurin, V. A.; Pierce, J. G.; Kagan, V. E.; Wipf, P.; Kanai, A. J.; Greenberger, J. S., The mitochondria-targeted nitroxide JP4-039 augments potentially lethal irradiation damage repair. *In Vivo* **2009**, *23* (5), 717-726; (c) Frantz, M.-C.; Skoda, E. M.; Sacher, J. R.; Epperly, M. W.; Goff, J. P.; Greenberger, J. S.; Wipf, P., Synthesis of analogs of the radiation mitigator JP4-039 and visualization of BODIPY derivatives in mitochondria. *Org. Biomol. Chem.* **2013**, *11* (25), 4147-4153.
88. Wipf, P.; Xiao, J.; Stephenson, C. R. J., Peptide-like molecules (PLMs): A journey from peptide bond isosteres to Gramicidin S mimetics and mitochondrial targeting agents. *Chimia* **2009**, *63* (11), 764-775.
89. (a) Wipf, P.; Nunes, R. L.; Ribe, S., Water-accelerated organometallic chemistry: Alkyne carboalumination – sulfinimine addition and asymmetric synthesis of allylic amines. *Helv. Chim. Acta* **2002**, *85* (10), 3478-3488; (b) Wipf, P.; Kendall, C.; Stephenson, C. R. J., Dimethylzinc-

mediated additions of alkenylzirconocenes to aldimines. New methodologies for allylic amine and C-cyclopropylalkylamine syntheses. *J. Am. Chem. Soc.* **2002**, *125* (3), 761-768.

90. Lloyd-Jones, G. C., Palladium-catalyzed α -arylation of esters: Ideal new methodology for discovery chemistry. *Angew. Chem. Int. Ed.* **2002**, *41* (6), 953-956.

91. Liu, X.; Hartwig, J. F., Palladium-catalyzed arylation of trimethylsilyl enolates of esters and imides. High functional group tolerance and stereoselective synthesis of α -aryl carboxylic acid derivatives. *J. Am. Chem. Soc.* **2004**, *126* (16), 5182-5191.

92. (a) García-Fortanet, J.; Buchwald, S. L., Asymmetric palladium-catalyzed intramolecular α -arylation of aldehydes. *Angew. Chem. Int. Ed.* **2008**, *47* (42), 8108-8111; (b) Taylor, A. M.; Altman, R. A.; Buchwald, S. L., Palladium-catalyzed enantioselective α -arylation and α -vinylation of oxindoles facilitated by an axially chiral *P*-stereogenic ligand. *J. Am. Chem. Soc.* **2009**, *131* (29), 9900-9901; (c) Liao, X.; Weng, Z.; Hartwig, J. F., Enantioselective α -arylation of ketones with aryl triflates catalyzed by difluorophos complexes of palladium and nickel. *J. Am. Chem. Soc.* **2007**, *130* (1), 195-200.

93. Chieffi, A.; Kamikawa, K.; Åhman, J.; Fox, J. M.; Buchwald, S. L., Catalytic asymmetric vinylation of ketone enolates. *Org. Lett.* **2001**, *3* (12), 1897-1900.

94. Dai, X.; Strotman, N. A.; Fu, G. C., Catalytic asymmetric Hiyama cross-couplings of racemic α -bromo esters. *J. Am. Chem. Soc.* **2008**, *130* (11), 3302-3303.

95. Lou, S.; Fu, G. C., Enantioselective alkenylation via nickel-catalyzed cross-coupling with organozirconium reagents. *J. Am. Chem. Soc.* **2010**, *132* (14), 5010-5011.

96. Rudolph, A.; Lautens, M., Secondary alkyl halides in transition-metal-catalyzed cross-coupling reactions. *Angew. Chem. Int. Ed.* **2009**, *48* (15), 2656-2670.

97. Poulsen, T. B.; Bernardi, L.; Bell, M.; Jørgensen, K. A., Organocatalytic enantioselective nucleophilic vinylic substitution. *Angew. Chem. Int. Ed.* **2006**, *45* (39), 6551-6554.

98. Skucas, E.; MacMillan, D. W. C., Enantioselective α -vinylation of aldehydes via the synergistic combination of copper and amine catalysis. *J. Am. Chem. Soc.* **2012**, *134* (22), 9090-9093.

99. Kim, H.; MacMillan, D. W. C., Enantioselective organo-SOMO catalysis: The α -vinylation of aldehydes. *J. Am. Chem. Soc.* **2007**, *130* (2), 398-399.

100. (a) Stevens, J. M.; MacMillan, D. W. C., Enantioselective α -alkenylation of aldehydes with boronic acids via the synergistic combination of copper(II) and amine catalysis. *J. Am. Chem. Soc.* **2013**, *135* (32), 11756-11759; (b) Krautwald, S.; Sarlah, D.; Schafroth, M. A.; Carreira, E. M., Enantio- and diastereodivergent dual catalysis: α -Allylation of branched aldehydes. *Science* **2013**, *340* (6136), 1065-1068.

101. King, A. E.; Ryland, B. L.; Brunold, T. C.; Stahl, S. S., Kinetic and spectroscopic studies of aerobic copper(II)-catalyzed methoxylation of arylboronic esters and insights into aryl transmetalation to copper(II). *Organometallics* **2012**, *31* (22), 7948-7957.
102. Casitas, A.; King, A. E.; Parella, T.; Costas, M.; Stahl, S. S.; Ribas, X., Direct observation of Cu^I/Cu^{III} redox steps relevant to Ullmann-type coupling reactions. *Chem. Sci.* **2010**, *1* (3), 326-330.
103. King, A. E.; Huffman, L. M.; Casitas, A.; Costas, M.; Ribas, X.; Stahl, S. S., Copper-catalyzed aerobic oxidative functionalization of an arene C–H bond: Evidence for an aryl-copper(III) intermediate. *J. Am. Chem. Soc.* **2010**, *132* (34), 12068-12073.
104. Pei, L.; Qian, W., Cu^I/L-proline-catalyzed coupling reactions of vinyl bromides with activated methylene compounds. *Synlett* **2006**, *2006* (11), 1719-1723.
105. Allen, A. E.; MacMillan, D. W. C., Enantioselective α -arylation of aldehydes via the productive merger of iodonium salts and organocatalysis. *J. Am. Chem. Soc.* **2011**, *133* (12), 4260-4263.
106. (a) Nagib, D. A.; Scott, M. E.; MacMillan, D. W. C., Enantioselective α -trifluoromethylation of aldehydes via photoredox organocatalysis. *J. Am. Chem. Soc.* **2009**, *131* (31), 10875-10877; (b) Allen, A. E.; MacMillan, D. W. C., The productive merger of iodonium salts and organocatalysis: A non-photolytic approach to the enantioselective α -trifluoromethylation of aldehydes. *J. Am. Chem. Soc.* **2010**, *132* (14), 4986-4987.
107. Hall, D. G., Structure, Properties, and Preparation of Boronic Acid Derivatives. In *Boronic Acids*, Wiley-VCH Verlag GmbH & Co. KGaA: 2011; pp 1-133.
108. Horning, B. D.; MacMillan, D. W. C., Nine-step enantioselective total synthesis of (–)-vincorine. *J. Am. Chem. Soc.* **2013**, *135* (17), 6442-6445.
109. Molander, G. A.; Cadoret, F., Synthesis of the stereogenic triad of the halicyclamine A core. *Tetrahedron Lett.* **2011**, *52* (17), 2199-2202.
110. Pereira, S.; Srebnik, M., Hydroboration of alkynes with pinacolborane catalyzed by HZrCp₂Cl. *Organometallics* **1995**, *14* (7), 3127-3128.
111. Kontokosta, D.; Mueller, D. S.; Wang, H.-Y.; Anderson, L. L., Preparation of α -imino aldehydes by [1,3]-rearrangements of *O*-alkenyl oximes. *Org. Lett.* **2013**, *15* (18), 4830-4833.
112. (a) Ko, E.; Liu, J.; Perez, L. M.; Lu, G.; Schaefer, A.; Burgess, K., Universal peptidomimetics. *J. Am. Chem. Soc.* **2010**, *133* (3), 462-477; (b) Valverde, I. E.; Bauman, A.; Kluba, C. A.; Vomstein, S.; Walter, M. A.; Mindt, T. L., 1,2,3-Triazoles as amide bond mimics: Triazole scan yields protease-resistant peptidomimetics for tumor targeting. *Angew. Chem. Int. Ed.* **2013**, *52* (34), 8957-8960.

113. Pietruszka, J.; Witt, A., Synthesis of the Bestmann-Ohira reagent. *Synthesis* **2006**, 2006 (24), 4266-4268.
114. Samulis, L.; Tomkinson, N. C. O., Preparation of the MacMillan imidazolidinones. *Tetrahedron* **2011**, 67 (23), 4263-4267.
115. Edafiogho, I. O.; Scott, K. R.; Moore, J. A.; Farrar, V. A.; Nicholson, J. M., Synthesis and anticonvulsant activity of imidooxy derivatives. *J. Med. Chem.* **1991**, 34 (1), 387-392.